AD NUMBER

AD481769

LIMITATION CHANGES

TO:

Approved for public release; distribution is unlimited.

FROM:

Distribution authorized to U.S. Gov't. agencies and their contractors; Critical Technology; APR 1966. Other requests shall be referred to Air Force Armament Laboratory, Attn: ATWR, Eglin AFB, FL 32542-0000. This document contains export-controlled technical data.

AUTHORITY

AFATL ltr, 1 aug 1977

ATL-TR-66-29

Relative Motion Simulation Study

by

P. J. Ferrara

General Electric Company

APRIL 1966

AIR FORCE ARMAMENT LABORATORY
RESEARCH AND TECHNOLOGY DIVISION
AIR FORCE SYSTEMS COMMAND
EGLIN AIR FORCE BASE, FLORIDA

481769

481769

ATL-TR-66-29

RELATIVE MOTION SIIULATION STUDY

by

P. J. Ferrara
General Electric Company

FOREWORD

This final report was prepared by the Advanced Technology Programs Section of the Re-entry Systems Department, General Electric Company, Philadelphia, Pennsylvania on U.S. Air Force Contract No. AF 08(635)4911, Task No. 7848, title, "Relative Motion Simulation Study." This contract was administered under the cognizance of Mr. Charles Simpson, and Mr. James Bloomquist, Targets and Scorers Division, Air Force Armament Laboratory, Eglin Air Force Base, Florida.

The work covered by this report was performed between February, 1965 and December 1965 under the direction of Mr. Peter J. Ferrara, Program Manager. The principal technical contributors were Messrs. R. Phillips and W. Yager.

Information in this report is embargoed under the Department of State International Traffic In Arms Regulations. This report may be released to foreign governments by departments or agencies of the U. S. Government subject to approval of (controlling AFATL, RTD, AFSC, Eglin AFB, Florida), or higher authority within the Department of the Air Force. Private individuals or firms require a Department of State export license.

This technical report has been reviewed and approved.

William W. Metz

WILLIAM W. METZ
Chief
Targets and Scorers Division

ABSTRACT

The objectives of this study contract were to analyze the system requirements and establish design criteria for a relative motion simulation facility able to test and evaluate air-to-air or space mission scoring systems. In the pursuit of these objectives, numerous present and forseeable future scoring systems were studied and their essential features abstracted. The relative motion characteristic of the two classes of intercept was analyzed and the significance of maneuver capability evaluated. Those aspects of an intercept observable by scorers were summarized both quantitatively and qualitatively. With these general requirements in hand, various techniques for mechanizing the intercept simulation were considered. The technique finally selected as most practical employed a projection system whose line-of-sight was rotated by a high-performance, DC servo motor, driven open-loop in a manner duplicating the real-time sweep of the missile to target displacement vector. Relative velocity/miss distance ratios up to 500 can be simulated exactly, and ratios up to 1000 simulated acceptably, using this technique. Hardware implementation will be simple and straightforward, and all major components are obtainable off-the-shelf. A preliminary design was developed for a facility capable of accommodating L- and S-band radar scorers and both active and passive optical scorers. The design allows extension to higher radar frequencies or to infrared by modular replacement of components, without major redesign.

TABLE OF CONTENTS

TABLE OF CONTENTS (Cont)

LIST OF ILLUSTRATIONS

LIST OF ILLUSTRATIONS (Cont)

LIST OF ILLUSTRATIONS (Cont)

1.0 INTRODUCTION

1.1 Summary

The basic performance requirement under this Relative Motion Simulation Study contract has been stated as follows:

> "...study, research and definition of design criteria for a technique to realistically simulate the relative motion that occurs between advanced air-to-air, and other advanced future weapons systems and their respective targets."
>
> (R&D Exhibit NR ATT 65-8)

Our work on this requirement has proceeded in two phases. Phase I was primarily concerned with the invention of a suitable simulation technique and systems studies to establish its realm of usefulness. Phase II was concerned mostly with the hardware implementation of that technique.

In general, the studies of Phase I may be said to have shown that a facility built around a certain high-performance DC servo motor--the Incredyne--can accommodate all presently forseeable types of optical and radar scorers and can simulate the significant features of an intercept with a high degree of realism. It was shown that a wide range of air-to-air, and space missions could be simulated using this technique. Sufficient analysis was carried out to show the reasonableness and general workability of such a facility. Mechanisms for generating the most important features of a realistic intercept were described and their performance criteria outlined. To some extent the actual hardware which might be employed was tentatively identified. In Phase II, this work has been extended to a more detailed description of the most important elements of an actual facility design.

1.2 Design Approach

In the study phase of this work, we considered the potential of the several basic types of scoring systems and tried to foresee the avenues of development which might be followed as the technology advanced. We then developed the conceptual design of a simulator with capabilities general enough to accommodate anything we could see to be reasonably forthcoming. It was a sophistocated facility which could simulate an intercept in realistic detail. The cost of realism comes high, however. For the present and immediate future, we feel such refinement in simulation is not justified. Consequently, in the design phase of the work, we stripped down our original concept to include only the most essential features. It is this stripped down simulator whose detailed description is presented in this report.

1.3 Preliminary Design

Although our contractual requirement included only a statement of the criteria on which a design could be based, we decided to go further and identify more accurately the most

vital parts. Once the simplified facility was defined, it was a natural second step to survey the range of available key hardware items to make sure suitable components were readily available. In the process of making such a survey, intended basically to insure feasibility, it was reasonable and natural to select those particular items of hardware deemed most suitable. The result was significant head start toward a practical facility design.

1.4 Cost Estimate

Having defined a system, including certain essential actual hardware to realize it, we were in a fairly good position approximately to cost that system. The final result, then, includes somewhat more than was required by the contract. We feel that carrying the work through these extra steps lends additional force and credibility to the basic facility concept and represents a useful bonus to our customer.

1.5 Design Philosophy

In approaching the task of design, we were mindful of the primary requirement that what we recommend represents a practical and workable facility realizable at sensible cost. Three very useful rules to follow in such a case are: (1) use the simplest possible design; (2) use a modular design, employing common subsystems wherever possible and allowing for upgrading by modular replacement; and (3) use off-the-shelf hardware generally with minimum reliance on special component development. Wherever possible, these rules were applied throughout the work.

2.0 SYSTEM DESIGN CONCEPTS

The facility recommended in this report includes two major subfacilities: an optical intercept simulator designed to exercise optical scoring systems, and a radar intercept simulator designed to exercise radar scoring systems.

The facilities described here are limited to the simulation of a rectilinear relative intercept, that is, one during which neither target nor scorer undergoes acceleration. A zero acceleration intercept is completely characterized by two independent variables, which we choose to take as the miss distance R_0 and the maximum angular velocity Ω. The significant features of a rectilinear intercept are diagrammed in Figure 1. Analysis has shown that this form of intercept is an adequate approximation to most practical cases of interest.

2.1 Optical Intercept Simulator

By optical intercept simulator, we refer to a device which simulates the intercept observables which a scoring system employing optical sensors could detect and measure. We have divided optical scoring systems into two classes: passive and active. By active optical system, we mean one which illuminates its target, the only present example being the laser rangefinder. By passive optical system, we refer to one which observes a self-luminous or independently illuminated target. There are several types of passive devices at present. The optical intercept simulator described here can accommodate passive systems alone or linked passive and active systems such as the PERSEAS/laser.

2.1.1 Passive Intercept Simulator. A general view of the passive optical intercept simulator is shown in Figure 2. Essentially it operates as follows. A fixed lens projects an image of a target outline through a rotating diagonal mirror into a large spherical zone field mirror. The scoring system under test is placed in the simulator so that the field mirror images the diagonal mirror onto the scorer aperture. Thus generally all light leaving the projector enters the scorer, regardless of the angular position of the diagonal mirror. In thus conserving light from the projector, the field mirror allows target brightness to range even up to that of the projector source without excessive power requirements.

The projection lens is focused at a point between the focus and the surface of the field mirror, chosen so that after relay by the field mirror the virtual image seen by the scorer is at or beyond the hyperfocal distance of the scorer lens. Thus the image will always be in focus for the scorer.

The angular position of the target as seen by the scorer depends on the rotational position of the diagonal mirror. The diagonal mirror is fixed to the shaft of a high-performance, DC servo motor, the Printed Motors, Inc. Incredyne. A programmed control system drives the motor so that its angular shaft position $\theta(t)$ closely duplicates the angular position of the target during an intercept.

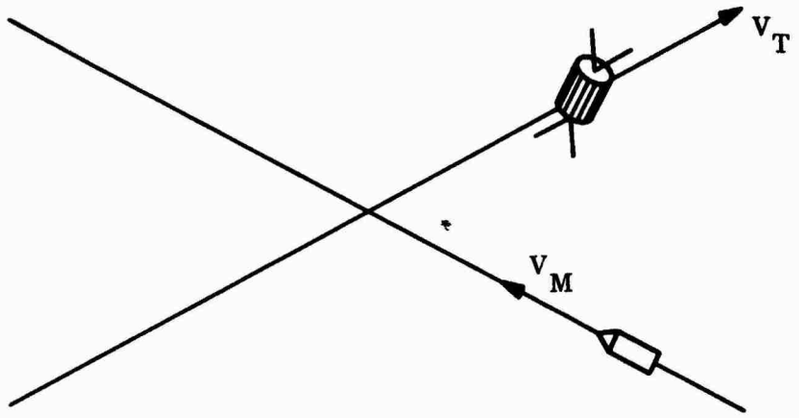

ANY ZERO ACCELERATION INTERCEPT MAY BE REDUCED TO A RECTILINEAR INTERCEPT RELATIVE TO ONE BODY CONSIDERED AS FIXED.

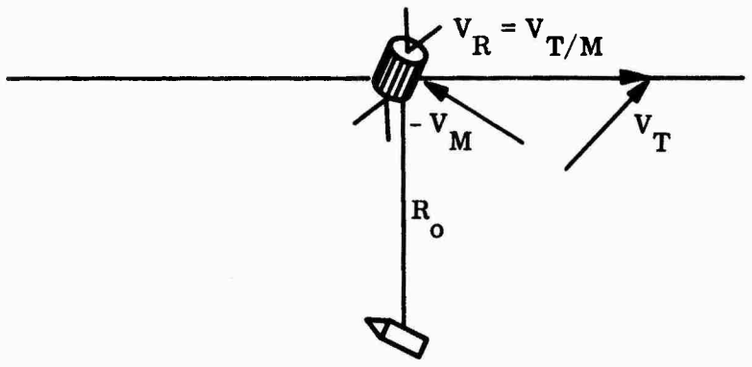

THE INTERCEPT IS COMPLETELY DEFINED BY TWO VARIABLES. THE MOST CONVENIENT ARE.....

R_o = MISS DISTANCE

V_R = RELATIVE VELOCITY

Ω = V_R/R_o MAXIMUM ANGULAR VELOCITY

Figure 1. Rectilinear Intercept Parameters

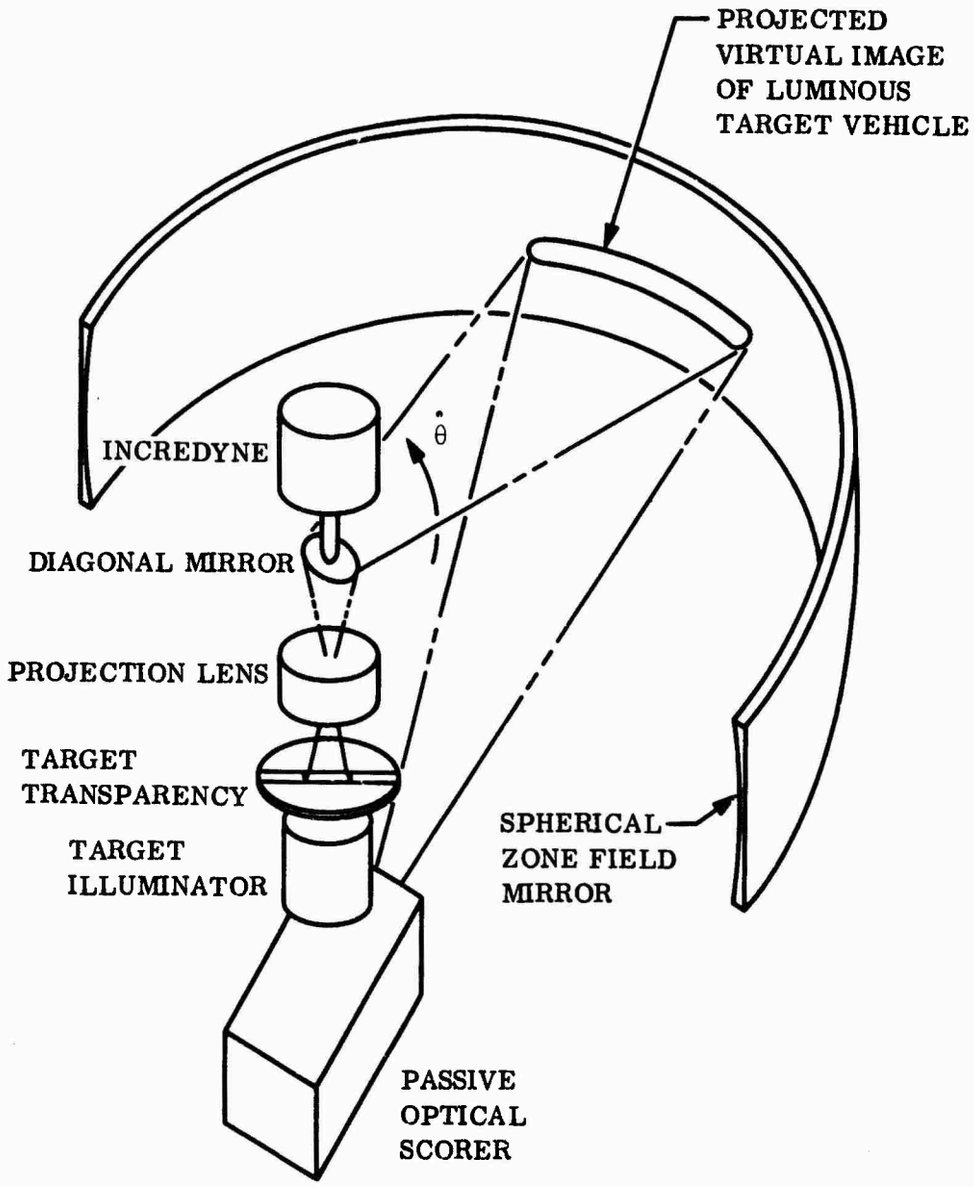

Figure 2. Basic Concept of Passive Optical Intercept Scorer

The target outline in the projector is electrically driven and is programmed to vary the apparent size of the target realistically as it sweeps past during the intercept.

In summary, the passive optical intercept simulator can duplicate the angular size and position of a target, as well as its brightness, throughout a rectilinear intercept.

2.1.2 Active Intercept Simulator. The main features of the active optical simulator are illustrated in Figure 3. The operation of the active simulator is basically the same as that of the passive simulator, except for the projection system. The essential function of the active intercept simulator is to present a moving target to the laser rangefinder. This moving target should be equivalent to a physical reflecting body of constant size moving with constant velocity in a straight line. In the active intercept simulator, this function is performed by projecting a photosensitive window onto a reflective fence in such a way that its size and velocity remain constant. A proper range return is obtained only when a laser beam is properly directed and hits the target. The reflective fence is essential if both the ranging and tracking capabilities of an active scoring system are to be tested. The tracking capabilities alone may be tested by substituting for the reflective fence a field mirror such as used in the passive simulator. This alternate arrangement has the advantage of compactness, if space is limited. A second method of achieving compactness is to fold the reflective fence with mirrors. This arrangement is discussed in the section of this report dealing with the radar intercept simulator.

2.1.3 Integration of Passive and Active Simulators. In present practice, the laser rangefinder cannot function independently. It may be foreseen that future laser scorers will have sufficient power and sufficient pulse repetition frequency to operate as omnidirectional pulse radars but, for the near future, the laser will have to operate with limited beamwidths and in conjunction with some direction sensing system, as the PERSEAS/laser combination. Therefore, a means must be provided in the simulator to accommodate linked passive and active systems. The means proposed is diagrammed in Figure 4.

For a proper test of linked systems, it is essential that active and passive systems see exactly the same target. For a closed-loop drive, independent motors could be used. But for the open-loop system recommended here, the only means of positive linkage is to drive both simulators with a common motor. Fortunately, the Incredyne is double-ended, and this arrangement is perfectly feasible. There is the disadvantage that the inertia loading this motor is increased, which may result in some degradation of performance. On the other hand, tracking lasers are not likely to find much use in small miss-distance intercepts anyway, so this disadvantage may be more apparent than real.

It does not appear possible to use the same optics for both active and passive simulators simultaneously. Therefore, it will be necessary physically to separate the two associated parts of an active/passive trajectory scorer such as the PERSEAS/laser system. One of the ground rules of our approach in the Phase I study part of this work was that such physical separation of cable connected subsystems was allowed. The relative displacement required in the present design is: rotation through 180 degrees and physical separation by 39 inches. Other configurations might reduce the physical separation considerably.

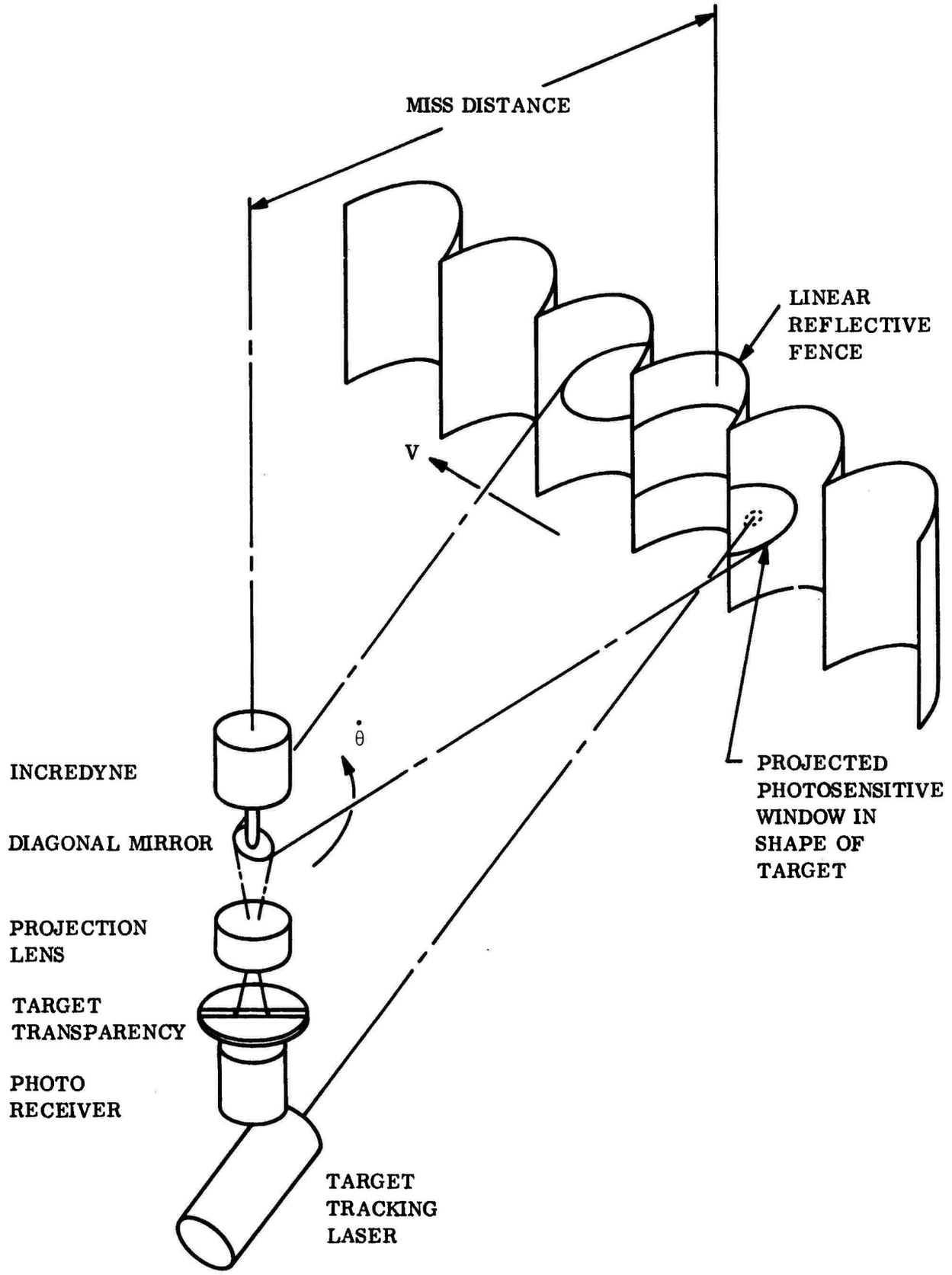

Figure 3. Basic Concept of Active Optical Intercept Simulator

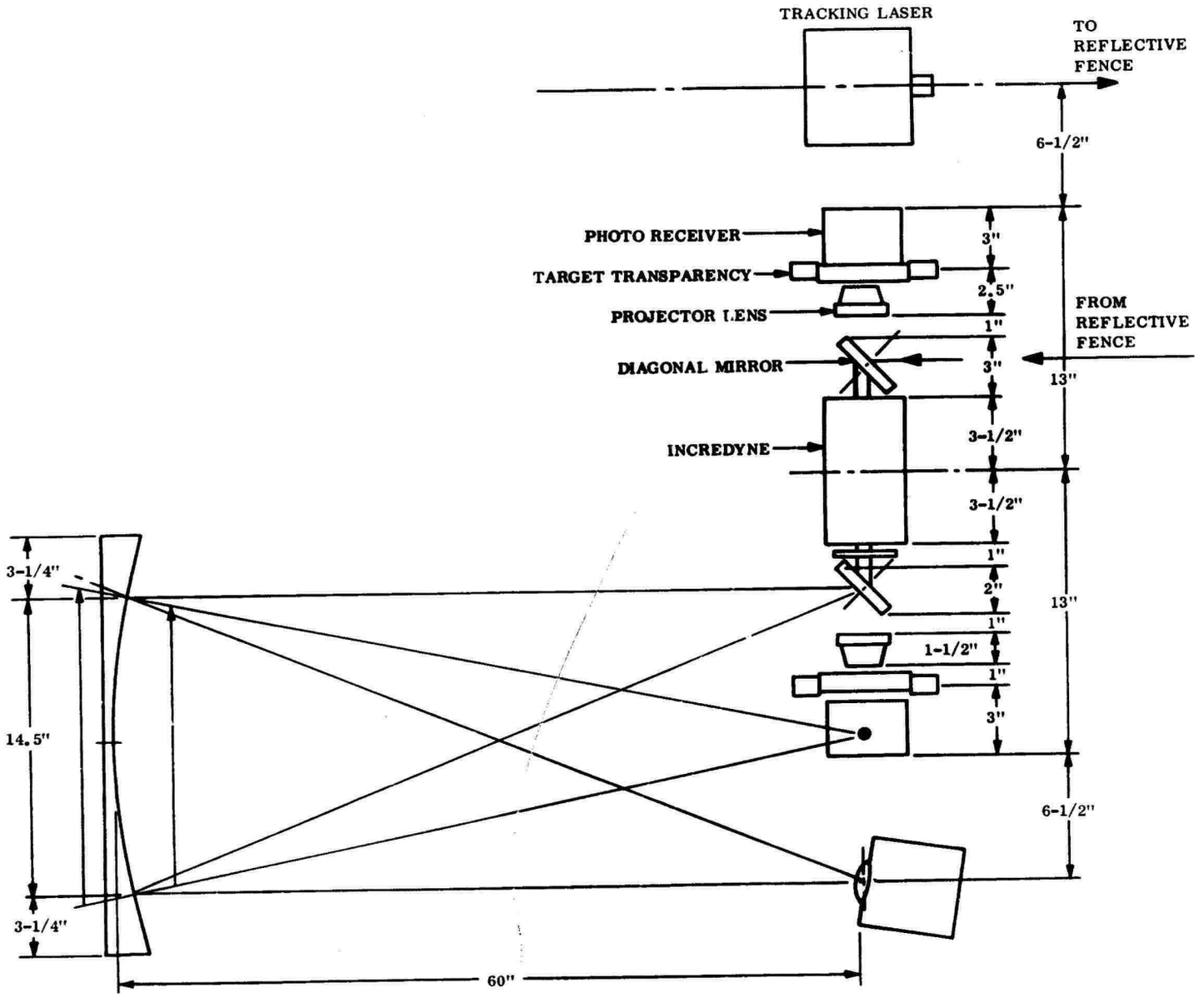

Figure 4. Integration of Active and Passive Optical Simulators

2.2 Radar Intercept Simulator

2.2.1 Proposed Design. The general scheme is illustrated in Figure 5. A block diagram of the operation is shown in Figure 6. The concept is as follows: The scoring system is mounted in a radar-anechoic room containing antennas for communicating with the scorer under conditions approximating free-space. The output signal of the scorer, carrier plus all modulation, is received, suitably processed, and then imposed on a CW laser beam through an electro-optical modulator. The laser beam serves as the carrier for the complete radar signal. This laser beam is then swept across a suitably reflective rectilinear fence in such a way that the range function R(t) is duplicated on a full geometric scale, real time basis. The returned signal will then contain the same time delay and doppler modulation as would the RF signal returned from a real intercept. Furthermore, if the reflective fence has structure to it, the return will include a scintillation pattern which adds to the realism. This returning laser beam is then demodulated to yield the intercept-modulated RF, and after suitable processing this signal is broadcast to the scoring system receiver. Except for an additional instrumental time delay, the scoring system will receive a return of its own radiated signal which should be closely similar to the return from a real intercept.

Although the system is extendable to shorter wavelengths, the design recommended here is limited to L- and S-bands only.

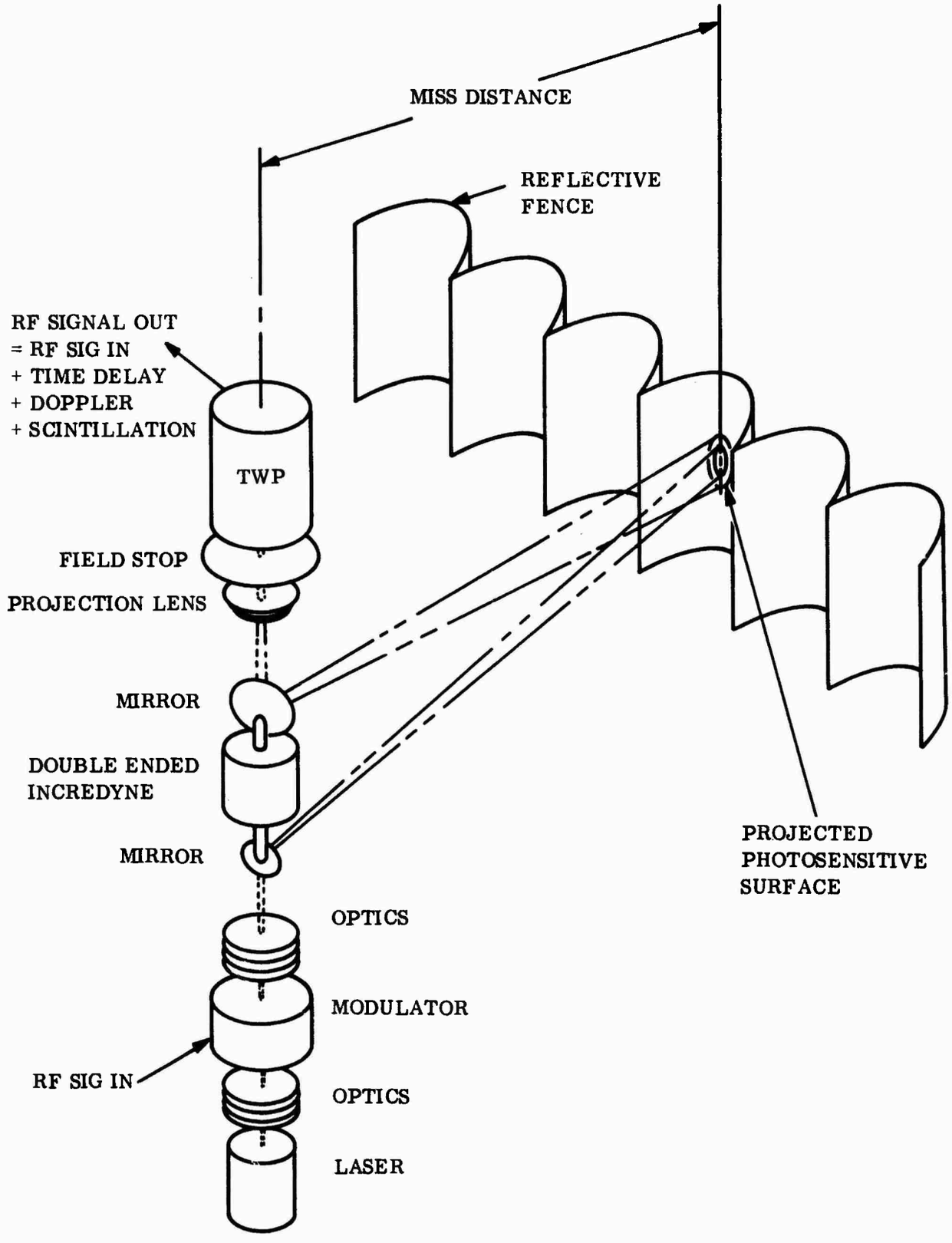

Figure 5. Basic Concept of Radar Intercept Simulator

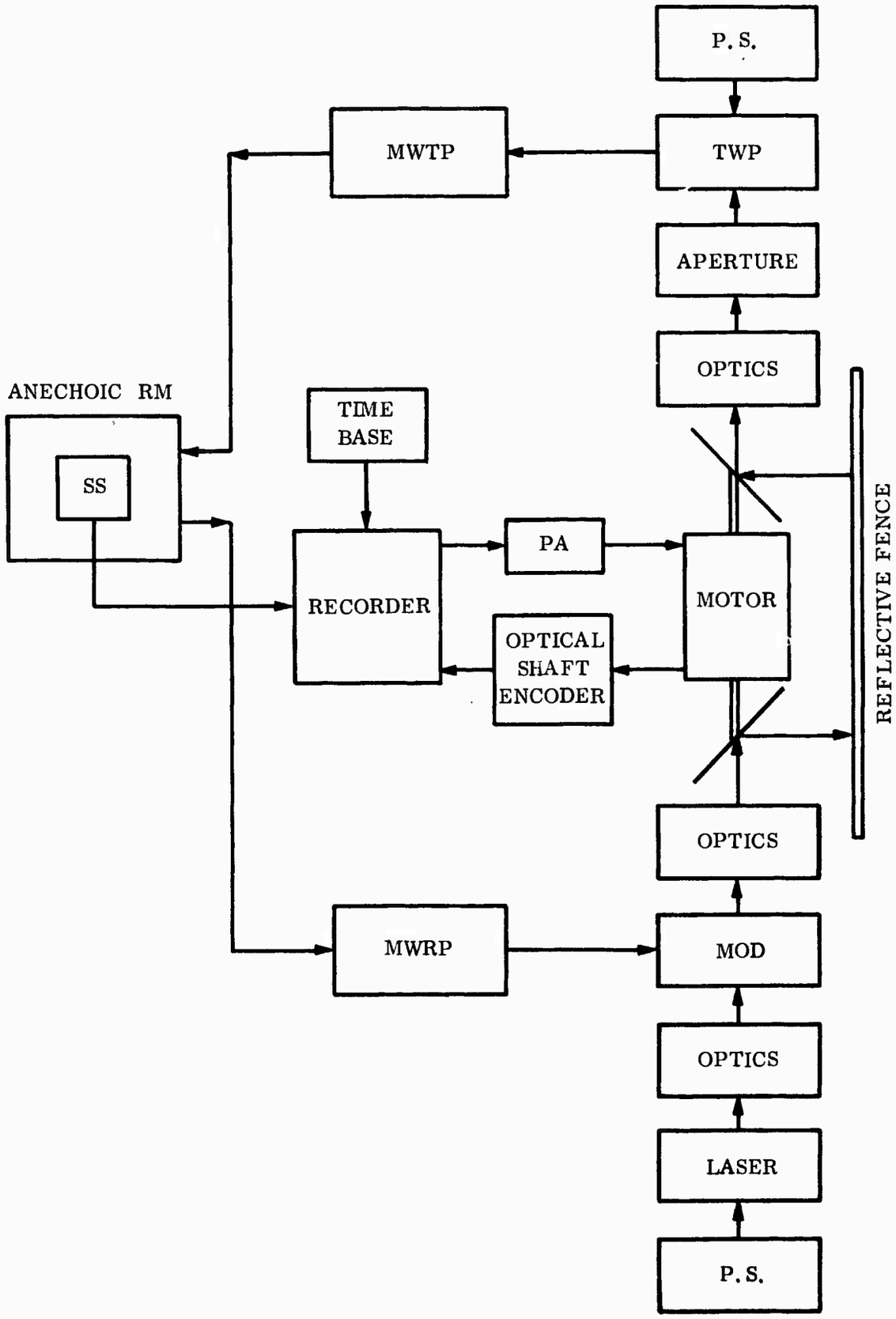

Figure 6. Radar Intercept Simulator

3.0 DESIGN JUSTIFICATION

3.1 Scoring System Survey

3.1.1 General. The design of a relative motion simulator depends on the particular scoring systems which it must accommodate. Hence, numerous scoring systems both in existence and under development were surveyed in order to establish basic requirements for a relative motion simulation facility. The scoring systems surveyed included miss-distance indicators and trajectory scorers intended to be carried either in the target or the missile. Ground tracking systems or systems which require a third vehicle as an observer were not included. The systems noted in this survey are listed below.

3.1.2 Scoring Systems.

3.1.2.1 Optical and IR.

PERSEAS (Photo Electric Rotating Slit Elevation and Azimuth Sensor)

Multicamera Systems (several)

Diamond Fuze EOS

IR Cooperative Scoring System

Reflecting Cone IR Scorer

Tri-Pulse Optical MDI

Laser Rangefinder (GE)

Monocular Rangefinder (GE-STRANGER)

WADC 2-Camera TV System

GE Acquisition and Tracking Subsystem

3.1.2.2 Radar Systems.

PARMIS

PARAMI

AN/USQ-11 NOL Single Path Doppler

AN/USQ-6 Raytheon Double Path Doppler

AN-USQ-7 Firetrac

Radioplane FM-CW Proximity Scorer

Interstate FM MDI

Bidops

GC Dewey Autoscore

NOL 10 ms Pulse Radar

DOFL 10 ns Pulse Radar

3.1.2.3 Radioactive Systems.

Franklin GNO-Gamdar

Engineering Specialities - ESCO

Stanley Aviation

Giannini

3.1.2.4 Other Systems.

Librascope (Electrostatic)

Hughes Magnetometer (Magnetic Flux)

Aeromic (Acoustic)

Swedish Lyth-22 (Acoustic)

FEI - (Acoustic)

3.1.3 Summary of Operational Types. A summary of scoring systems classified by their mode of operation are identified as follows.

3.1.3.1 Optical and IR.

Direction Finding - PERSEAS

Echo Ranging - GE Laser

Focal Ranging - GE STRANGER

Parallax Ranging - Diamond EOS

Stadia Ranging - GE Acquisition and Tracking Subsystem

3.1.3.2 Radar.

Echo Ranging - NOL Pulse Radar

Cooperative Echo - PARAMI

SP Doppler - AN/USQ-11

DP Doppler - AN/USQ-6

Doppler Cycle Counter - Autoscore

Multifrequency Doppler - Bidops

Phase Comparison - Firetrac

3.1.3.3 Radioactive.

Calibrated Source - inverse square ranging - ALL

3.1.3.4 Electrostatic.

Field Anomaly - Librascope

3.1.3.5 Magnetic.

Field Anomaly (Hughes) Magnetometer

3.1.3.6 Acoustic.

Calibrated overpressure - Swedish Lyth-22

Arrival at displaced microphones - FEI

3.1.4 Recent Advances. The new scoring systems which are under development or have just become operational reflect the direction of growth in the field and, further, fix the operational requirements of the motion simulator. The following are considered the most important in this category.

3.1.4.1 PERSEAS/Laser. The Photoelectric Rotating Slit Elevation and Angle Sensor is under development by the University of Texas in cooperation with General Electric. It receives reflected light (visible) from the vehicle to be scored and determines elevation and azimuth angle (position) of this vehicle. This information is used to point a

laser ranging device. The vehicle is tracked in this manner through a part of the relative trajectory, usually not including the distance of closest approach. The miss distance is calculated from the angle and angle rate plus range and range rate information then acquired using the assumption of rectilinear motion.

PERSEAS is intended to be a space mission scorer which may be used for non-cooperative targets. It will be a trajectory scorer.

3.1.4.2 Autoscore. The Dewey Autoscore is a radar doppler cycle counter which records scalar miss distance for non-cooperative targets or missiles. It is capable of scoring misses of 0 to 200 feet with a reported accuracy of ±3 percent. The system employs a carrier frequency of 1780 mc.

3.1.4.3 Bidops. Bidops registers scalar miss distance in real time by detecting the doppler phase difference between two reflected CW radar signals. It scores non-cooperative targets in the speed range 500 to 6000 ft/sec over miss distances of 0 to 150 feet with an accuracy of ±4.5 feet. It has carrier frequencies of 1713.78 mcs and 1716.23 mcs. It is adaptable by modification to intercept at 25,000 ft/sec and miss distances of 2000 feet.

3.1.4.4 Franklin MDI. The Franklin radioactive scorer is a cooperative miss-distance indicator. The system determines miss distance by counting gamma emission at the target from a radioactive tag on the projectile. Readout is provided directly in feet in real time. The system is provided with its own motion simulator which is used to calibrate the system before flight tests.

The system can score in the velocity range of 600 to 6000 ft/sec with accuracy of ±10 percent or ±3 feet (whichever is greater). Its range indication is 3 to 100 feet.

3.1.5 Survey Results. Scoring system development is in the direction to improve cost, size, weight, and accuracy of operational systems or to provide additional scoring capability. The additional capability not presently provided by operational systems is for high velocity intercepts and large miss distance with trajectory scoring. These broad objectives are reflected by the development trends discovered in the scoring system survey. The important features of these trends are outlined as follows:

Optical and IR: Imaging and image analyzing systems; laser ranging.

Radar: Non-cooperative; doppler; high frequency; (toward K-Band)

The proposed simulation facility is designed to test advanced scoring systems having these characteristics.

3.2 Optical Intercept Sensors

The optical sensors which will observe an intercept may be conveniently classified into two general types: passive and active. Passive sensors respond to radiation originating

at the target. This radiation may be either natural or the result of some augmentation device. Active sensors irradiate the target and respond to reflected radiation. Sensors may also usefully be classified according to whether they extract information concerning direction $\theta(t)$, range $R(t)$, or both. The simulation problems are somewhat different for these several classes of devices.

3.2.1 Passive Optical Sensors. In its simplest form, a passive optical sensor is merely a device which responds in some way to the presence of light. The full capabilities of a passive optical sensor appear, however, only when a lens is added.

Although perfect imagery is possible only for one set of conjugates, in general, a good lens performs a complete three-dimensional mapping of a luminous surface in object space into image space. Since the coordinates of image space are accessible to measurement, this means that in principle the full three-dimensional character of a target surface can be deduced from measurements made to locate the image surface. This principle is illustrated in Figure 7.

Referring to Figure 7, the accuracy with which x, y, and z can be determined falls off rapidly with increasing range and F/number. Furthermore, the technique necessary for accurate measurement of (z'-f) is not always practical. It may take too much time, for instance. Consequently, imaging sensors are commonly used in ways which make only partial use of their capabilities. An ideal passive optical sensor would continuously read out x'(t), y'(t), and z'(t), and, therefore, would generate the object space coordinates x, y, and z for all times t. Practical devices are less sophisticated and make progressively less use of the information in the image, as suggested by the following list, in rough order of decreasing complexity:

a. Continuous readout of x', y', z' (ideal sensor)

b. Continuous readout of centroidal x', y' (some tracking transducers)

c. Sampling of all x', y' for selected t (photography)

d. Sequential scan of x', y', (TV, PERSEAS)

e. Sequential scan of z' for limited x', y' (GE-STRANGER)

f. Read t for fixed f(x', y') (EOS)

g. Read t for fixed z', all x', y' (optical range gate)

Although passive optical sensors are inherently capable of generating range information, the more usual application is to generate angle information only

$$\frac{x'}{z'} \approx \frac{x'}{f} \; ; \; \frac{y'}{z'} \approx \frac{y'}{f}$$

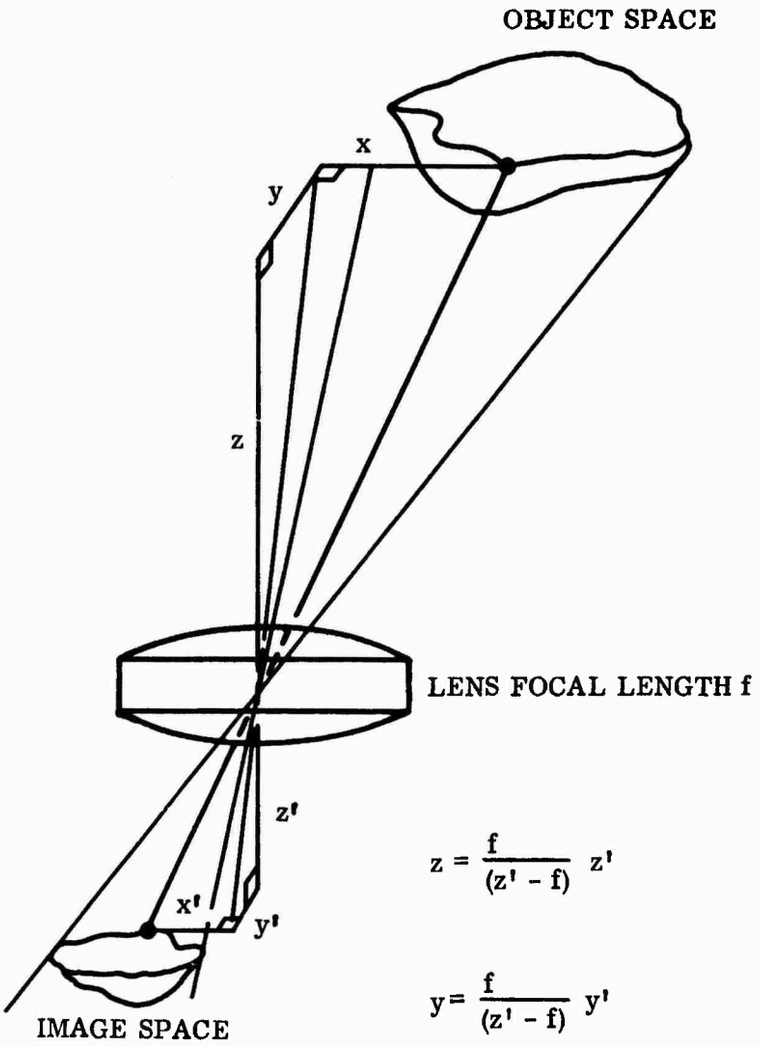

Figure 7. Mapping Properties of a Passive Optical Sensor

The presence of a known baseline somewhere in the system will allow range to be computed. In general, there are two types of such systems: those based on the stadia principle and those based on parallax. These are illustrated in Figure 8.

3.2.2 Active Optical Sensors. Active optical devices are those which make use of the laser for target illumination. The laser has a very limited beamspread and to get a return, it must be pointed in the direction of the target. This is accomplished either by slaving the laser to an associated direction sensor (PERSEAS, TV/laser systems) or by scanning the field with the laser, whose beam is deflected systematically into a raster pattern by moving optical elements (Westinghouse and GE systems), ultrasonic standing wave cells (United Aircraft), or other devices. Pointed lasers at present have limited application to scoring systems for two reasons:

a. The enormous angular accelerations characteristic of close intercepts places severe mechanical demands upon the servo pointing system, and

b. The high pulse power requirement limits the pulse repetition rate.

These two limitations are related. The pulse power requirements are high because the target must be observed at a relatively great distance. It must be observed at a relatively great distance because the pointing system cannot move fast enough to follow it when it gets close. There is every reason to believe that the present methods of beam deflection can be dramatically improved and that rapid deflection over a wide field will soom be possible. The use of active optical sensors in scoring systems can, therefore, be expected to increase.

3.2.3 Basic Simulation Requirements. The basic intercept simulation requirements for passive and active optical sensors may be summarized as follows:

a. Passive Optical Sensors require a moving, luminous image with full-scale duplication of size, direction $\theta(t)$, and optical range $R(t)$.

b. Active Optical Sensors require a moving reflective target with full-scale duplication of size, direction $\theta(t)$, and physical range $R(t)$.

By optical range, we mean the light rays received by the sensor must appear to diverge from a point at $R(t)$. It is not essential that a real source be located at the physical distance R.

By physical range, on the other hand, we mean that a reflective target must be physically located at this range $R(t)$. Thus, we see that the intercept simulation problems are appreciably different for the two types of sensors.

Although no imaging systems are known to be in use for scoring which make full use of the available image information, it is perfectly reasonable to expect that systems making greater use of image information than at present will appear.

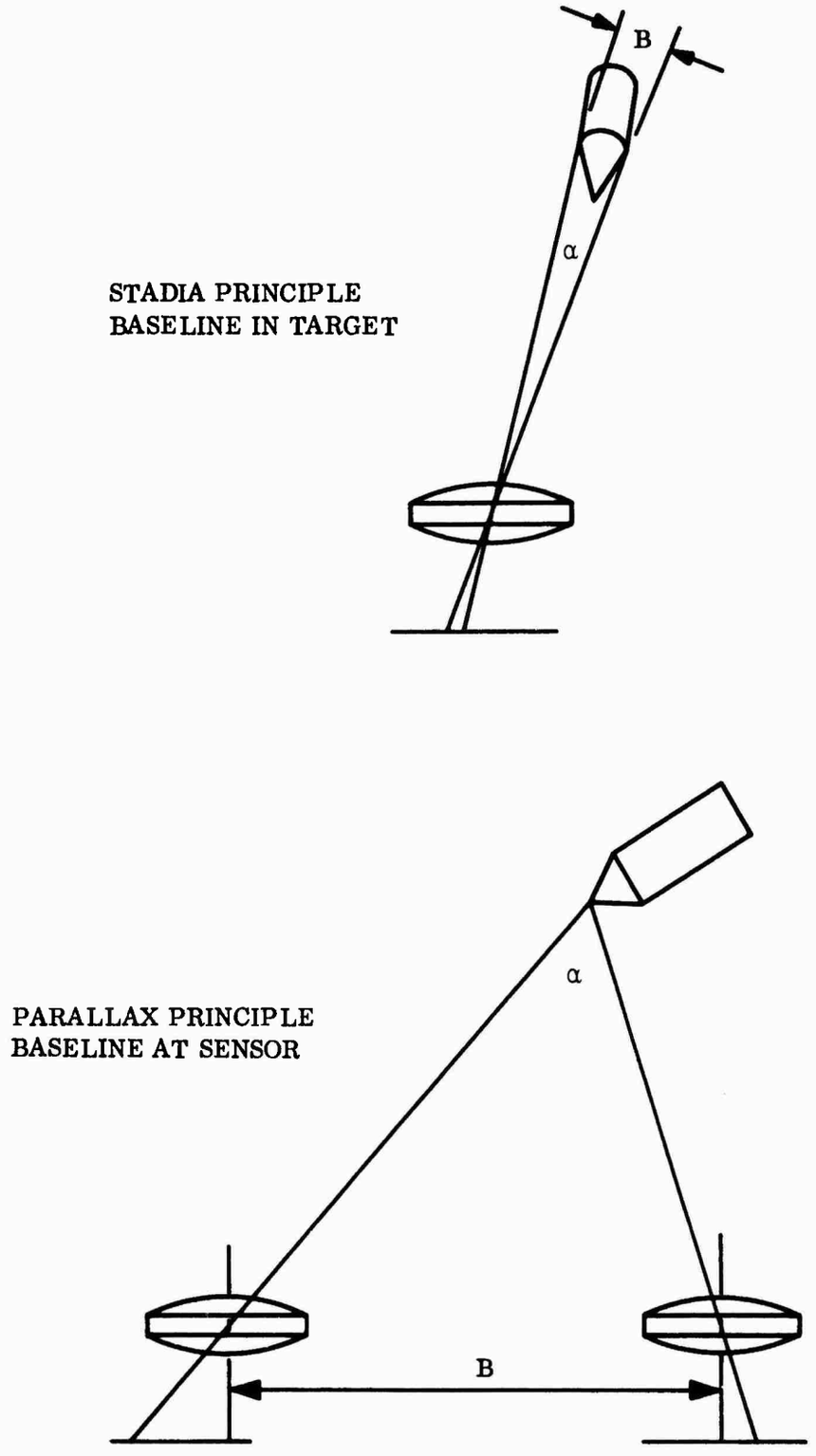

Figure 8. Range Systems Based on Stadia and Parallax Principle

Since the requirement in this study is to devise a simulator which can accommodate reasonably foreseeable future systems rather than presently existing systems, it is appropriate that the simulator have the most general capability possible, even though it exceeds the requirements of any present scoring sensor. Therefore, the passive optical simulator should ideally have the capability to generate and present to the sensor a luminous target for which the coordinates x(t), y(t), and z(t) are duplicated full-scale. Thus, any future systems of greater sophistication than present systems, up to and including the ideal sensor, can be accommodated for test. The inclusion of full-scale duplication of optical range is important to optical fuzes and terminal guidance systems as well as to scoring systems, since all are designed to operate in the region of small z (under 100 meters) where usefully accurate measurements of z' are possible. In the present design, optical range simulation is omitted, but it can be added later as the need arises.

The operation of both passive and active optical sensors involves real geometric displacement inside the sensor corresponding to external motion of the target. Therefore, the simulator must incorporate an element of real geometric motion in its operation.

3.3 Basic Technical Problem

Both passive and optical sensors have in common the requirement that intercept simulation include the full-scale duplication of direction $\theta(t)$. The angular accelerations involved in practical intercept situations become extremely large (See Section 4.0). This implies severe mechanical demands upon the simulator. If it were possible to rotate a line-of-sight in such a way that it faithfully duplicated the angular function $\theta(t)$ then this mechanism could be used to develop a rotating projection system. With a rotating projection system, the basic intercept simulation requirements for both types of sensors could be met, as Figures 9 and 10 illustrate. Thus, we may say that the problem of rotating a line-of-sight in such a way as to meet the severe acceleration demands is the basic technical problem in intercept simulation.

3.3.1 Basic Technical Solution. The simple and direct way to generate a rotating line-of-sight is to reflect a fixed line-of-sight in a rotating 45-degree diagonal mirror. This idea is illustrated in Figure 11. If this device were to be used, then the servo motor driving the mirror would have to be able to duplicate the function $\theta(t)$. A survey of available high-performance servo motors revealed one motor which had the necessary capability: the INCREDYNE, manufactured by Printed Motors, Inc., of Glen Cove, Long Island. Since the feasibility of developing such motion in a motor is crucial to any design developing along the lines so far suggested, this matter is examined in further detail in a later section.

3.4 Radar Intercept Sensors

3.4.1 Active RF Devices. All present RF scoring systems are active systems. Cooperative systems exist in which transmitter and receiver are in separate vehicles,

PASSIVE OPTICAL SYSTEMS

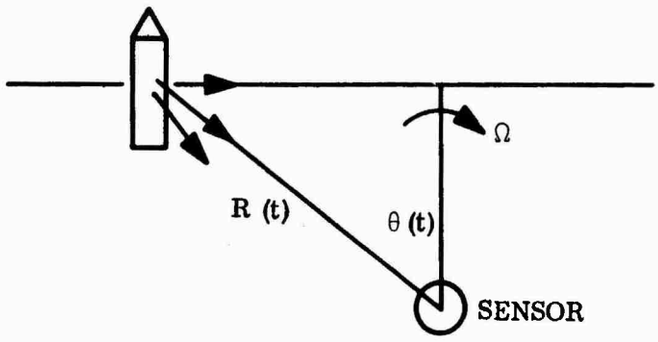

SENSOR OBSERVES
MOVING LUMINOUS
TARGET IN
DIRECTION θ (t)
AT RANGE R (t)

BASIS OF SIMULATION

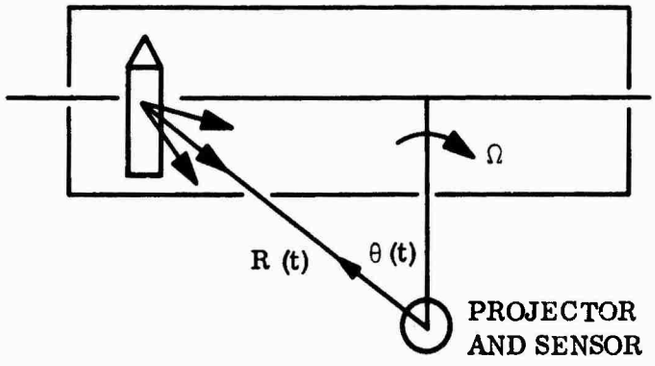

ROTATING PROJECTION
SYSTEM PLUS
SUITABLE REFLECTOR

Figure 9. Passive Optical Systems

ACTIVE OPTICAL SYSTEMS

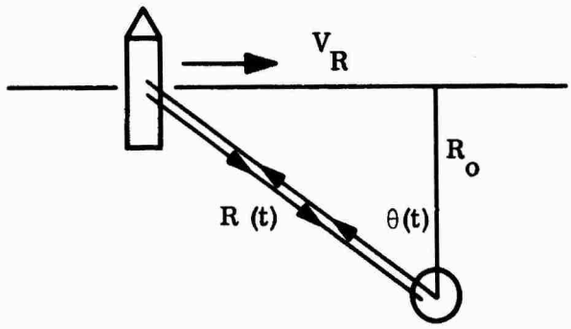

SOURCE
AND SENSOR

SENSOR SEES RADIATION
FROM MOVING REFLECTOR
AT DISTANCE R (t)
AND DIRECTION θ (t)

BASIS OF SIMULATION

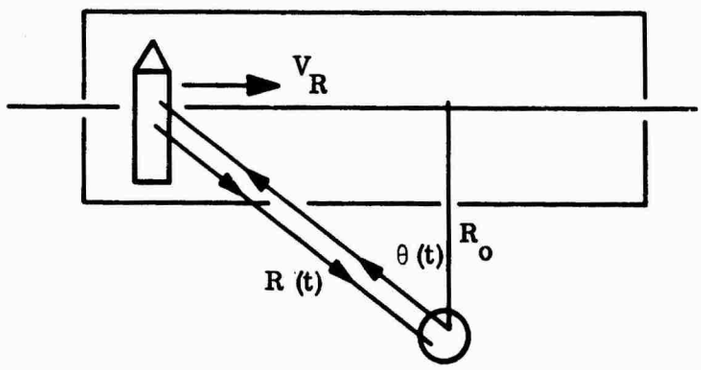

PROJECTOR
AND SENSOR

MOVING PROJECTION
OF PHOTOSENSOR
APERTURE ON TO
REFLECTIVE SURFACE
AT DISTANCE R (t)

Figure 10. Active Optical Systems

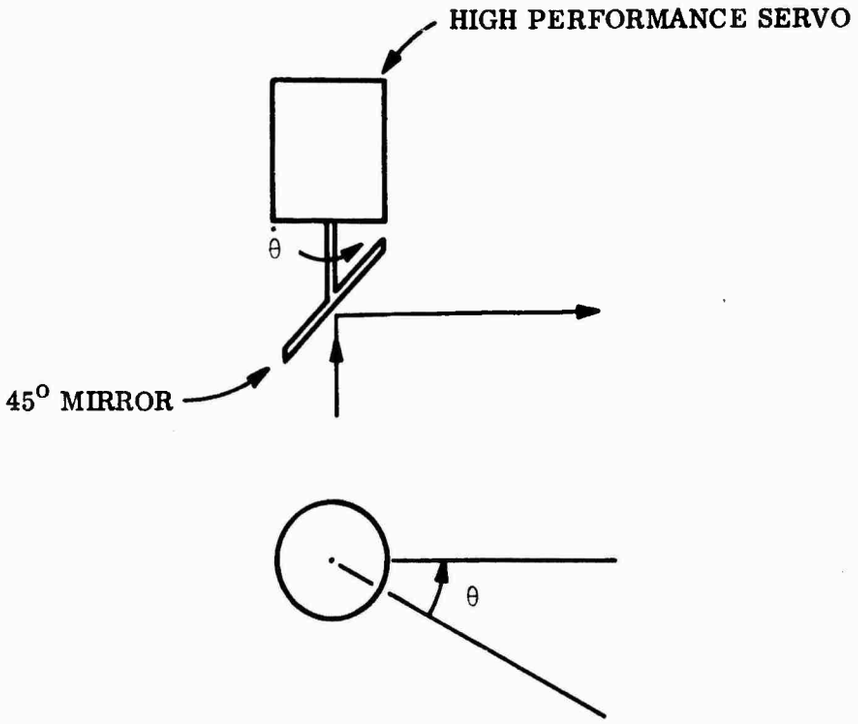

ROTATING LINE OF SIGHT CAN BE PRODUCED BY REFLECTING IN ROTATING 45-DEGREE MIRROR DRIVEN BY A HIGH-TORQUE, LOW-INERTIA MOTOR

Figure 11. Basic Technical Solution to Line-of-Sight Rotation Problem

but these are not properly passive systems. Passive systems are not likely to be developed for two reasons:

a. Sufficiently strong natural sources of RF do not exist to provide vehicle illumination, and

b. At the relatively long wavelengths involved, only coherent signals can yield a return with sufficient information entrained to serve for scoring purposes.

High angular accelerations and narrow beamwidths cannot be combined in a single antenna package except for very short wavelengths. Consequently, active RF scoring systems are not presently, and are not likely to become in future, pointing systems in the way that active optical systems are pointing systems. Instead, they are conventionally omnidirectional, low-power radar systems radiating generally a CW, sometimes a pulse signal.

Intercept information is entrained in the modulated signal returned by the reflecting target.

3.4.2 General Simulation Requirements. The RF scoring system in operation radiates an omnidirectional signal or signals. During intercept, this signal is returned by reflection from the target vehicle. The original signal has been modulated by the intercept and information regarding this intercept is entrained in the modulation. The most important elements of intercept modulation are:

a. Time delay

b. Doppler

c. Scintillation

d. Inverse fourth power range attenuation

The radar intercept simulator must be a device which accepts the scorer transmission, modulates it in such a way as to duplicate realistically the effects of an intercept, and then returns the modulated signal to the scorer receiver. The essential feature of such a simulator is a very wide-band, continuously-variable, delay line operable throughout the radar region to time delays as short as 10 nanoseconds.

3.4.3 Design Philosophy. Present RF scoring systems operate at frequencies up to S-band. It is reasonable to foresee these operating frequencies going higher because of the improvement in ranging accuracy and the reduction in size which ensue. Our design philosophy has been to devise a facility which has the most general capability possible in order to accommodate future scoring systems as they come along. Our design goal, then, is a facility whose inherent usefulness extends throughout the radar range and as far above S-band as is presently practicable. Furthermore, since the limits of practicability will expand as industrial development in this field continues, the design

of the simulator should be modular so that improved subsystems can be substituted as the state of the art advances.

3.4.4 Delay Line Problems. We may first consider whether any commercially available delay device will serve in the simulator. To be satisfactory the delay device or devices must be operable throughout the microwave region from L-band to K-band. To accommodate any reasonable type of scorer, bandwidth should be ±30 percent of nominal band center. Efficiency is important. A maximum insertion loss of 20 db is desirable; otherwise, multiple stages of microwave amplification must be resorted to. An essential requirement is a lack of distortion, whether of amplitude, frequency or phase.

Present microwave delay devices which might be considered here are all acoustic delay lines. No continuously variable delay lines are available, although work in this area is being done, and all known devices fall short of the present requirements in one or more respects. Fixed delays are available, but the shortest is 500 ns. Operating frequencies are limited to L-band and S-band, although development work up to K-band is in progress.

Bandwidth available does not exceed 10 percent. Insertion losses are high, on the order of 45 db at 1 Gc, increasing to 75 db at higher frequencies. Coupling to the acoustic medium is a serious problem, transducer efficiencies at present being no more than 1 percent.

Acoustic delay lines are dispersive and, therefore, introduce phase distortion. Passband and mode conversion characteristics generate considerable amplitude and frequency distortion and spurious pulses are a serious problem. In short, available delay devices do not appear suitable as a basis for simulator design.

3.4.5 Proposed Simulator Design. We saw in the previous sections that the radar simulator must in essence constitute a form of delay line. We also saw that no practical delay lines are available having characteristics approaching those required. Therefore, we must invent a suitable delay line. Our design philosophy allows us to do this if our invention amounts only to a unique assembly of practical and available subsystems and components. No substantial reliance on product development is allowed.

In our earlier treatment of the optical intercept simulator, we were obliged to devise a scheme for generating a moving target suitable for testing laser tracking systems. It would appear that this same device can be adapted to serve as just the sort of delay line required. The general scheme was illustrated in Figure 5.

4.0 RELATIVE MOTION SYSTEM REQUIREMENTS

4.1 Trajectory Parameters and Simulation Regimes

It is desirable that the intercept simulator have the most general capability possible, as we have indicated before. The targets against which missiles may be deployed fall into three general classes: aircraft, Space Mission No. 1, and Space Mission No. 2. Insofar as possible, the simulator should be designed to duplicate the missile/target relative motion for each of these three classes of intercept.

At least at the moment of minimum separation, any intercept may be defined by the two parameters miss distance (R_o) and relative velocity (V_R). The possible combinations of these two differ, however, for the three classes of intercept. These several domains may be delimited approximately as follows:

Air-to-Air

R_o = zero to 200 feet; 10 feet typical

V_R = 200 to 6000 fps; 1000 fps typical

Space Mission No. 2

R_o = 25 to 150 feet, 100 feet typical

V_R = 12,000 to 43,000 fps; 25,000 fps typical

Space Mission No. 1

R_o = 1000 to 6000 feet; 3000 feet typical

V_R = 18,000 to 40,000 fps; 25,000 fps typical

These parametric domains are displayed graphically in Figure 12.

4.2 The Rectilinear Approximation

The apparatus described in this report is designed to simulate a rectilinear relative intercept--that is, one in which neither missile nor target undergoes acceleration. Of course, in general, this is not true of any intercept. Nevertheless, it is a reasonable basis of design for two reasons. First, the basic purpose of the intercept simulation is to test the ability of a scoring system or related device to perceive and record an object moving at intercept velocities. For such a test, considering the infinite number of possible relative trajectories, a rectilinear path is as useful and demanding as any other. Second, for many practical cases, the rectilinear trajectory is a good approximation anyway. We can prove this rather simply.

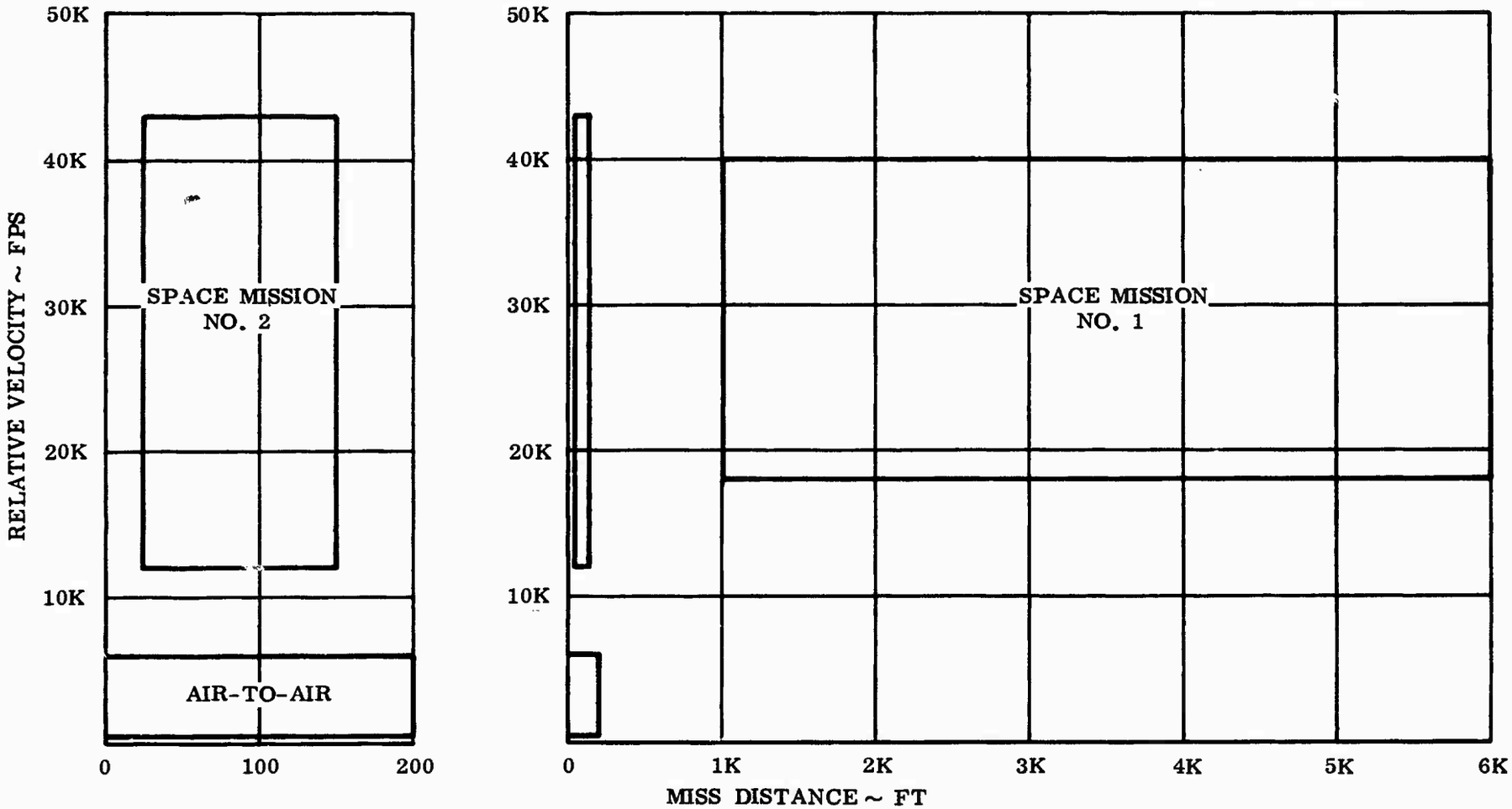

Figure 12. Intercept Parametric Domains

The kinematics of a maneuvering relative intercept are diagrammed in Figure 13 for the three cases of head-on attack, flank attack, and tail chase. It is assumed here, first of all, that the target is non-maneuvering, all acceleration being done by the attacking missile. It is also assumed that the speed of the missile is constant and that maneuver is limited to constant lateral acceleration only. None of these assumptions is rigorously true, but they are sufficiently close to the truth to serve as the basis of our argument.

Consideration of the vector diagrams of Figure 13 shows that all departure from a rectilinear intercept is due to the missile acceleration vector A_m. In general, the direction of the vector A_m, for a relative velocity to the right, will always be in the lower right hand quadrant. This acceleration vector may be resolved into components in the $\hat{r}$ and $\hat{t}$ directions. The effect of the $\hat{t}$ component is to increase the velocity along the path. The effect of the $\hat{r}$ component is to rotate the vector V_R and generate a curvilinear relative trajectory instead of a rectilinear one.

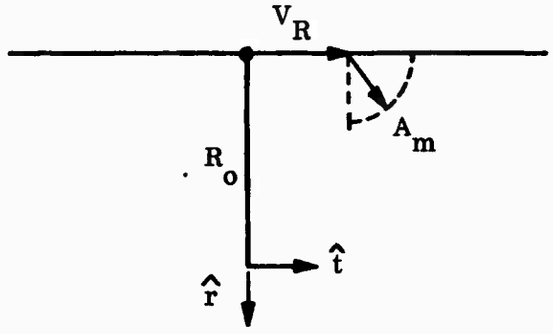

We wish now to reach some conclusion regarding the domain over which rectilinear approximation is adequate. To a first approximation, we may take A_m to be constant and entirely in the $\hat{r}$ direction. This assumption is the most conservative. The resulting trajectory is then a parabola with vertex at the miss-distance point. The displacement from the rectilinear path is given by $\Delta = 1/2\ A_m t^2$ where t here is time.

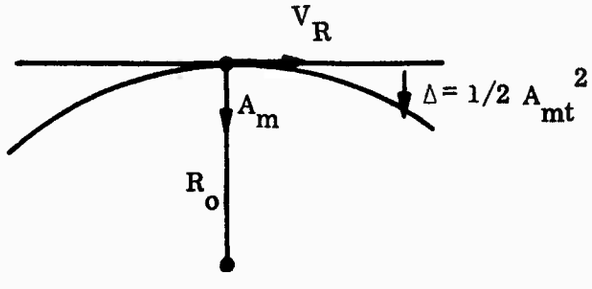

Now, to establish a domain of adequacy, we must first set some criterion of adequacy. We will adopt here the same criterion used in later sections; that the separation between intended and actual trajectories not exceed one-half the characteristic dimension of the vehicle, which we take to be 10 feet. Thus,

$$\frac{1}{2} A_m t^2 \leq 5$$

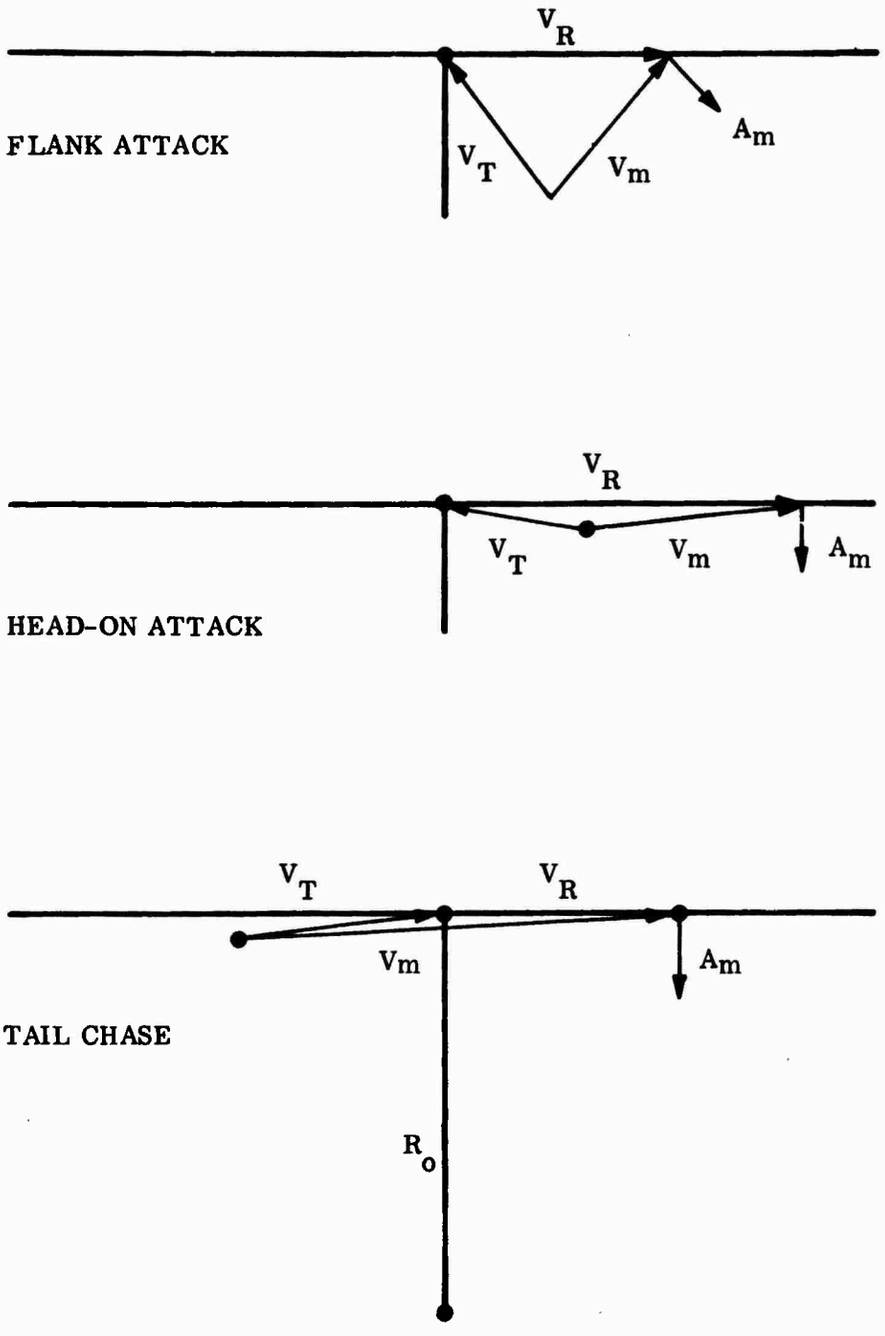

Figure 13. Kinematics of Maneuvering Relative Intercept

Now if we take R_{mx} as the maximum range to be simulated, R_o as the miss distance, and V_R as the relative velocity, then from simple trigonometry

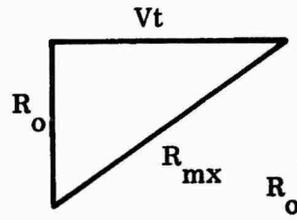

$$R_o^2 = R_{mx}^2 - V^2t^2$$

But from the previous result $t^2 \leq 10/A_m$. Hence,

$$R_o^2 \geq R_{mx}^2 - \left(\frac{10}{A_m}\right) V_R^2$$

On a plot of V_R versus R_o, this equation represents a family of elliptical quadrants. The intercept with the R_o axis depends on the maximum range required. That with the V_R axis depends on the lateral acceleration of the missile. All combinations of R_o and V_R above the ellipse can be satisfactorily simulated according to the criterion of a 5-foot maximum error.

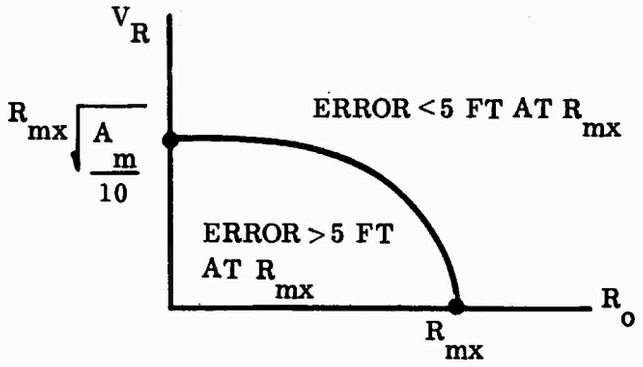

As an example of a maneuvering missile, we may take the Sidewinder. The average lateral acceleration of a Sidewinder in the course of an intercept up to 40,000 feet is about 9g. Using this value for A_m, the domain boundary equation may be written

$$R_o^2 \geq R_m^2 - \left(\frac{10}{9 \times 32.2}\right) V_R^2$$

$$R_o^2 \geq R_m^2 - 0.0345\, V_R^2$$

The domain boundaries for various values of R_{mx} have been plotted in Figure 14. We may conclude from these displays that a rectilinear intercept is a good approximation for all anti-satellite and anti-ICBM intercepts for ranges up to 1000 feet, but that

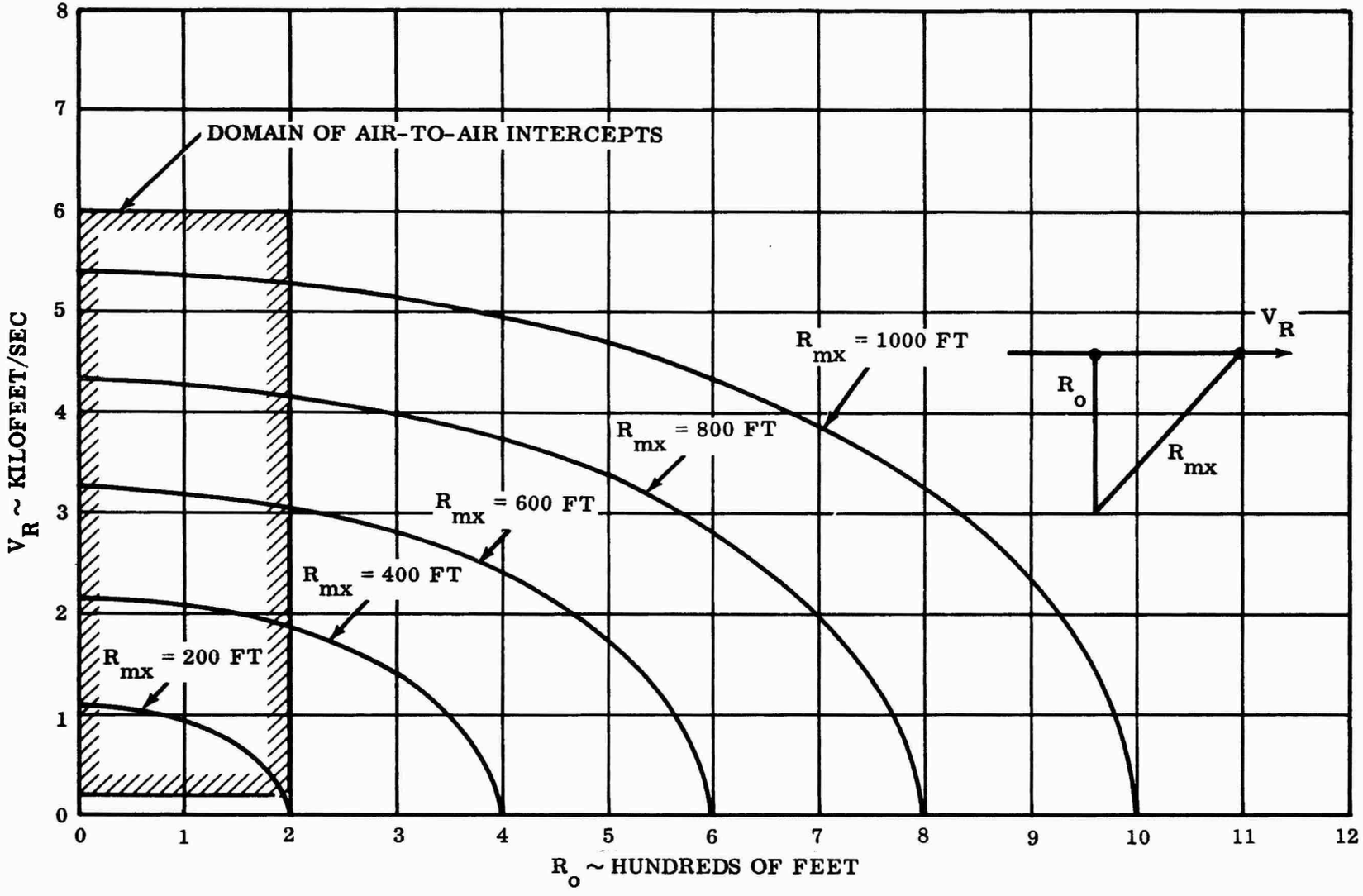

Figure 14. Domains of Validity, Rectilinear Approximation to Maneuvering Intercept for Sidewinder Missile

satisfactory simulation for the slower air-to-air intercepts will be limited to perhaps 200 feet. These figures are, of course, conservative.

4.3 Parametric Functions of a Rectilinear Intercept

Having established that the rectilinear case is an adequate approximation to most intercepts of interest, and having shown that a rotating mirror is an appropriate technique for effecting the intercept simulation, we next must examine the angular functions associated with the rectilinear case and consider how performance of the motor driving the mirror may limit the (R_o, V_R) domain which it is possible to simulate.

The significant angular functions are the velocity $\dot{\theta}$, acceleration $\ddot{\theta}$, and jerk $\dddot{\theta}$. These functions are derived by straightforward differentiation. The formulas are displayed below.

Let

$$\Omega = \frac{V_R}{R_o}$$

Then

$$\theta = \tan^{-1}(\Omega t)$$

and

$$\dot{\theta} = \frac{\Omega}{1 + \Omega^2 t^2}$$

$$\ddot{\theta} = \frac{-2\Omega^3 t}{(1 + \Omega^2 t^2)^2}$$

$$\dddot{\theta} = \frac{6\Omega^5 t^2 - 2\Omega^3}{(1 + \Omega^2 t^2)^3}$$

For generality of discussion, it is more convenient to work in terms of the dimensionless variables $\dot{\theta}/\Omega$, $\ddot{\theta}/\Omega^2$, $\dddot{\theta}/\Omega^3$. These dimensionless functions are plotted in Figures 15 through 17.

The limitation on motor performance can be expressed in terms of maximum angular acceleration. Setting the jerk equal to zero, solving for Ωt, and substituting in the expression for angular acceleration, it may be shown that

$$\ddot{\theta}_{max} = 0.65\,\Omega^2$$

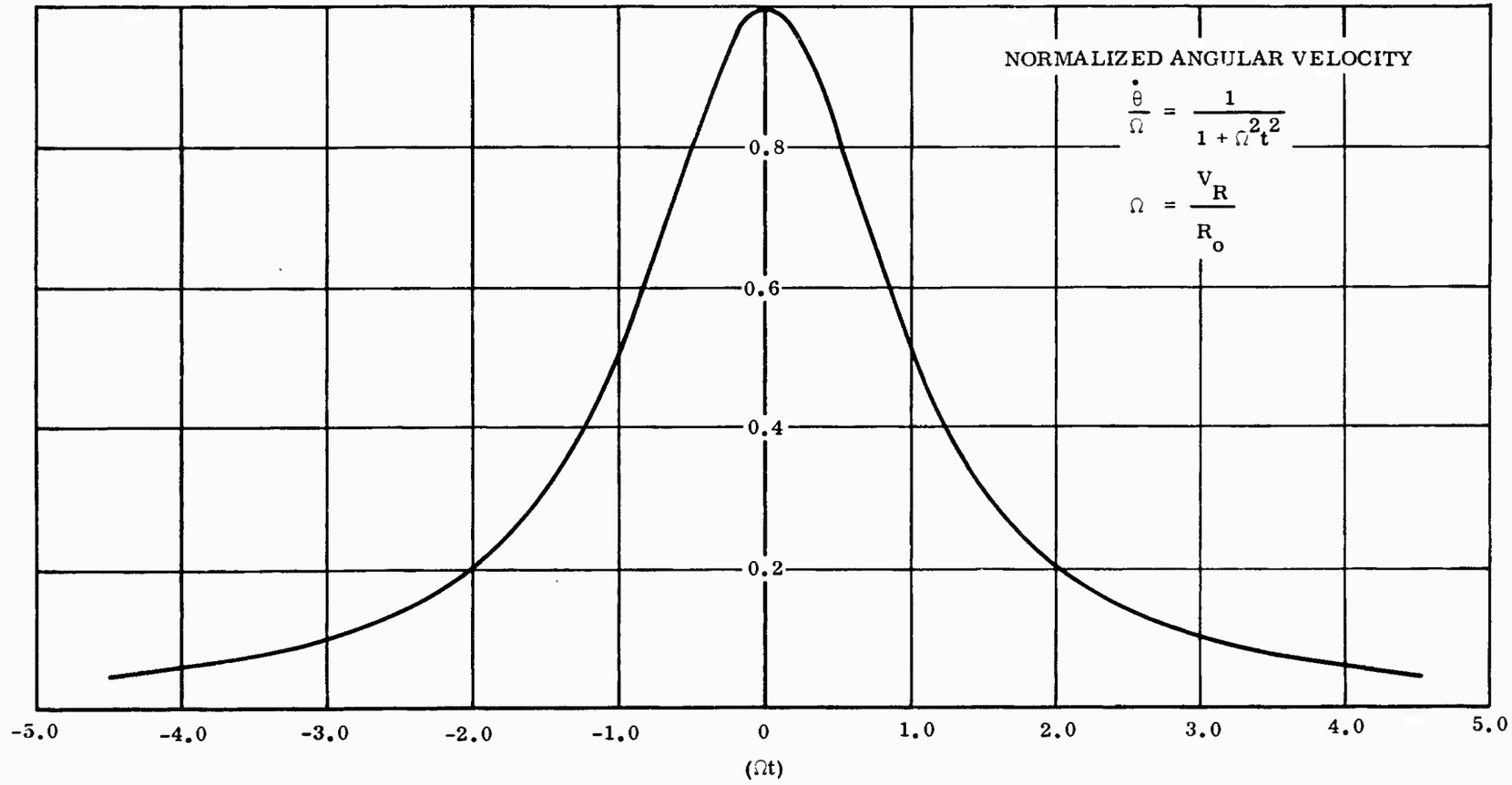

Figure 15. Normalized Angular Velocity for Rectilinear Intercept

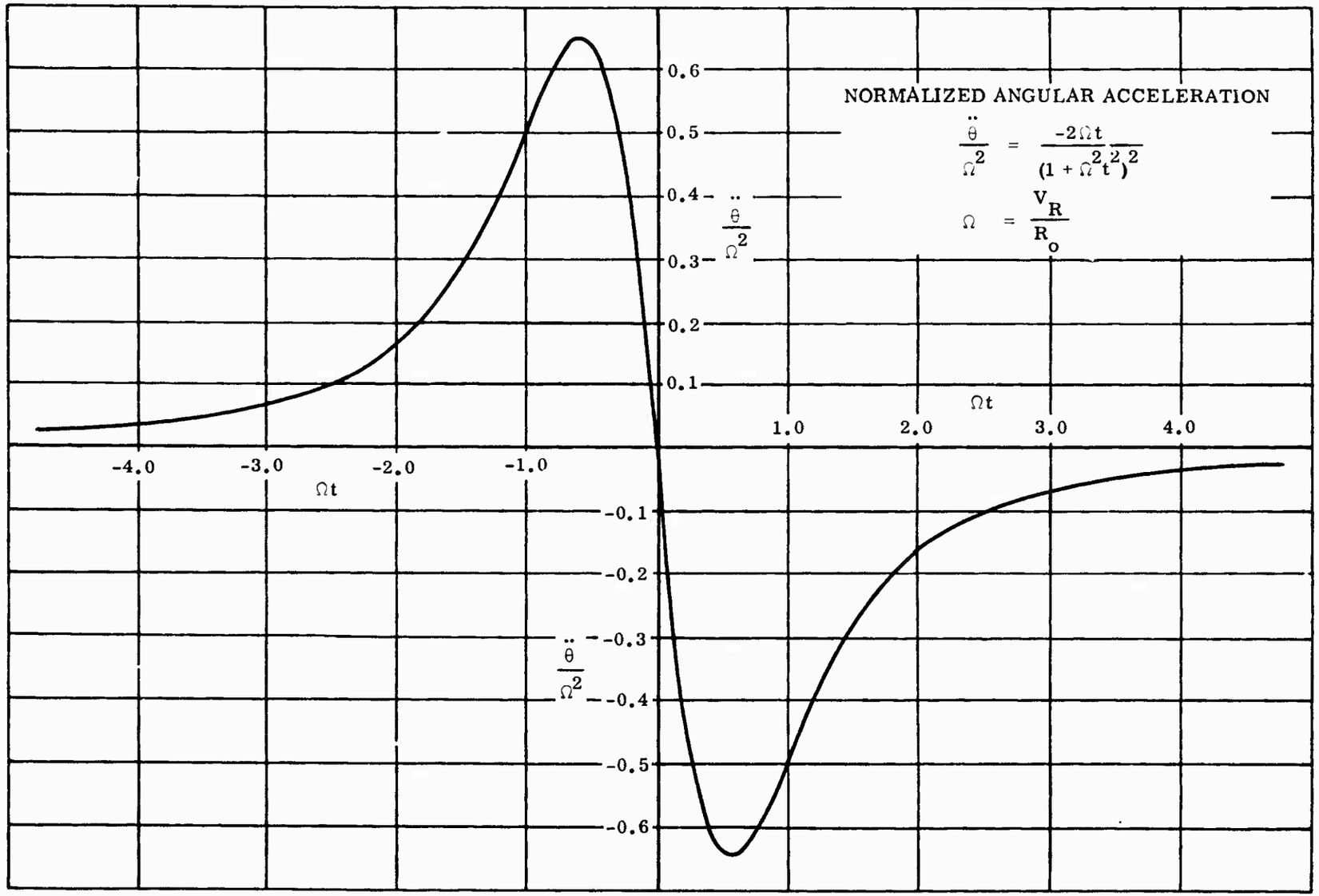

Figure 16. Normalized Angular Acceleration for Rectilinear Intercept

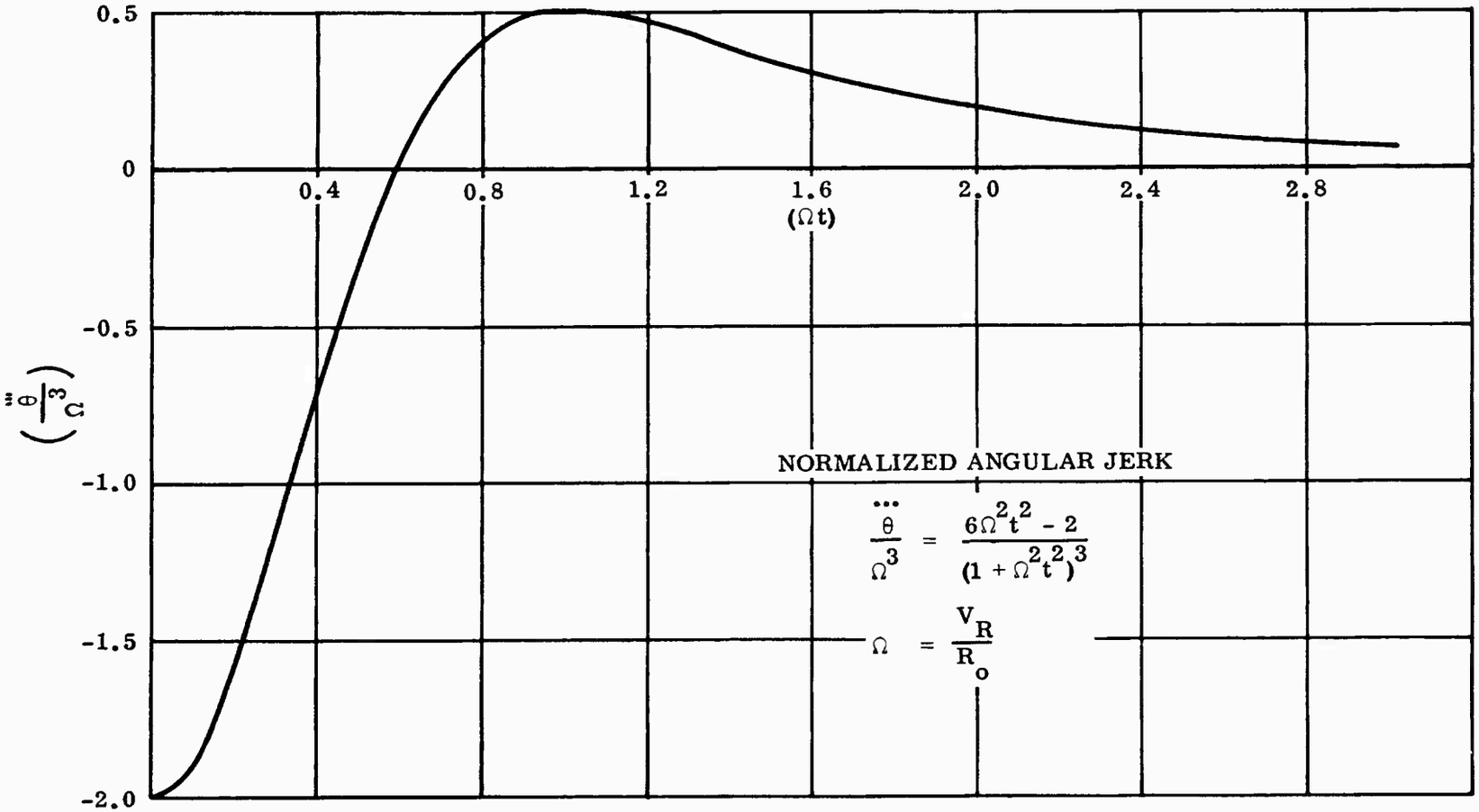

Figure 17. Normalized Angular Jerk for Rectilinear Intercept

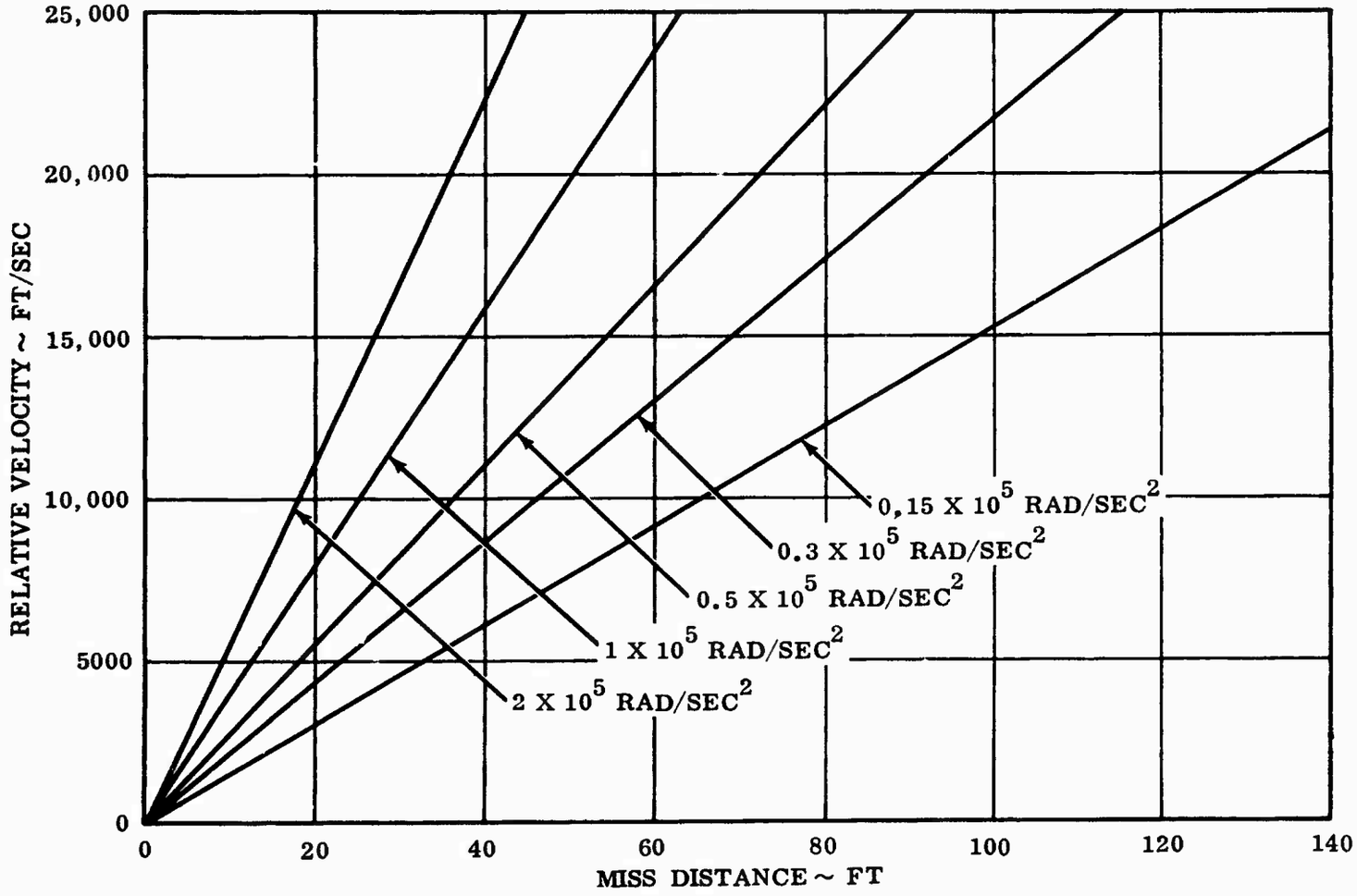

Figure 18. Maximum Angular Acceleration

Hence, on an (R_0, V_R) diagram, an angular acceleration limit corresponds to a straight line through the origin. This is illustrated in Figure 18.

4.4 Target Observable Requirements

A non-cooperative scoring system senses some observable characteristics of the vehicle to be scored while a cooperative system detects some signal which has been artificially generated for the purpose of scoring. The equipment for generating the artificial signal is usually considered to be part of the scoring system and would be supplied with it. There are a large number of physical principles upon which cooperative scoring systems could depend, while the number of observables for non-cooperative systems is restricted. The observable characteristic for non-cooperative scorers must be generated by the relative motion simulator and mechanized so that it supplies a true representation to the scorer. One result of the scoring system survey has been to identify two observable characteristics upon which all practical non-cooperative scorers depend: reflected light (visible or infrared), and reflected radar signals.

For each of the non-cooperative scorer classes (radar and visible or infrared), the signal strength at the scorer will depend on the particular vehicle, plus the time varying range and aspect. The time varying signal from a vehicle is called signature.

The relative motion simulator will be required to produce optical, infrared, and radar signatures of various vehicles, more or less accurately, depending on the mode of operation to the particular scorer being tested. The present purpose is to specify the limits of operation of the signal producing apparatus in the motion simulator so that it will be capable of producing specific signatures. These limits are derived as follows:

4.4.1 Optical.

4.4.1.1 Image Size. Image size is properly described in terms of angular subtense and depends on the physical size of the simulated target and its distance from the scorer. The maximum demand upon the simulator will occur when the vehicle is at the miss distance. For the class of air-to-air targets, we may take the minimum miss distance R_0 to be 5 feet. For Space Mission No. 2, we may take it to be 50 feet. Maximum dimensions of some present air-to-air missiles are as follows:

Falcon:	7 feet
Genie:	9 feet
Sidewinder:	9 feet
Sparrow:	12 feet

It will be reasonable to take 10 feet as typical of this class of vehicle. At a miss distance of 5 feet, the image will subtend 90 degrees. This may be taken as the maximum practical requirement on image size.

Satellites vary much more in size than do air-to-air missiles. Among the largest are the following:

Agena: 16 feet

Pegasus: 100 feet

At an assumed miss distance of 50 feet, the maximum demand on image size is again 90 degrees, in this case for the Pegasus. Satellites designed to be inconspicuous will subtend a considerably smaller angle.

An angular subtense of 90 degrees may, therefore, reasonably be taken to be the maximum simulation requirement.

4.4.1.2 Image Brightness. The brightness of self-luminous targets will depend on their temperature. The brightness of non-self-luminous targets will depend on the local illumination at the vehicle and its reflective properties. Self-luminous targets are discussed in Paragraph 4.4.2, Infrared.

The most significant type of target illumination is sunlight. At high altitudes the value of sunlight may be taken as 14 lumens/cm^2. If a target is a diffuse reflector, the greatest brightness it can exhibit is $14/\pi = 4.5$ stilb, and this may be taken as an upper limit for this type of reflector. Perfect plane specular surfaces can in principle exhibit a brightness equal to that of the sun, 200,000 stilb, but for numerous reasons, this ideal case need not be considered. Practical surfaces, however, which may be curved and intermediate between specular and diffuse, can produce a glint which is of sufficient duration to be observed in a scanning system. The extent of this glint can be estimated from observations of satellite scintillation and measurements of optical cross section for complex bodies. Complex satellites are frequently observed to scintillate as much as 5 magnitudes or 20 db peak to peak. If we take this as a measure of the possible brightness variation, then we may say that the maximum surface brightness which must be simulated is 20 db above a perfect diffusor, or 450 stilb.

4.4.2 Infrared.

4.4.2.1 Radiance. The surface temperature of satellites may be expected to range from 200°K to 400°K. The radiance of such satellites will be typically that of a grey body at those temperatures, if sunlight is absent. In daylight, the infrared appearance of a target vehicle is due primarily to reflected sunlight. The apparent radiance in any spectral window $\Delta\lambda$ is $(I_{\Delta\lambda})/\varphi$, where $I_{\Delta\lambda}$ is the solar irradiance in that window and φ is the effective solid angle of reflection. As in the case of visible reflection, we may take φ to vary from π to $\pi/100$. Reflectivity with sufficient accuracy for the present purpose may be taken as unity for aluminum vehicles.

4.4.3 Radar. Non-cooperative radar scorers illuminate their target with a transmitted signal and receive a reflected signal for scoring. The reflected signal is distinguished by a frequency and a signal strength. The frequency of the reflected signal is determined by the transmitted frequency and by the relative velocity of the target. The reflected signal strength is fixed by the transmitted power, radar cross section of the target, and by range. Cross section and frequency requirements are summarized below.

4.4.3.1 Radar Cross Section. Space targets have been identified which have radar cross sections of 0.003 meter^2 to more than 100 meters^2. Some of these targets can have ±40 db scintillation due to changing aspect during an intercept.

4.4.3.2 Frequency Bands. Radar frequencies of interest extend from L-band to K-band. Immediate requirements extend only to S-band, however.

5.0 FACILITY CAPABILITY

5.1 Introduction

It was shown in an earlier section of this report that a rectilinear intercept is adequately representative of all intercepts to which real scorers might be exposed. Therefore, a simulator designed to test scoring systems need simulate only a rectilinear intercept to provide an adequate test. The simulator system described in this report has been designed to do just that. It remains to establish the domain of miss-distance and relative velocity over which the performance of the simulator may be considered adequate.

We begin by considering the case of perfect simulation.

5.2 Mirror Driving System

The central element in the proposed simulator system is a 45-degree mirror driven in such a way as to duplicate the intercept azimuth (θ) as a function of time. In this section, we consider how this mechanical requirement can be met.

5.2.1 Mirror Moment of Inertia. Assume an aluminum mirror of the following dimensions:

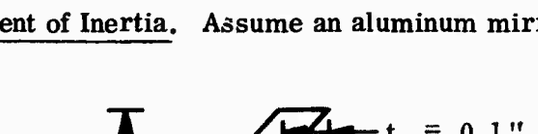

The density of aluminum is:

$$\rho = 0.00404 \ \frac{\text{oz-sec}^2}{\text{in}^4}$$

The polar moment of inertia of the mirror is:

$$J = \frac{1}{2} Mr^2 = \frac{1}{2} (\pi r^2 \rho t) r^2 = \frac{1}{2} (\pi)(1)(0.00404)(0.1)(1) = 0.00064 \text{ oz-in-sec}^2$$

Neglecting the effect of the shaft, $J = 0.001$ oz-in-sec^2

5.2.2 Motor Driving Voltage. The driving voltage function needed to produce the displacement $\theta = \tan^{-1} \Omega t$ can be deduced from the basic motor equations:

$$E = k_e \dot{\theta} + \left(\frac{r_m}{k_T}\right) T + \left(\frac{L}{k_T}\right) \dot{T}$$

$$T = T_F + \left(\frac{1}{r_d}\right) \dot{\theta} + J \ddot{\theta}$$

where

E = Terminal voltage, volts

T = Total torque, oz-in

T_f = Friction torque, oz-in

J = Total polar moment of inertia, in-oz-sec^2

L = Motor inductance, henrys

k_e = Back voltage constant, volts/(rad/sec)

k_t = Torque constant, oz-in/ampere

r_m = Total machine resistance, ohms

r_d = Damping torque constant, (rad/sec)/oz-in

The numerical values of these significant parameters for the Incredyne are as follows:

T_f = 4.5 oz-in

J = 0.003 oz-in-sec^2 (motor) + 0.001 (mirror) = 0.004 oz-in-sec^2

L = 200 x 10^{-6} henrys

k_e = 0.091 volts/(rad/sec)

k_t = 13.0 oz-in/ampere

r_m = 0.74 ohm

r_d = 140 (rad/sec)/oz-in

Combining the two basic motor equations, we may write:

$$E = \left(k_e + \frac{r_m}{k_T r_d}\right)\dot{\theta} + \left(\frac{r_m}{k_T}\ J + \frac{L}{k_T r_d}\right)\ddot{\theta} + \left(\frac{LJ}{k_T}\right)\dddot{\theta} + \left(\frac{r_m}{k_T}\right)\ T_F$$

Substituting numerical values yields:

$$E = (0.091)\,\dot{\theta} + (2.28 \times 10^{-4})\,\ddot{\theta} + (6.15 \times 10^{-8})\ \dddot{\theta} + 0.26$$

It is useful to put this equation into a form using the dimensionless angular variables $\left(\frac{\dot{\theta}}{\Omega}\right), \left(\frac{\ddot{\theta}}{\Omega^2}\right), \left(\frac{\dddot{\theta}}{\Omega^3}\right)$. Taking $\Omega = 500$ rad/sec,

$$E = 45.5\left(\frac{\dot{\theta}}{\Omega}\right) + 57.0\left(\frac{\ddot{\theta}}{\Omega^2}\right) + 7.7\left(\frac{\dddot{\theta}}{\Omega^3}\right) + 0.26$$

This driving voltage is displayed in Figure 19.

5.2.3 Motor Current. The current drawn by the motor may be calculated from:

$$I_m = \frac{T}{k_T} = \frac{T_F}{k_T} + \left(\frac{1}{r_d k_T}\right)\dot{\theta} + \left(\frac{J}{k_T}\right)\ddot{\theta}$$

Substituting numerical values and converting to dimensionless angular functions for $\Omega = 500$ rad/sec yields

$$I_m = 0.275\left(\frac{\dot{\theta}}{\Omega}\right) + 77.0\left(\frac{\ddot{\theta}}{\Omega^2}\right) + 0.35$$

A plot of this function is displayed in Figure 20.

5.3 Limitations on Motor Performance

The basic limitation on motor performance is the peak current which can be accepted without thermal damage. The manufacturer declares that 50 amperes is a practical maximum for short duty cycle operation, although this figure has been exceeded in special tests. On the basis of this recommendation, we have adopted 50 amperes as a design maximum.

We note from the preceeding calculation that $I_m = \left(\frac{J}{k_T}\right)\ddot{\theta}$ approximately. Therefore, the limitation on motor current is also effectively a limitation on acceleration. If current is limited to 50 amperes, acceleration is limited to 162,000 rad/sec^2. The example illustrated in Figure 20 indicates that if a rectilinear intercept is to be duplicated faithfully, a practical limit to the range of simulation is the case $\Omega = 500$ rad/sec. We next wish to examine the limitations on performance when simulation is allowed to be less than faithful.

5.4 Basic Motor Deflection Requirement

Figure 21 illustrates the angular path of a target during a rectilinear intercept as a function of the parameter Ωt. On this dimensionless plot, slope $= \left(\frac{\dot{\theta}}{\Omega}\right)$ and rate of

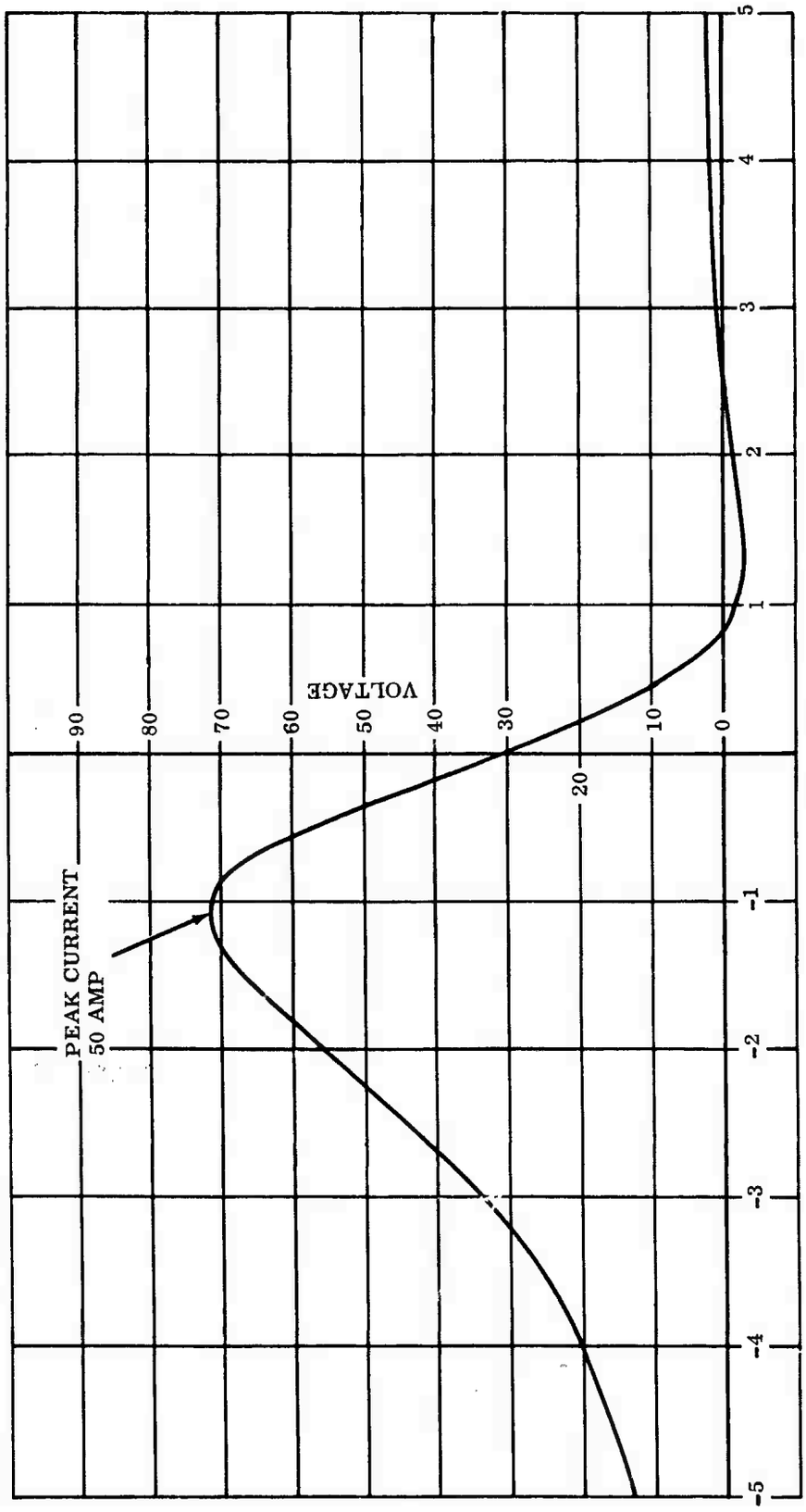

Figure 19. Voltage Function for PMI Incredyne at $\Omega = 500$ r/s, $\ddot{\theta}_{max} = 162,000$ r/s^2

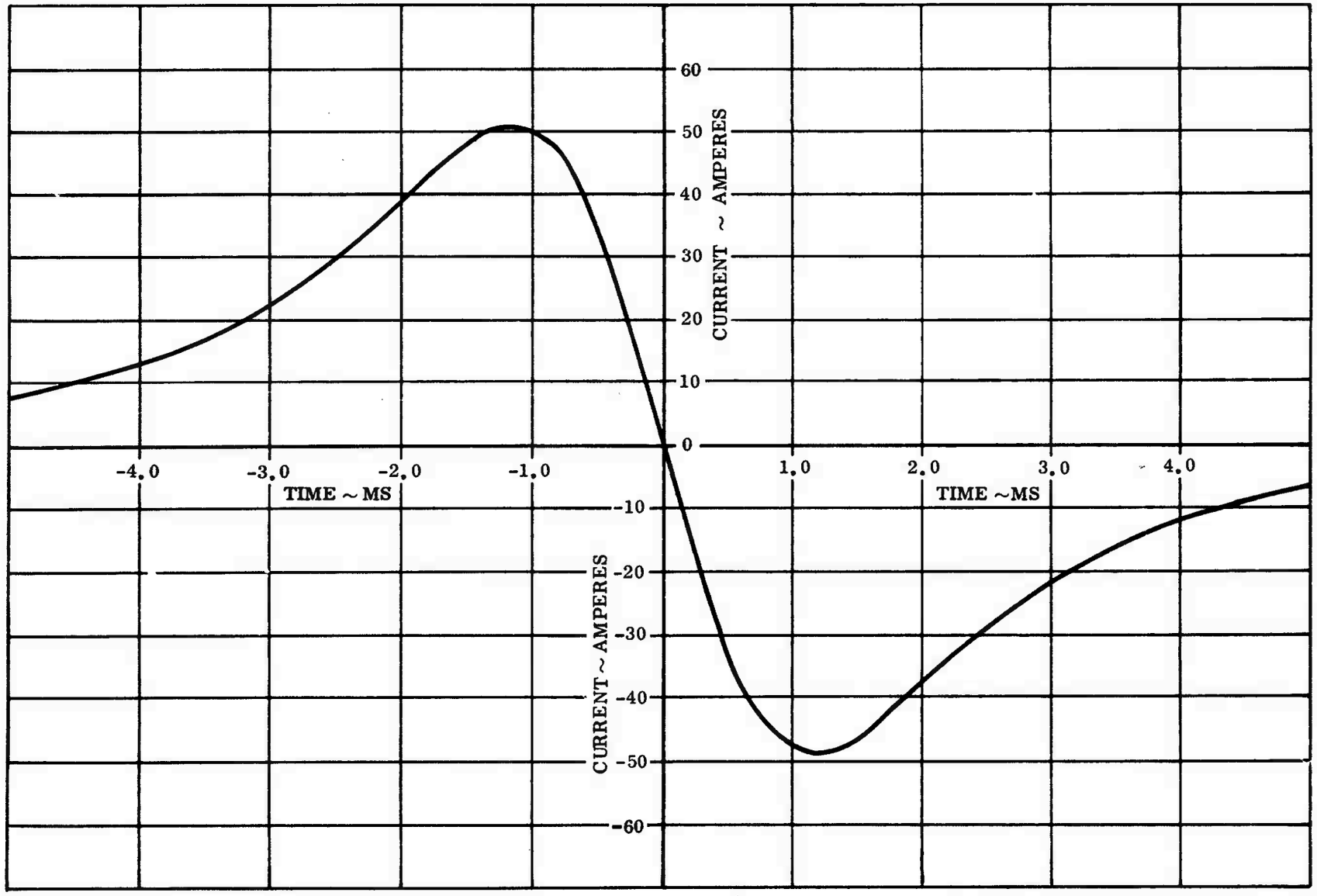

Figure 20. Current Drawn by PMI Incredyne at $\Omega = 500$ r/s, $\ddot{\theta}_{max} = 162,000$ r/s^2

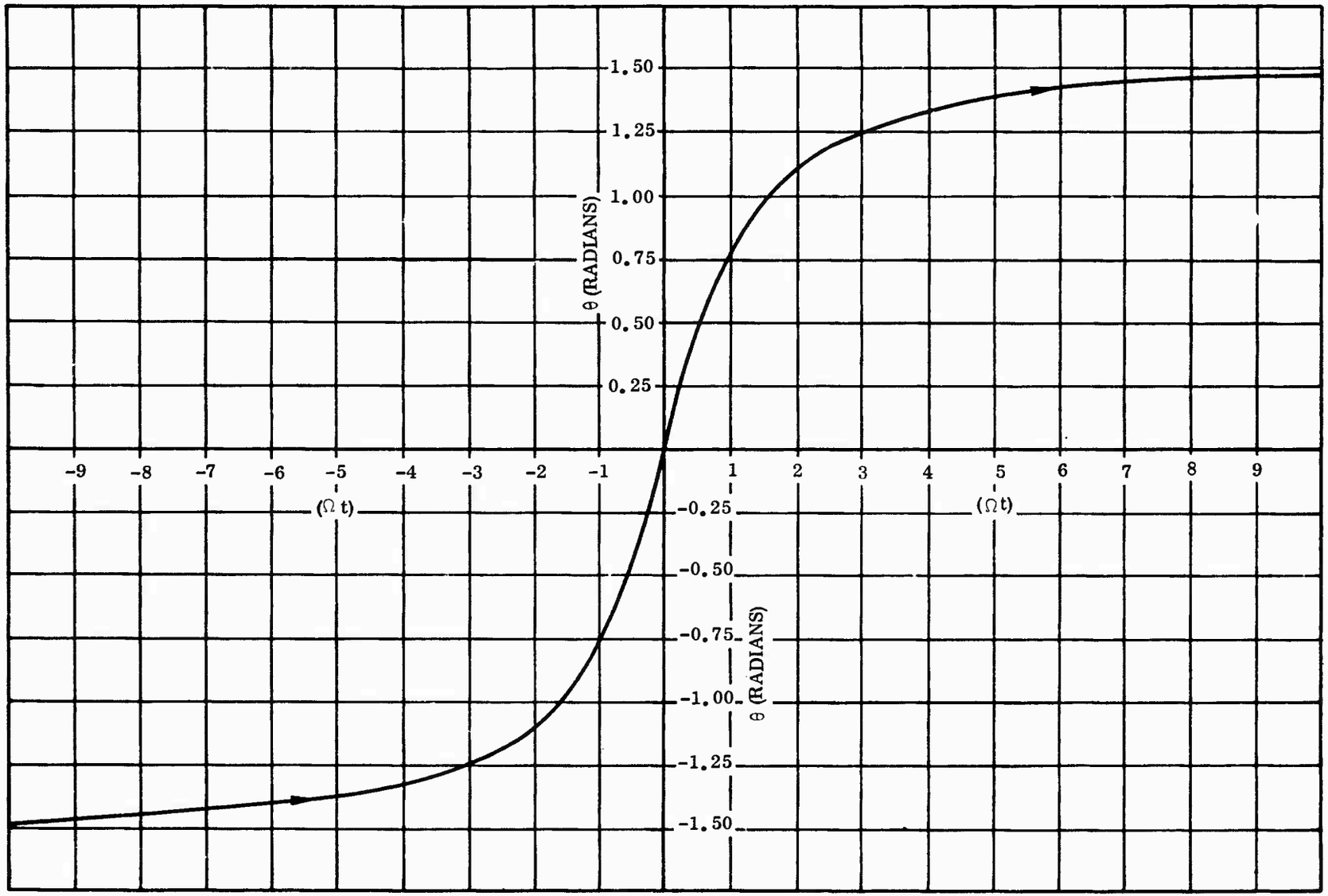

Figure 21. Angular Path in a Rectilinear Intercept

change of slope $= \left(\frac{\ddot{\theta}}{\Omega^2}\right)$. As plotted, it is essentially an arctangent curve, since $\tan\theta = \Omega t$. The object of the motor control system is to follow this angular path within some acceptable envelope of error.

It was just shown that this angular path can be followed exactly, without exceeding the acceleration limits of the motor, for intercepts in which $\Omega \leq 500$ rad/sec. By "exactly" we mean that the envelope of error will be determined only by accidental variations in the applied voltage or the motor constants and not by any basic limitation in the motor performance. The significance of these sources of error has not been treated in this study because, in the case of the motor, the information is not available and must be obtained by experiment and, in the case of the voltage, because the design of the control system has not yet been sufficiently detailed to allow a solution.

In this section we consider what sort of error envelope may be deemed acceptable and what implications such an envelope may have for the motor control problem. In particular, we examine two questions:

1. Is it possible to use simpler driving functions and still maintain adequate simulation; and

2. Is it possible to achieve effective simulation for cases of $\Omega > 500$ without exceeding accelerations limitations by following an angular path which, although imperfect, is still within an acceptable error envelope?

5.5 Criterion of Acceptable Error

The first requirement is to decide what constitutes adequate simulation. The criterion adopted here is that the simulated position on the trajectory should differ from the intended position by no more than half the vehicle length.

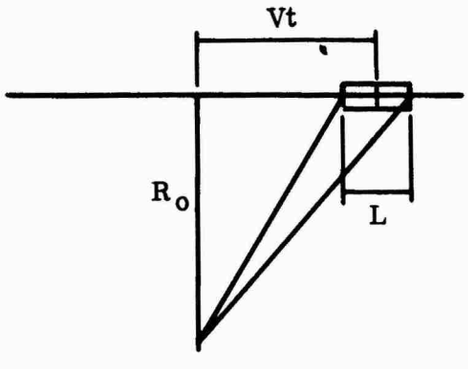

Thus $\Delta Vt = \pm \frac{L}{2}$ and $\Delta(\Omega t) = \pm \frac{1}{2} \frac{L}{R_o}$. The acceptable error envelope, therefore, depends on miss distance: the smaller the miss distance, the less accurate need the simulation be--which is all to the good.

Elsewhere in this study, we have adopted as a typical target dimension L = 10 feet. We assume the same here. We consider first what would appear to be the worst case: R_o = 5 feet. For $R_o = 5$, $\frac{L}{2R_o} = \Delta(\Omega t) = 1$. The error envelope for this case has been plotted in Figure 22. We see that this represents a very loose simulation requirement indeed. For the case of $\theta = 0$ intended, it would seem that $\Delta\theta$ could be as much as 45 degrees. Actually, we must impose a rather more severe criterion. If both branches of the intercept are to be simulated to an equal standard, and if the limitation on angular path is basically one of acceleration, then symmetry demands that the angular path pass through the point ($\theta = 0$, $\Omega t = 0$). Subject to this constraint, then, the angular path may wander anywhere within the envelope and still be satisfactory.

5.6 Possibility of Voltage Pulse Motor Drive

The next point to consider is the manner in which the motor may be driven. To follow the proper angular path exactly, it is necessary to drive with a continuously varying voltage function, as has been shown earlier. An easier method of driving would be with voltage pulses. We now examine this possibility.

The differential equation of motion for the Incredyne has been derived earlier. In its general form, it may be written using dimensionless variables

$$E = a + b\left(\frac{\dot{\theta}}{\Omega}\right) + c\left(\frac{\ddot{\theta}}{\Omega^2}\right) + d\left(\frac{\dddot{\theta}}{\Omega^3}\right)$$

where E is the applied terminal voltage. When we consider treating pulses, we deal with integrals. Thus, we write

$$\int (E-a)\, d(\Omega t) = b\int\left(\frac{\dot{\theta}}{\Omega}\right) d(\Omega t) + c\int\left(\frac{\ddot{\theta}}{\Omega^2}\right) d(\Omega t) + d\int\left(\frac{\dddot{\theta}}{\Omega^3}\right) d(\Omega t)$$

Now let $A_E = \int (E-a)\, d(\Omega t)$ be the area under a voltage pulse,

$A_A = \int\left(\frac{\ddot{\theta}}{\Omega^2}\right) d(\Omega t)$ be the area under an acceleration pulse, and

$A_V = \int\left(\frac{\dot{\theta}}{\Omega}\right) d(\Omega t)$ be the area under the velocity curve in the interval $d(\Omega t)$.

We note also that over a pulse $\int \frac{\dddot{\theta}}{\Omega^3}\, d(\Omega t) = 0$. Hence, we may write

$$A_E \doteq bA_V + cA_A$$

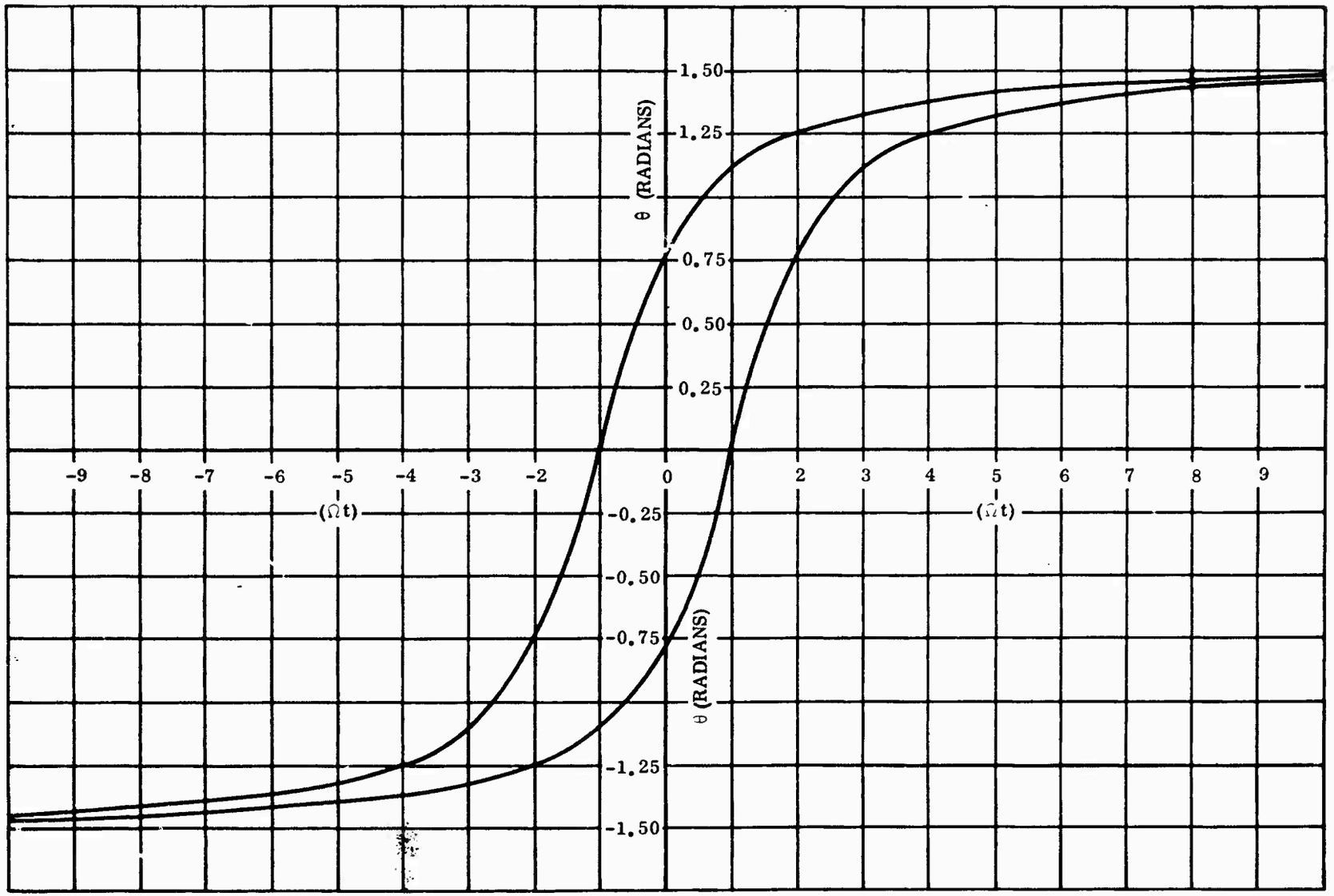

Figure 22. Allowable Angular Displacement Error Envelope for $L/2R_o = 1$

or

$$A_A = \frac{1}{c} A_E - \frac{b}{c} A_V$$

Now

$$A_V = \int \frac{\dot{\theta}}{\Omega} \, d(\Omega t) = \left(\Sigma A_A + \frac{A_A}{2} \right) d(\Omega t)$$

where ΣA_A represents the sum of all previous pulses A_A.

Thus

$$A_A = \frac{1}{c} A_E - \frac{b}{c} \left(\Sigma A_A + \frac{A_A}{2} \right) d\,\Omega t$$

or

$$A_A = A_E \left(\frac{2}{2c + b\, d(\Omega t)} \right) - \left(\frac{2b\, d(\Omega t)}{2c + b\, d(\Omega t)} \right) \Sigma A_A$$

Hence, a train of short voltage pulses may be considered equivalent to a train of acceleration pulses. If the voltage pulses are of constant amplitude, however, the resulting train of acceleration pulses is of steadily diminishing amplitude. But this need not concern us here. We only need to show that driving with a train of voltage pulses is equivalent to driving with a train of acceleration pulses. Put another way, if we analyze the problem of driving the motor in terms of acceleration pulses, we are assured these can be realized in the form of voltage pulses. Next we consider how to develop a train of acceleration pulses which will generate the required angular path.

5.7 Development of Pulse Driving Function

The relation between acceleration pulses and angular displacement is mathematically identical to the relation between load and deflection in a beam. Therefore, in seeking simple and conveniently realizable motor driving functions, we may take advantage of the large body of technique invented to solve analogous problems in structural mechanics. In the present case, it will be convenient to use the moment-area method.

Consider again the function $\theta(\Omega t)$. If we intend to simulate the central 2000 feet of an intercept from a miss distance of only 5 feet, we must work from $\Omega t = -200$ to $\Omega t = +200$. The problem, therefore, becomes one of devising a sequence of acceleration pulses which will cause the angular path to enter the error envelope at $\Omega t = -200$, pass through the origin, and leave the error envelope beyond $\Omega t = +200$. As time progresses from $\Omega t = -200$ to zero, we may imagine pulses of acceleration to be applied at intervals. The moment-area theorems applied to this problem may be stated as follows:

1. The slope of the path $\left(\frac{\dot{\theta}}{\Omega} \right)$ at any point Ωt equals the sum of the areas under an acceleration diagram to the left of that point.

2. The deflection θ at any point Ωt equals the sum of the moments, taken about that point, of all areas under an acceleration diagram to the left of that point.

The application of these theorems is illustrated in Figure 23. Note that, for illustrative purposes, the acceleration curve consists of a sequence of rectangular pulses. Actually such pulses may not be physically realizable. This does not matter in the solution, however. What we need to work with are the areas under the pulse envelopes and the centroids of the pulses. The actual form of the pulse may be chosen to be anything convenient. The form chosen affects the peak current and the shape of the transition curve in the neighborhood of the pulse only.

Figures 24 through 26 illustrate a sequence of acceleration pulses and the resulting angular path computed for the case of R_o = 5 feet, R_{max} = 1000 feet. From Ωt = -200 to Ωt = -10, the pulses are calculated to generate an angular path which follows the proper arctangent curve. After Ωt = -10, the path selected is that requiring the least acceleration. Note that the last acceleration pulse has a value of 0.39. If this represents the area under a rectangular pulse whose duration is, say, $\Delta(\Omega t) = 2$, the peak acceleration is $\left(\frac{\ddot{\theta}}{\Omega^2}\right) = 0.195$. On the other hand, the peak acceleration for completely faithful simulation of this same intercept is 0.65. The peak current drawn by the motor is only 15 amperes instead of 50. Thus, by replacing strict simulation with approximate simulation, we have dramatically lessened the demand on the motor. A corollary to this is that by replacing strict simulation with approximate simulation we may be able to exceed the limitation $\Omega \leq 500$ by a considerable margin without exceeding the 50-ampere limit on motor current. We will examine that possibility next.

5.8 Enlargement of Operating Domain

The general angular path to follow for minimum acceleration is that shown schematically in Figure 27. The strongest acceleration pulse occurs at the point B, and is of a magnitude to change the slope of CB to the slope of BA. The magnitude of this required acceleration pulse is a function of the miss distance R_o, since $\Delta(\Omega t) = L/2R_o$. To calculate this maximum pulse, we need to know the coordinates of points A, B, and C.

The point A is found from the relation:

$$\frac{\theta_A}{(\Omega t)_A + \Delta} = \left(\frac{\dot{\theta}}{\Omega}\right)_A$$

where: $\Delta = \Delta(\Omega t) = \frac{L}{2R_o}$. Point B is found from a knowledge of point A and the relation:

$$\frac{\theta_B}{(\Omega t)_B - \Delta} = \left(\frac{\dot{\theta}}{\Omega}\right)_A$$

$$\theta_A = \left[\left(\frac{\ddot{\theta}}{\Omega^2}\right)_1 (\Delta \Omega t)_1 (\Omega t)_1 + \left(\frac{\ddot{\theta}}{\Omega^2}\right)_2 (\Delta \Omega t)_2 (\Omega t)_2 + \ldots \right]$$

θ_A = Σ (MOMENTS ABOUT A OF ACCELERATION AREAS TO LEFT OF A)

$$\left(\frac{\dot{\theta}}{\Omega}\right)_A = \left[\left(\frac{\ddot{\theta}}{\Omega^2}\right)_1 (\Delta \Omega t)_1 + \left(\frac{\ddot{\theta}}{\Omega^2}\right)_2 (\Delta \Omega t)_2 + \ldots \right]$$

$\left(\frac{\dot{\theta}}{\Omega}\right)_A$ = Σ (ACCELERATION AREAS TO LEFT OF A)

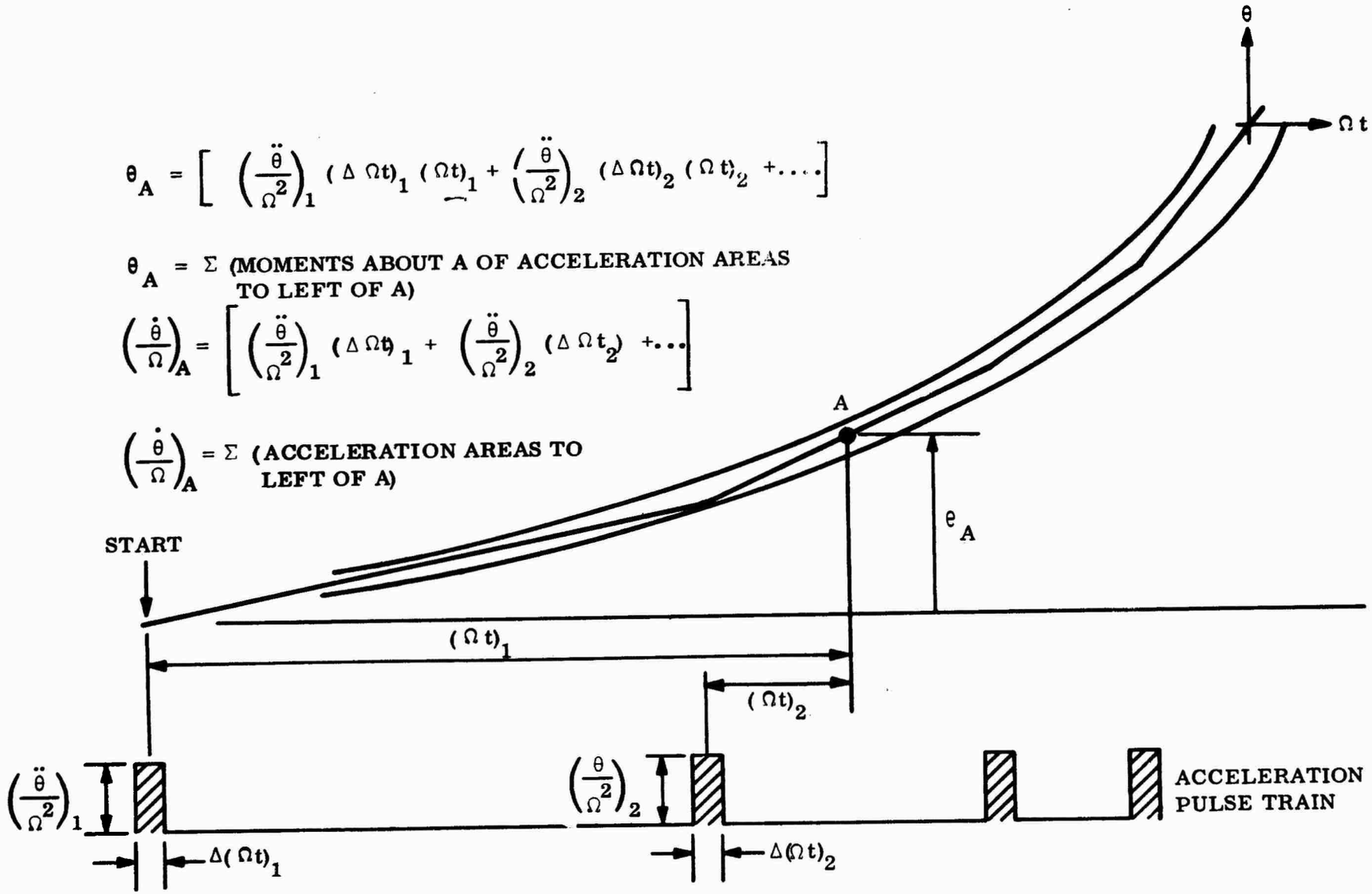

Figure 23. Application of Moment Area Method to Motor Deflection Computation

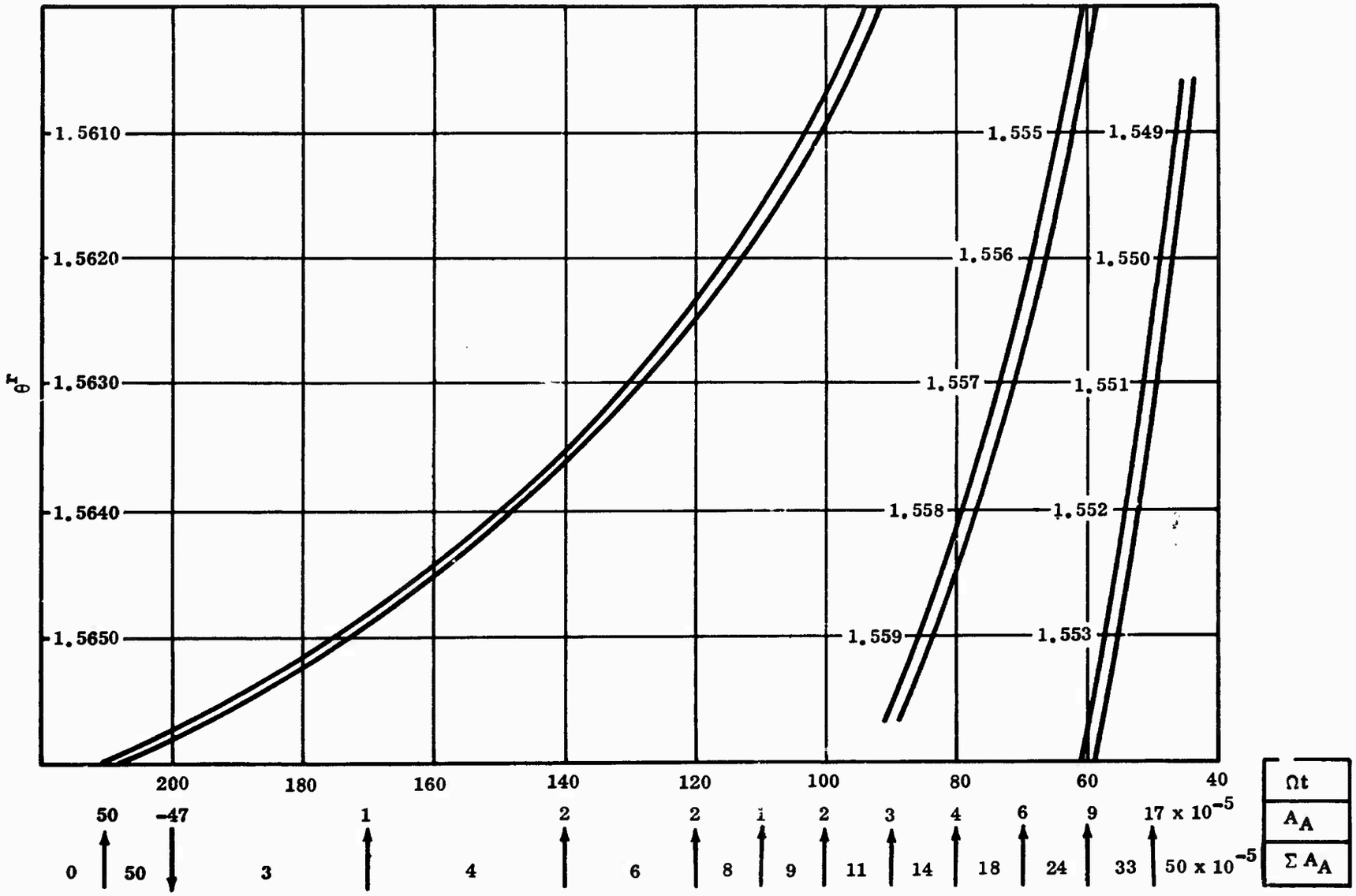

Figure 24. Error Envelope and Acceleration Pulse Sequence for R_o = 5 Feet, R_{mx} = 1000 Feet (Sheet 1)

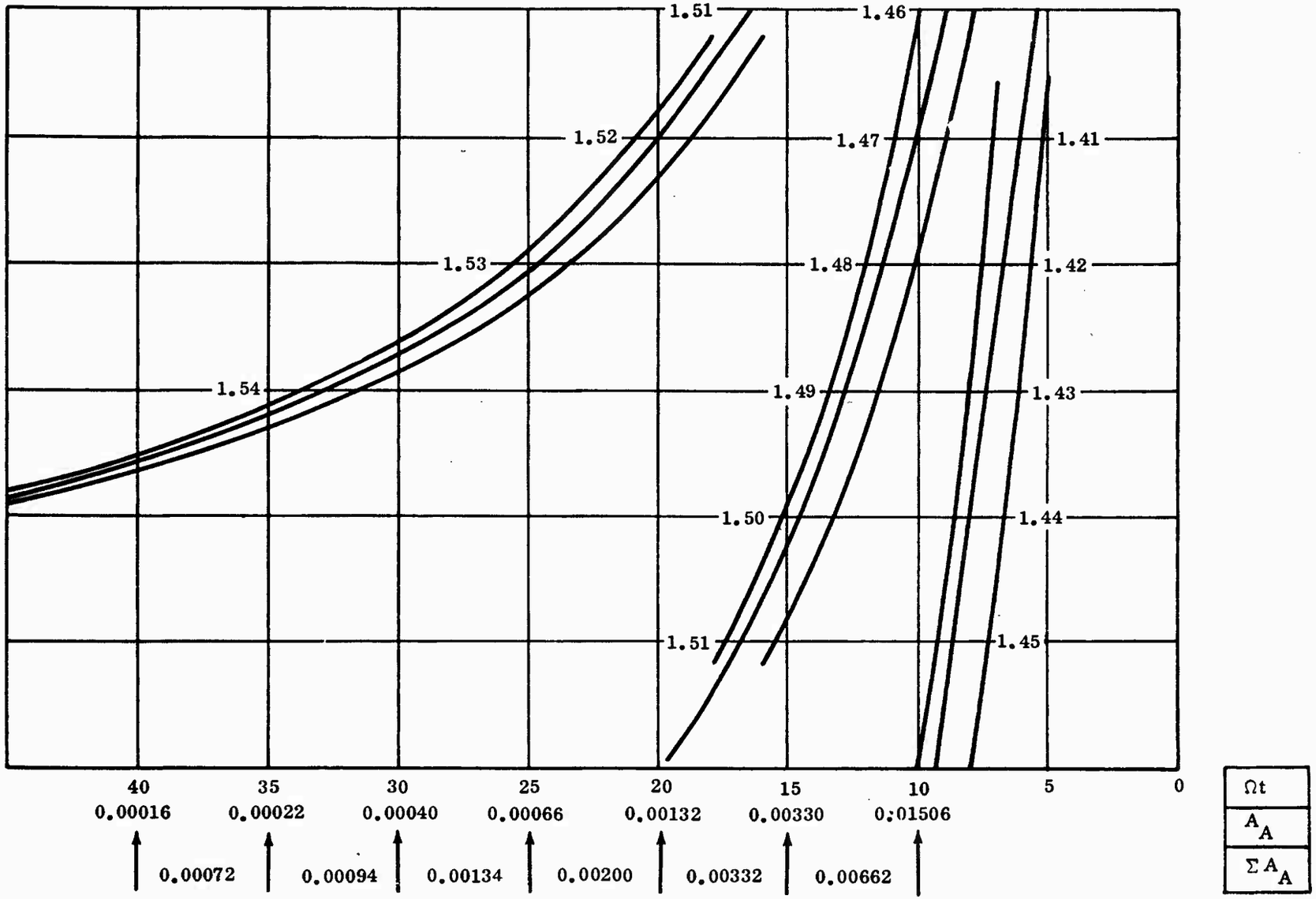

Figure 25. Error Envelope and Acceleration Pulse Sequence for R_o = 5 Feet, R_{mx} = 1000 Feet (Sheet 2)

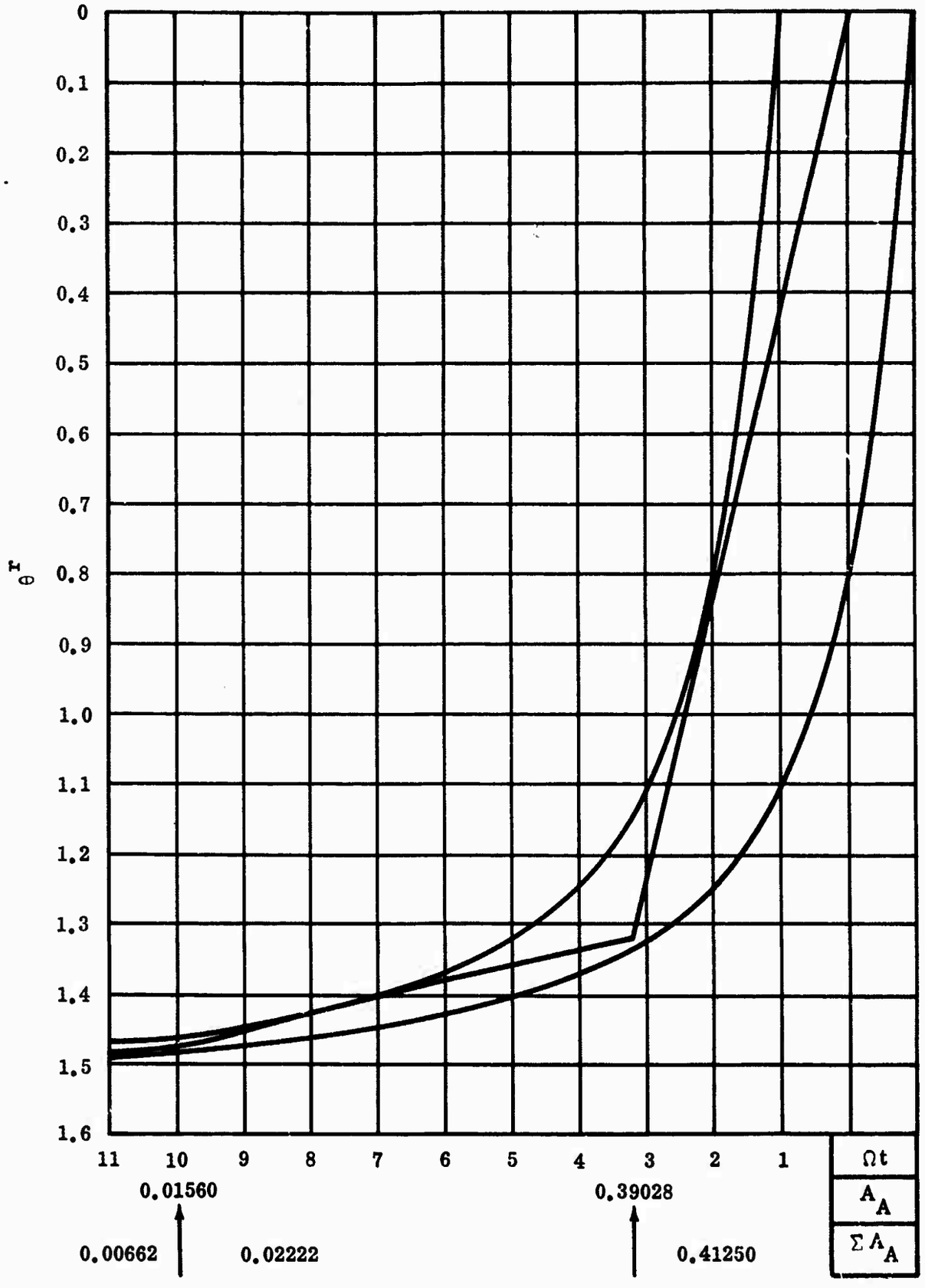

Figure 26. Error Envelope and Acceleration Pulse Sequence for R_o = 5 Feet, R_{mx} = 1000 Feet (Sheet 3)

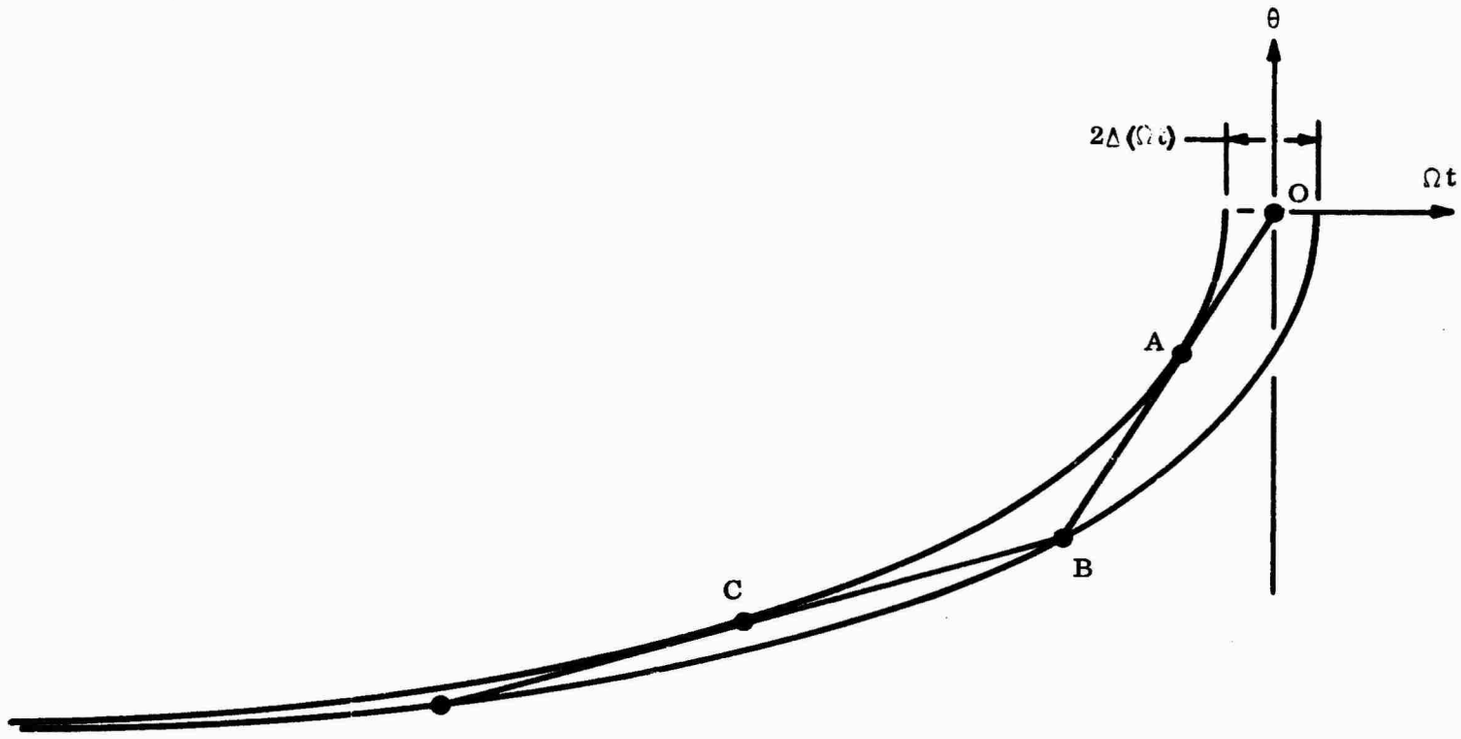

Figure 27. Angular Path for Minimum Acceleration within Allowable Error Envelope

Knowing point B, point C is then found from the further relation:

$$\frac{\theta_C - \theta_B}{(\Omega t)_C - (\Omega t)_B} + 2\Delta = \left(\frac{\dot{\theta}}{\Omega}\right)_C$$

The solution for points A, B, and C is conveniently carried out by semigraphical means, making use of general curves of θ and $\left(\frac{\dot{\theta}}{\Omega}\right)$. Thus, the solution for A follows from the construction:

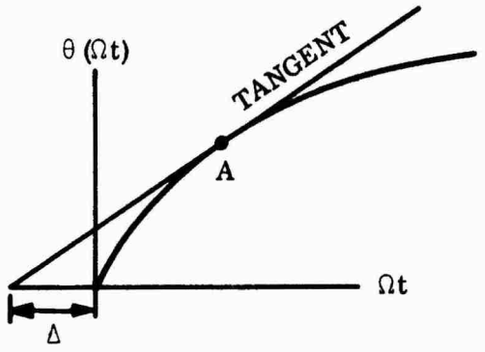

That for B from the construction:

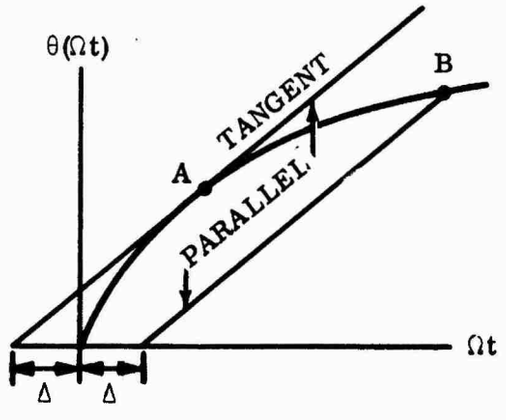

and that for C from the further construction:

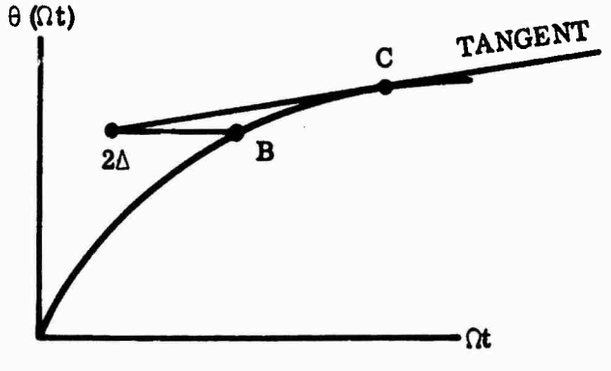

In general, the tangents are drawn graphically, the slopes of those tangents determined from measurements, and the points of tangency then found from the curve of slope $\left(\frac{\dot{\theta}}{\Omega}\right)$ versus angle.

Once the points A, B, and C are found, the final acceleration pulse is given by:

$$A_B = \left(\frac{\dot{\theta}}{\Omega}\right)_A - \left(\frac{\dot{\theta}}{\Omega}\right)_C$$

If we assume a rectangular pulse of duration $\Delta(\Omega t) = 2$, the peak acceleration is:

$$\left(\frac{\ddot{\theta}}{\Omega^2}\right)_{max} = \frac{1}{2} A_B$$

and the equivalent maximum relative velocity V_r for a 50-ampere maximum current is given by:

$$V_R = R_o \sqrt{\frac{50}{2.28 \times 10^{-4} \left(\frac{\ddot{\theta}}{\Omega^2}\right)_{max}}}$$

The final result of this calculation is displayed in Figure 28. From it, we deduce that, if maintaining target position within ± 5 feet throughout the intercept represents adequate simulation, then the performance domain may be extended beyond the apparent limit of $\Omega = 500$ by a factor of approximately two without exceeding the allowable maximum current in the motor.

5.9 Validity of Target Radar Return Simulation

The purpose of this section is to determine how well the microwave-modulated, laser system target return simulates the actual radar return from a moving target. We first define the actual radar return. Then we find the simulated return of the laser system. These results are compared to show the validity of the simulation.

In the case of actual radar, targeting information of range, range rate, azimuth, elevation, polarization component amplitude, and polarization component relative phase is obtained. For the purposes of this application, however, the analysis will be restricted to range information, although the results obtained can be extended to cover the simulation validity of other information parameters.

The radar range return from a moving target illuminated by microwave frequency energy contains, in general, both scintillation effects and doppler effects. These effects can be

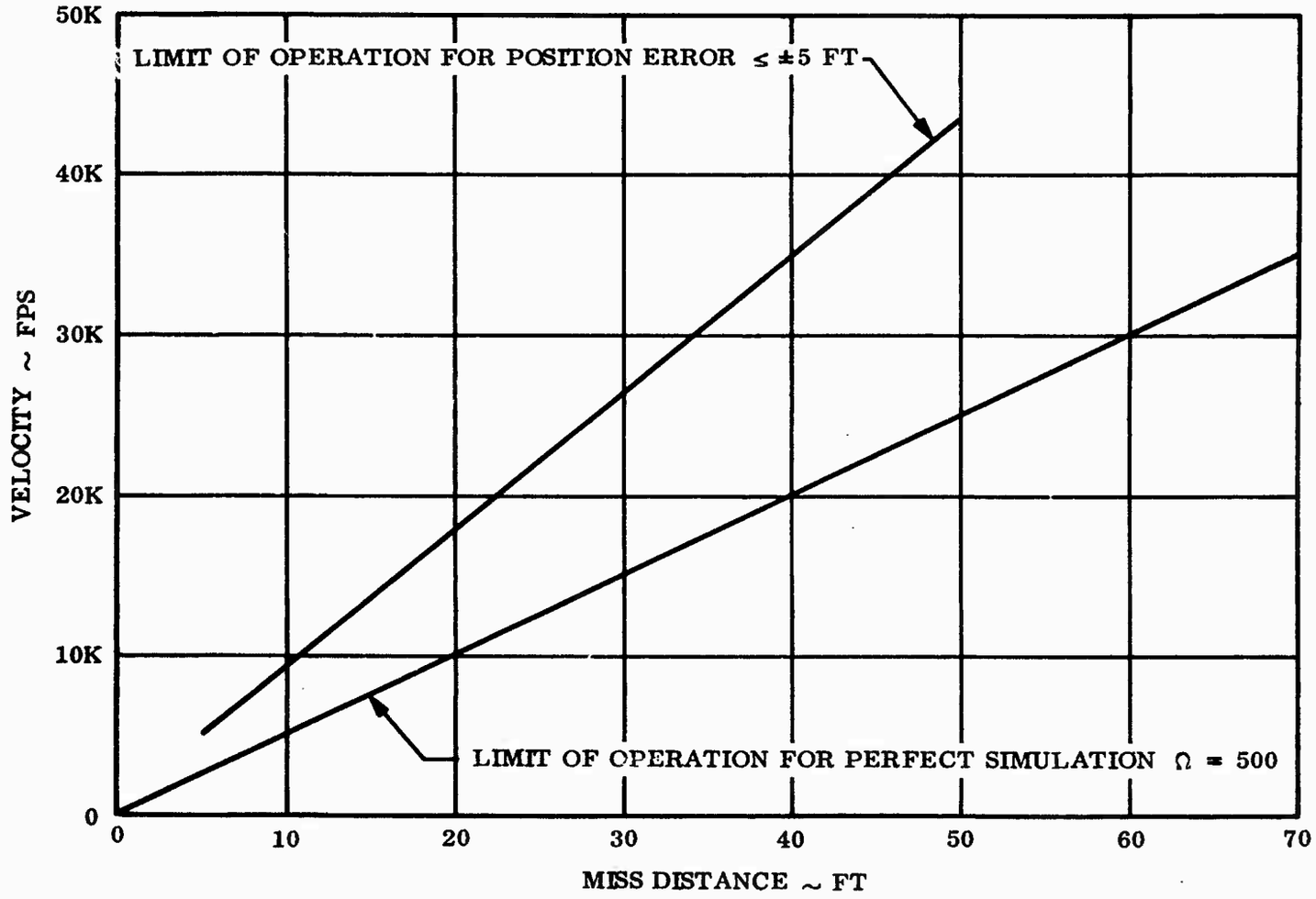

Figure 28. Enlargement of Operating Domain for Imperfect Simulation

translated into amplitude modulation and angle modulation of the transmitted microwave carrier. Coherent signals are assumed throughout.

In the simulation system, the original microwave carrier, which may or may not be amplitude, phase or frequency modulated, in turn amplitude modulates a coherent laser beam. The laser beam is caused to rotate in a plane at a predetermined angular velocity. The rotating beam impinges on a stationary target fence. A reflection is produced at the fence, energy is returned to the point of illumination, and is detected. The reflected energy is converted down to the microwave frequency spectrum, and is then modified in power level so as to duplicate the levels expected for an actual target return. The operations of converting the microwave signals up and down in frequency can be shown to introduce no erroneous information. Therefore, the problem reduces to that of showing that the laser system target return is of the same form as the actual radar target return.

5.9.1 True Radar Return. The actual radar return signal will first be analyzed to determined its mathematical form. Then the simulated return will be found. The results will be compared and the possible variances indicated.

For the microwave radar per se, and assuming the target is a point source for reflection, let the transmitted signal be the general complex function:

$$y(t) = K_e^{j\omega_o t}$$

where $\omega_o = 2\pi f_o$ and f_o is the microwave carrier frequency. After reflection, the return signal, in general, is both amplitude and phase modulated and can be represented as:

$$v(t) = a(t)e^{j\,[\omega_o t + \varphi(t)]}$$

where $a(t)$ is the complex amplitude modulation function and $\varphi(t)$ is the complex phase modulation function.

The total modulation is given by the function:

$$u(t) = a(t)\, e^{j\varphi(t)}$$

from which:

$$v(t) = u(t)\, e^{j\omega_o t}$$

But this is transformable into the frequency plane by the complex translation operation:

$$V(j\omega) = \int_0^\infty v(t)\, e^{-j\omega t}\, dt = \int_0^\infty u(t)\, e^{j\omega_o t}\, e^{-j\omega t}\, dt$$

$$= \int_0^\infty u(t)\, e^{-(j\omega - j\omega_o)t}\, dt$$

$$= U\left[j(\omega - \omega_o)\right]$$

This means that the frequency spectrum of the return signal, due to amplitude modulation or phase modulation or both, contains components only about the microwave carrier.

If

$$a(t) = A\,(1 + m_a \cos \omega_a t) = A\left[1 + \frac{m_a}{2}\left(e^{j\omega_a t} + e^{-j\omega_a t}\right)\right]$$

and

$$\varphi(t) = 0$$

then

$$u(t) = a(t)$$

and

$$v(t) = a(t)\, e^{j\omega_o t}$$

$$= A\left\{e^{j\omega_o t} + \frac{m_a}{2}\left[e^{j(\omega_o + \omega_a)t} + e^{j(\omega_o - \omega_a)t}\right]\right\}$$

So that if the target produces an amplitude modulated return signal, the frequency components become the carrier with side bands above the carrier and side bands below the carrier for each modulation frequency f_a generated.

If

$$a(t) = A$$

and

$$\varphi(t) = m_b \sin \omega_b t$$

where

$$m_b = \Delta\varphi$$

then

$$u(t) = A e^{jm_b \sin \omega_b t}$$

and

$$v(t) = A e^{j\omega_o t} e^{jm_b \sin \omega_b t}$$

By definition:

$$e^{jm_b \sin \omega_b t} = \sum_{k=-\infty}^{+\infty} J_K (m_b) e^{jk\omega_b t}$$

$$= J_o (m_b) + \left[J_1 (m_b) e^{j\omega_b t} + J_{-1} (m_b) e^{-j\omega_b t} \right]$$
$$+ \left[J_2 (m_b) e^{j2\omega_b t} + J_{-2} (m_b) e^{-j2\omega_b t} \right]$$
$$+ \left[J_3 (m_b) e^{j3\omega_b t} + J_{-3} (m_b) e^{-j3\omega_b t} \right]$$
$$+ \ldots$$

so that

$$v(t) = A \left\{ J_o (m_b) e^{j\omega_o t} \right.$$
$$+ \left[J_1 (m_b) e^{j(\omega_o + \omega_b)t} + J_{-1} (m_b) e^{j(\omega_o - \omega_b)t} \right]$$
$$+ \left[J_2 (m_b) e^{j(\omega_o + 2\omega_b)t} + J_{-2} (m_b) e^{j(\omega_o - 2\omega_b)t} \right]$$
$$+ \left[J_3 (m_b) e^{j(\omega_o + 3\omega_b)t} + J_{-3} (m_b) e^{j(\omega_o - 3\omega_b)t} \right]$$
$$\left. + \ldots \right\} .$$

This result shows that a multiplicity (k) of sidebands is produced in phase modulation. The amplitudes of the carrier and each of the sidebands a are proportional to the Bessel function of order k and of argument m_b (the modulation index).

Since the resulting target reflection due to frequency modulation is similar to that for phase modulation both effects can be called angle modulation. Mathematically the procedures are the same if the FM modulation index $m_b = \frac{\Delta\omega}{\omega_b}$.

5.9.2 Simulated Radar Return. Consider now the laser system. The radiated energy is reflected by the target fence while the beam is rotated at an angular velocity Ω. From the geometry of the system, $\Omega = \frac{V_R}{R_o}$, where V_R is the simulated target velocity and R_o is the minimum radial distance to the target. It is assumed here that the maximum Ω will be 500 radians per second, R_o will be 5 feet. Therefore, $V_{R_{max}} = 2500$ ft/sec. The doppler frequency shift at optical wavelengths is $f = \frac{c}{\lambda_L}\left(\frac{c+V}{c-V}\right)$

but

$$\frac{c+V}{c-V} = \frac{(c+V)(c+V)}{(c-V)(c+V)} = \frac{(c+V)^2}{c^2-V^2}$$

and since

$$c^2 \gg V^2, \quad \frac{c^2+2cV+V^2}{c^2-V^2} \cong 1 + \frac{2V}{c}$$

so that

$$f \cong \left(1 + \frac{2V}{c}\right)\frac{c}{\lambda_L}$$

or

$$\Delta f \cong \frac{2V}{\lambda_L} = \frac{2 \times 770 \text{ m/sec}}{6300 \times 10^{-10} \text{m}} = 2.43 \text{ Gc}$$

However, the percentage shift at optical wavelengths becomes:

$$\frac{\Delta f}{\frac{c}{\lambda_L}} = \frac{2.43 \times 10^9}{3 \times 10^8} \times 6300 \times 10^{-10} = 5 \times 10^{-6}$$

or 5 ppm. This is negligible shift in reflected optical wavelength and plays no part in the system response.

The transmitted radar microwave signal can be converted to laser frequencies by means of a microwave light modulator. This component allows amplitude or angle modulation of visible light at microwave rates. The device consists of a KDP crystal

supported by insulators in a microwave cavity. It turns out that the microwave E field, which is aligned parallel to the optical transmission axis, causes polarization modulation of the light beam. The equivalent light wave signal incident to the modulator from a coherent laser source can be written as:

$$z_o(t) = L\, e^{j\omega_L t}$$

where L is the E field equivalent amplitude and ω_L is the frequency of the incident light wave. The polarization modulation in effect produces phase modulation of the light beam so that the output of the modulator becomes:

$$z_1(t) = L e^{j(\omega_L t + \theta_m \cos \omega_m t)}$$

where ω_m is the microwave carrier frequency and θ_m is the maximum phase deviation. Thus angle modulation is available directly.

For amplitude modulation applications, the AM must be obtained indirectly. By using optical polarizers and an optical delay element, it is possible to obtain up to almost 100 percent linear modulation. The output then becomes:

$$z_1(t) = B\left[1 - 2J_1(2\theta_m)\cos \omega_m t\right] e^{j\omega_L t}$$

so that the modulation index is

$$m = 2J_1(2\theta_m)$$

It can be seen that the resulting AM is intimately related to the applied phase deviation.

The AM result is the only one of interest, since the detector is essentially an AM detector.

Therefore:

$$z_1(t) = B\left\{e^{j\omega_L t} - \frac{m}{2}\left[e^{j(\omega_L + \omega_m)t} + e^{j(\omega_L - \omega_m)t}\right]\right\}$$

This optical signal is then target modulated resulting in a new signal:

$$z_2(t) = u(t)\, z_1(t)$$

where u(t) is as defined earlier. Thus,

$$z_2(t) = u(t)\, e^{j\omega_L t} - \frac{m}{2}\, u(t)\, e^{j(\omega_L + \omega_m)t} - \frac{m}{2}\, u(t)\, e^{j(\omega_L - \omega_m)t}$$

This signal consists of three rotating vectors. In the following sketch, the vectors are plotted on a plane rotating at ω_L.

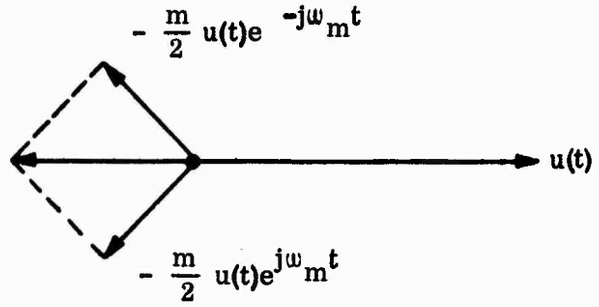

The resultant of the two sideband vectors is a vector collinear with the carrier vector and of the form:

$$\frac{m}{2}\,u(t)\,e^{j\omega_m t} + \frac{m}{2}\,u(t)\,e^{-j\omega_m t} = m\,u(t)\cos\omega_m t$$

The traveling wave phototube detector is a quantum detector, that is, the resulting output signal is proportional to the rate at which quanta of energy are received. In this case, the energy received is in the visible light spectrum. The TWP photocurrent is:

$$I_o = \frac{P_L\,\eta\,qe}{h\nu} = \frac{\frac{E_L}{t}\,\eta\,qe}{h\nu}$$

where P_L is the average input power

η is the quantum efficiency

qe is the electronic charge

and $h\nu$ is the quantum energy

or

$$I_o = k_E\,\frac{qe}{t}$$

where k_E is the converted energy ratio. Since the TWP is designed to respond the band of microwave frequencies about ω_m, the output current becomes:

$$i(t) = k_E\,m\,u(t)\cos\omega_m t$$

or

$$i(t) = k_E\,m\,u(t)\,\mathrm{Re}\left[e^{j\omega_m t}\right]$$

It can be seen that this equation can be put in the form:

$$i(t) = k\, u(t)\, e^{j\omega_m t}$$

This signal is proportional to $v(t) = u(t)\, e^{j\omega_0 t}$ if $\omega_m = \omega_0$. Since u(t) is general, this shows that a replica of the original target modulation can be simulated by the use of this technique.

The TWP output signal has only its amplitude adjusted to correspond with an expected range of radar receiver input levels. Therefore, since u(t) can be an amplitude or angle time varying function or both, the laser system provides a means for generating u(t) and for applying the resultant to the radar system under test as if the radar were receiving actual target returns.

5.10 Photometric Capability.

In passive optical intercepts, the target illumination is primarily by sunlight and earthlight. The surface properties of the target can be anything from dead black to specular, and the simulator should have the capability of duplicating as much of this range of conditions as possible. In an earlier section, we took the brightness of a perfect diffusor in sunlight as a minimum upper limit to this working range. Some white painted vehicles approximate this. Outside the earth's atmosphere, the solar illumination is 14 lumens/cm^2; therefore, a perfect diffusor would exhibit a brightness of $14/\pi = 4.5$ candles/cm^2. Consider now what this means in terms of the projection system. We consider first the use of a diffuse projection screen; second, the use of a spherical field mirror.

In general, the illumination on a projection screen is given by $E = BT\varphi$ lumens/cm^2, where B is the brightness of the projector source in candles/cm^2, T is the transmission efficiency of the system, and φ is the solid angle subtended at the screen by the exit pupil of the projector. If we suppose a xenon arc lamp such as the Osram XBO 450, an average source brightness of 45,000 candles/cm^2 is possible. Transmission wil run about 20 percent, so $E = 9000\varphi$. To duplicate sunlight, the projection solid angle must be $\varphi = \frac{14}{9000}$. But this implies the screen must be located 22.5 lens diameters away from the projector. Since we are limited to a projector aperture of about 2 inches, this means a screen less than 4 feet away. Thus to duplicate sunlight using a diffuse projection screen, a high power arc lamp and a short projection distance are required. To duplicate glint would not be practical at all. The trouble is, of course, that such a screen spreads light everywhere into a hemisphere, when it is actually needed only in the direction of the sensor.

When we project into the mirror, on the other hand, the sensor is actually looking at the projector source. Hence, except for transmission losses, and provided the aperture is filled, the luminous target can be as bright as the source. In the present case, the upper limit of target brightness would be

$$B = 9000\left(\frac{D_p}{D_S}\right)^2 \text{ candles/cm}^2$$

where D_p is the diameter of the projector lens and D_S is the diameter of the sensor lens. Thus, the use of a spherical mirror as the projection screen provides a tremendous potential range of brightness simulation. Glint would be easy to reproduce and image position could be as far away as infinity, if desired.

6.0 DETAIL SUBSYSTEM DESIGN, OPTICAL SIMULATOR

6.1 Subsystem Definition

The active and passive optical simulators may be resolved into two major subsystems. Basic to both, and to the radar simulator as well, is the mirror rotation subsystem. This is the central subsystem of the entire facility. Consequently it has been given major attention in what follows. The second major subsystem is the target projection subsystem. This differs in detail in the passive and active simulators, but the essential features are the same in both.

6.2 Mirror Rotation Subsystem

6.2.1 Conceptual Description. The central element in both optical and radar simulators is a high-performance, DC servo motor to which projection mirrors are attached. All angular functions are introduced into the intercept simulation through the rotation of this motor and attached mirrors. Since the most important features of the intercept simulation is the proper duplication of angular motion, the control of the motor may be said to be the central problem in the design of the simulator.

6.2.2 Control System Considerations. In deciding what method of control to use we considered the following:

1. The class of intercept intended is the rectilinear intercept. Whether the simulator exactly duplicates this intended intercept or not is not of paramount importance. Minor variations do not affect the basic demand made upon the scoring system. What is important is that whatever the intercept motion actually turns out to be, it be determinable with sufficient accuracy to allow evaluation of the scoring system. We take this requirement to mean that, in retrospect, the actual position of the target vehicle be determinable to within one milliradian.

2. The motor chosen, the PMI Incredyne, is the highest acceleration motor on the market. At small miss distances, the acceleration requirements demand that even this motor be driven to the limit of its capabilities. Open loop operation under these circumstances is easier than closed loop operation.

6.2.3 Recommended Method of Control. Therefore, in the interest of simplicity, economy, and effectiveness, our primary recommendation is that this motor be run open loop in a reasonably close approximation to the nominal intercept intended, and that the actual motor motion be monitored and recorded with sufficient accuracy to allow its position to be determined in retrospect to within one milliradian. The general scheme of control for accomplishing this is diagrammed in Figure 29.

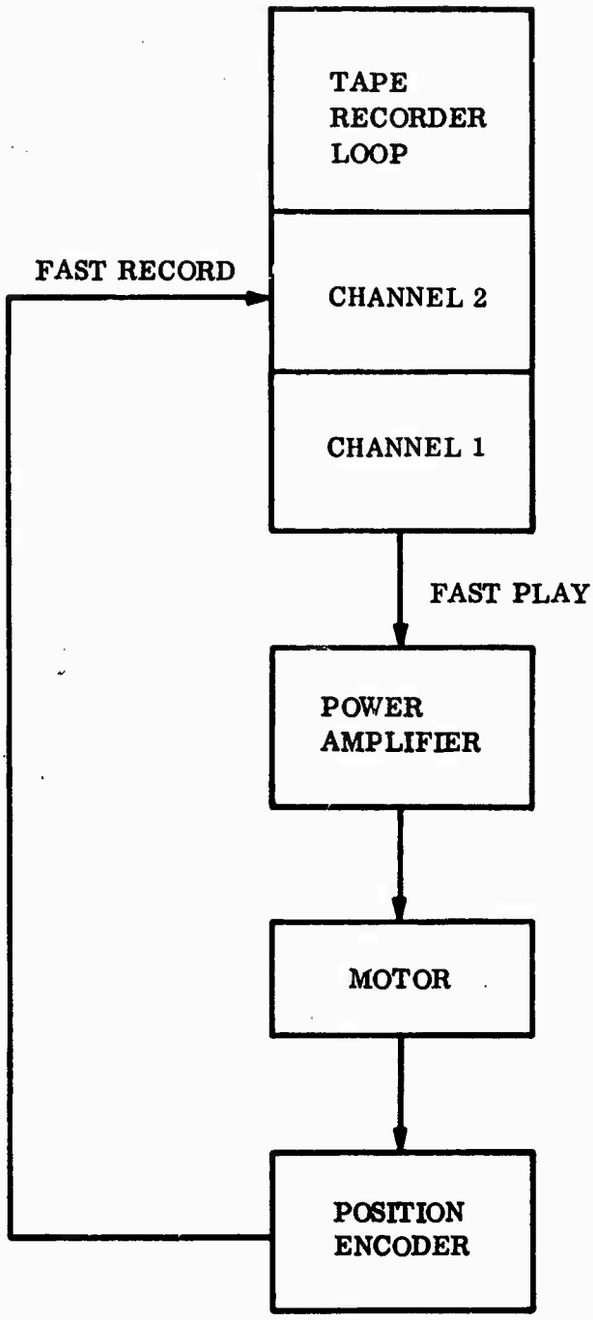

Figure 29. General Scheme of Control - Open Loop Drive / Record System

6.2.4 Alternate Closed Loop Control. Although closed loop control is more difficult, and is not, therefore, our primary recommendation, preliminary analysis shows it may indeed be feasible and that it merits further study.

6.2.5 Description of Control Action. The control action may be described as follows. One cycle of simulation involves 180 degrees of mirror rotation. The motor position is determined by the time history of the voltage applied to its terminals. The design voltage function, calculated from the nominal motor constants, was displayed earlier in Figure 19. It is applied through a power amplifier which is driven by a continuous loop high fidelity tape recorder. The signal on the tape loop originates with a hand drawn curve in a function generator, and is recorded at slow speed. A library of these hand drawn voltage functions, each representing a separate value of the parameter Ω (maximum angular velocity), can be assembled easily from a computation involving the motor constants. If necessary and desirable, these functions can be refined by an iterative process of calculation and subsequent correction, to allow for variation of the motor constants. This procedure is diagrammed in Figure 30.

Once a suitable driving function has been arrived at it is transferred from the function generator to one channel of the tape loop by slow speed recording. The original hand-drawn function graph is permanently retained for repeated re-use. We then have the means to generate a pattern of relative motion which, if not precisely identical to that of a rectilinear intercept, is certainly representative. Variations can be rationalized in terms of acceleration occurring during the intercept. As long as it can be accurately determined what the relative trajectory actually was during the simulation, it is not of vital importance that it conform to the special case of zero acceleration.

The tape loop in the multichannel recorder now serves both to drive the system and, simultaneously, to record the output of the simulator system and the scoring system under test. (It is assumed that some kind of output from the scoring system will be available for recording; otherwise, it is hard to see how a scoring system could be evaluated.) The tape then contains a complete record of the test input and output - all on a common time base. It may then be played out at slow speed onto a multichannel oscillograph to generate a permanent visual display for evaluation purposes. This driving and recording sequence is diagrammed in Figure 31.

6.2.6 Subsystem Components. The mirror rotation subsystem includes the components shown in the block diagram of Figure 32. These are:

1. Function generator
2. Multi-channel, wide-band, tape recorder/reproducer
3. Time base generator, separate or part of the recorder
4. Preamplifier with large dynamic range

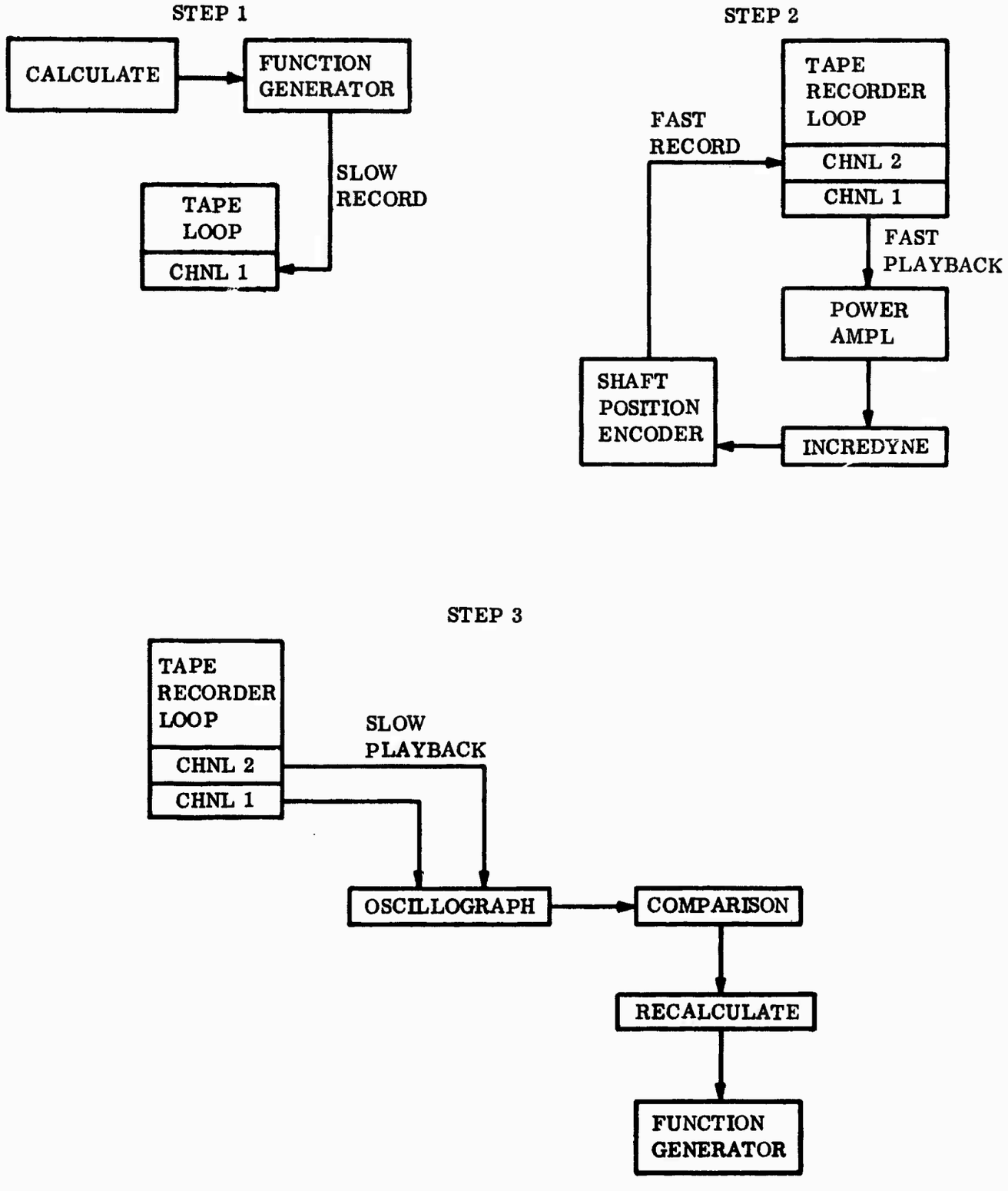

Figure 30. Development of Driving Function Library

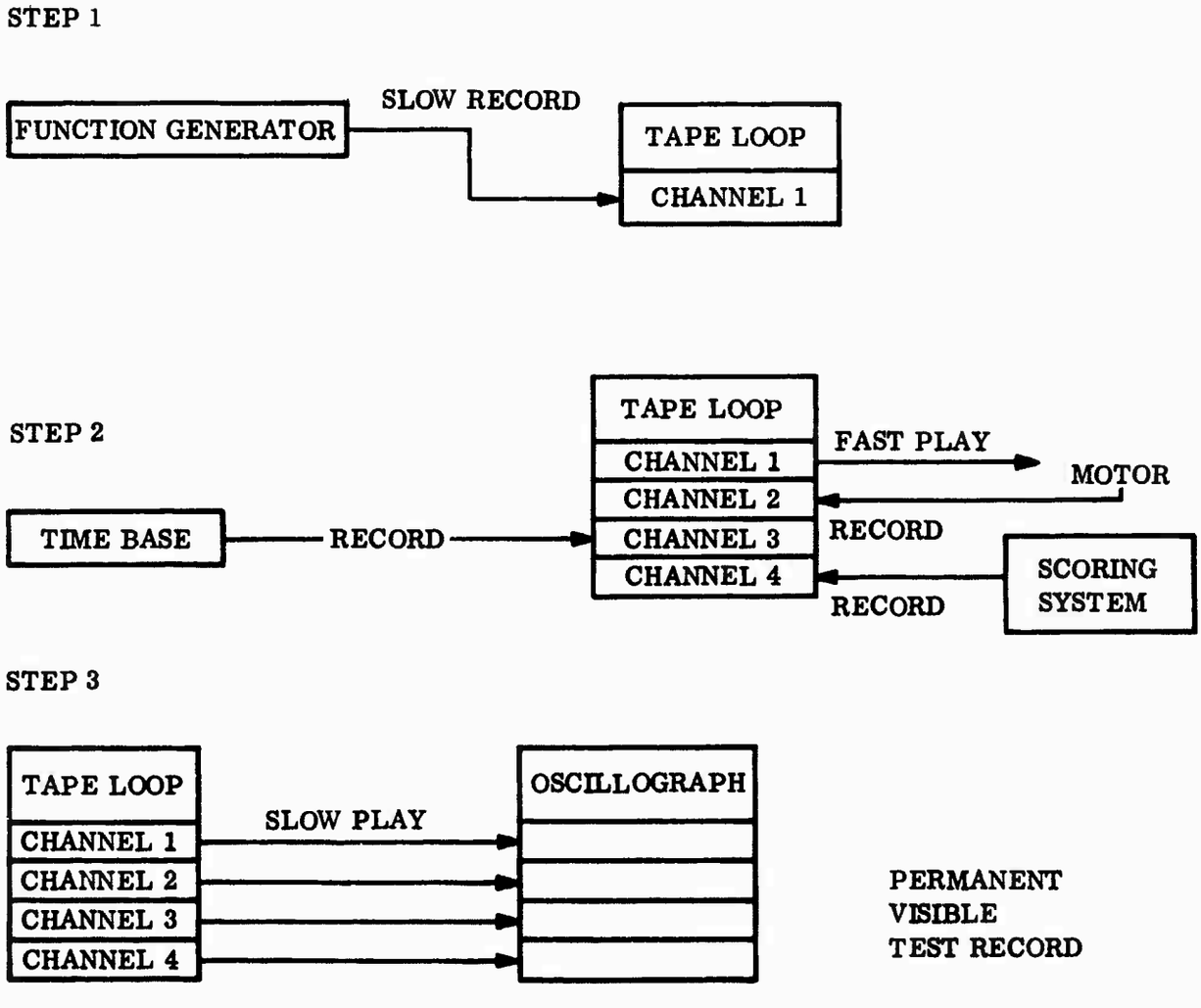

Figure 31. Development of Test Record

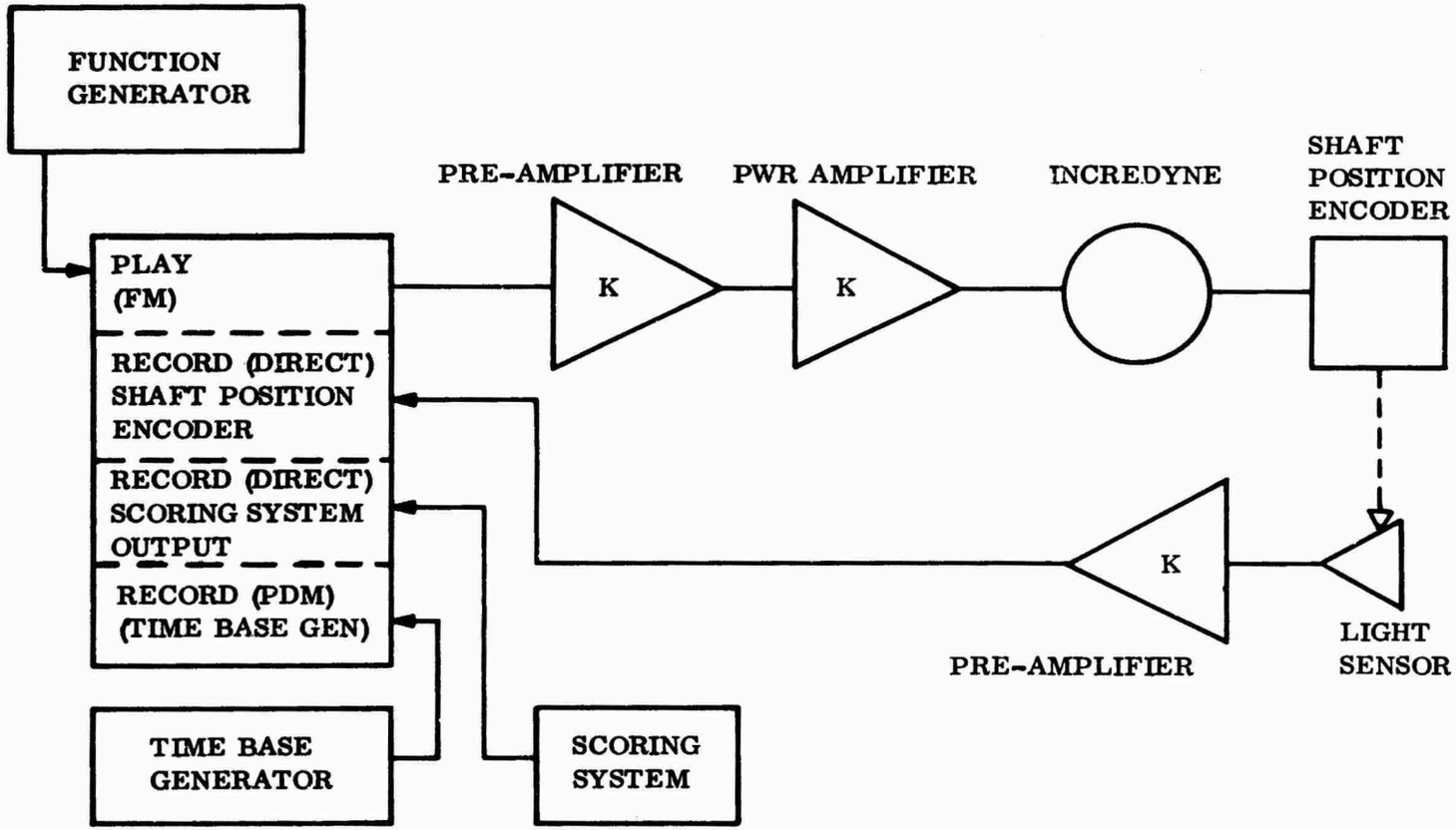

Figure 32. Mirror Rotation Subsystem

5. Power amplifier with large dynamic range

6. High current power supply

7. High acceleration DC servo motor

8. Shaft position encoder

6.2.6.1 Function Generator. A function generator selected would be a commercial unit manufactured by RI Controls and known as "Stata-Trak" or its equivalent. A metallized mylar 11-inch x 13-inch chart is divided into two sections by any single-valued hand-drawn function. The graph is then wound around a drum. As the drum rotates, a capacitative pickoff translates the hand-drawn graph into a DC output voltage in the ± 5 VDC range The cost of the Stata-Trak is $1946.

6.2.6.2 Tape Recorder/Reproducer. The basic requirements of the recorder/reproducer include the following:

1. A minimum of four channels, with a capability of simultaneously playing out one channel while recording on the other three.

2. A bandwidth of 125 kc, to accommodate the shaft position encoder.

3. A built-in time base generator with a pulse repetition frequency (PRF) of 111 kc or greater at 60 ips tape speed. A desirable feature would be the ability to reduce the PRF proportionally to the tape speed. The time base generator would use the direct recording mode.

4. The Play channel must have a frequency response down to DC. The maximum required will not exceed 300 cps, so the FM mode could be used.

These requirements can be met by an Ampex FR 1300. The cost of this unit is $12,000 without a time base generator. An integral time base generator would be $2000 additional.

In Table I is shown a schedule of record and play tape speeds for various values of the intercept parameter.

6.2.6.3 Preamplifier. The preamplifier requirements may be summarized as follows:

1. Input impedance: 4.5 KΩ

2. Output impedance: 500 Ω

3. Input range: 2.8 VDC

4. Output range: 80 VDC

5. Gain 30 maximum and variable

6. Bandwidth: DC to 1 Kc

These requirements can be met by two cascaded Philbrick Units. There are:

Booster - Model OS PB/100 100 V @ 10ma $85.00

Pre-Amp - Model PG SA 11 V @ 2.2ma $85.00

TABLE I. MAXIMUM ANGULAR VELOCITIES, TAPE SPEEDS, AND RATIOS

Ω rad/sec	T (Recorded Time) Milliseconds	T (Play) Milliseconds	Tape Speed (Record) ips	Tape Speed (Play) ips	Ratio TR/TP
500	640	20	1-7/8	60	32
250	↓	40	↓	30	16
125	↓	80	↓	15	8
62.5	↓	160	↓	7.5	4
31.25	↓	320	↓	3.375	2
15.625	↓	640	↓	1.875	1
7.812	↓	1280	3-3/4	1.875	0.5

6.2.6.4 Power Amplifier. The power amplifier requirements are as follows:

1. Input impedance: 25 K Ω to 50 K Ω

2. Output impedance: 0.01 Ω

3. R_{load}: 0.74 Ω static, 1.4 Ω dynamic

4. Input signal: ± 80 VDC P-P

5. Output signal: +70 VDC, - 10 VDC

These requirements are unusual and cannot be met by any commercial amplifier unit. The recommended design is based on a balanced bridge type push-pull circuit. The first advantage of this design over others considered is that power dissipation will be shared equally by the conducting transistors (either Q1 and Q4 or Q2 and Q3) as shown in the schematic, Figure 33. The second advantage is that only a single supply voltage will be necessary.

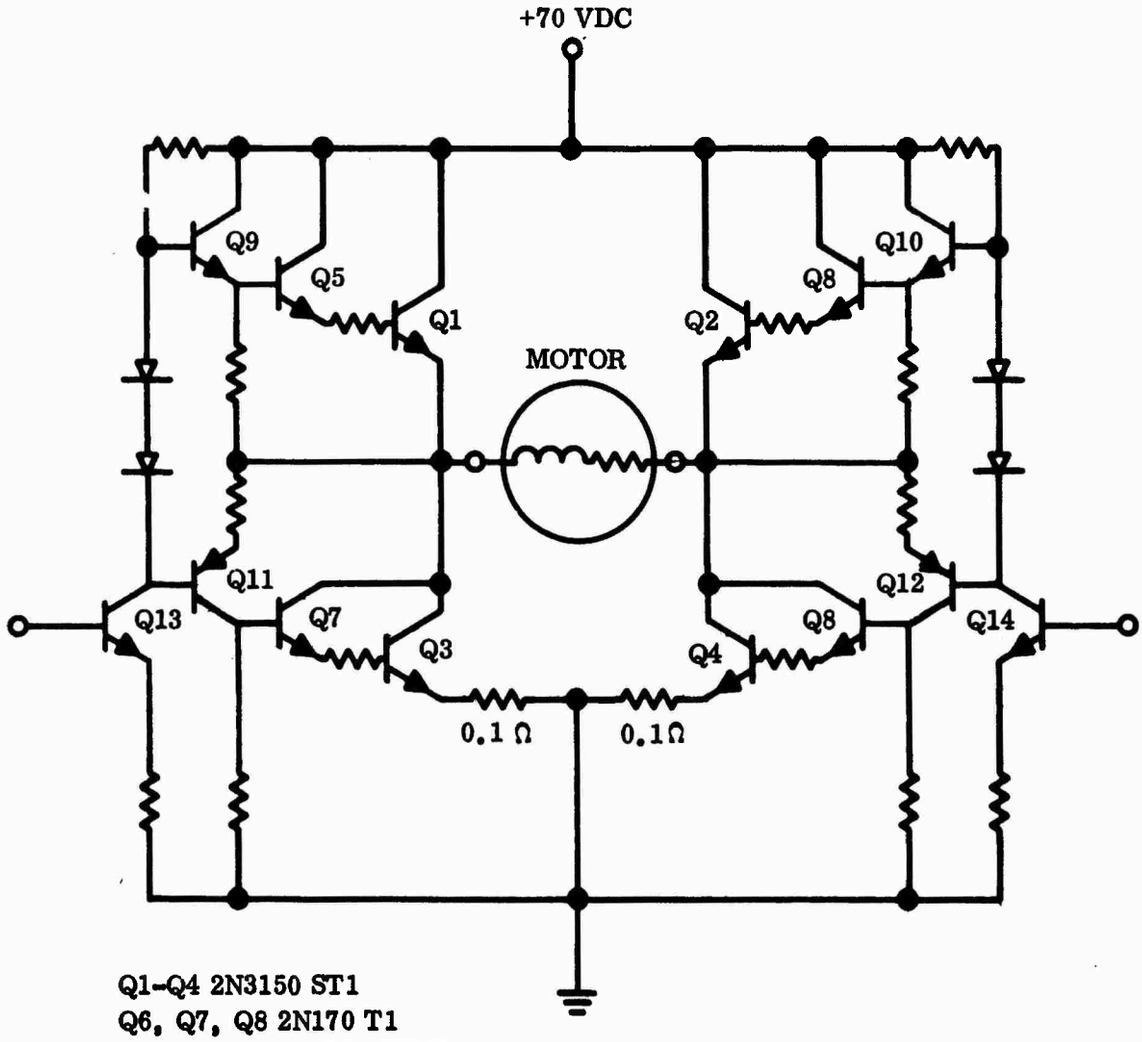

Q1-Q4 2N3150 ST1
Q6, Q7, Q8 2N170 T1
Q9, Q10, Q13, Q14 2N1711 T1
Q11, Q12 2N1132 (OR EQUIV)

Figure 33. Power Amplifier

Based on operating point data of I_c = 27a and V_{CB} = 35/2 V, the power dissipation (Q1 or Q4) will be 472 watts. Based on a duty cycle of 2 percent, it appears that Q1 can be a single 2N3150 transistor. The estimated cost for a complete amplifier would be approximately $1000.

6.2.6.5 Power Supply. The basic power supply requirement is one of high current, low output impedance, and hence, good regulation. These requirements may be summarized as follows:

1. Nominal output voltage: 80V ± 5V
2. Regulation: 1.3%
3. Output impedance: 0.02 Ω
4. Maximum output current: 50A

There are two ways to meet this requirement: with a commercial power supply or with batteries. A suitable commercial power supply is the Mid-East Electronics Model MS 77-50, rated at 80 VDC and 50 A. The cost is $2500. The same capability can be supplied by seven 12 V lead acid automotive storage batteries in series. A trickle charger can be installed to keep the batteries charged. A total of seven batteries and a trickle charger can be supplied for about $200.

6.2.6.6 High Performance DC Servometer. The analysis of the motor problem is presented in detail in Section 5.0 where it is shown that the PMI Incredyne will be suitable. Basically, the problem is one of obtaining a combination of high torque and low inertia. For the Incredyne, the maximum rated pulse torque is 1040 oz-in and the polar moment of inertia of the armature is only 0.003 oz-in-sec^2, suggesting a maximum angular acceleration of over 300,000 rad/sec^2. No other available motor is known to approach this figure. In fact, however, the actual maximum acceleration is limited by thermal damage at high currents. The Incredyne can accept up to 50 amperes at short duty cycles (a few percent) without performance degradation. Calculation has shown that the design maximum acceleration of 162,000 rad/sec^2 can be properly duplicated with this motor, and the manufacturer concurs.

6.2.6.7 Shaft Position Encoder. The shaft position encoder is basically a grating photo-etched around the periphery of a glass disk. The configuration of the grating is determined by the primary simulator requirement that the position of the shaft be determinable in retrospect to one milliradian. For the sake of simplicity, it is also desirable that the encoder require only a single recording channel.

Stress and inertia considerations make it desirable to keep the diameter of the encoder disk small, preferably two inches or less. On the other hand, the coarser the grating frequency the easier and cheaper to fabricate and the more accurate it will be. A reasonable accommodation to these various demands would be a disk two inches in diameter with a square wave grating of 250 cycles/inch around half its periphery.

Each cycle represents 4 milliradians. This would provide a least count of 2 milliradians, which should allow easy enough interpolation to 1 milliradian. The frequency response required of the recorder under the worst conditions (Ω = 500 r/sec) is $f = \frac{500\ r/s}{0.004\ r/cy} = 125$ kc, which is satisfactory.

There will be a total of 785 opaque lines around the semi-periphery of the disk. To allow easy counting, we can modulate this primary grating with a neutral density overlay in the form of a second square wave. A period ratio of 20 would provide a convenient count. A neutral density of 0.3 would provide a 2:1 voltage ratio in the recorded signal. The design of the shaft position encoder is shown in Figure 34.

More complicated encoders could be designed for automatic position readout, and this may prove desirable later. The present design will be adequate for interpretation of oscillograph recordings, which we expect will be the first method of analysis used.

To generate the shaft position signal, a light must be directed through the encoder into a photocell in such a way that it will be interrupted by the opaque lines in the grating. The design of this piece of equipment will be conventional and poses no serious problem. Estimated materials cost of the entire shaft encoder, including disk, pickoff and pre-amplifier, is $2000.

6.2.7 Subsystem Costs. Although precision costing cannot be done in some cases prior to actual component design, at least an approximate cost has been established for each component of the mirror rotation subsystem. The total subsystem cost is found as follows:

Component	Cost	Comment
1. Function generator	$1995	Purchased
2. Time Base generator	2000	Purchased as part of recorder
3. Multichannel tape recorder	12,000	Purchased (with 4 amplifiers)
4. Pre-amplifier	470	Includes 2 amp DC supply
5. Power amplifier	1000	In-house design
6. Power supply	2500	Purchased
7. Motor (Incredyne)	610	Purchased
8. Shaft position encoder	2000	In-house design
Total Costs	$22,575	Does not include design time

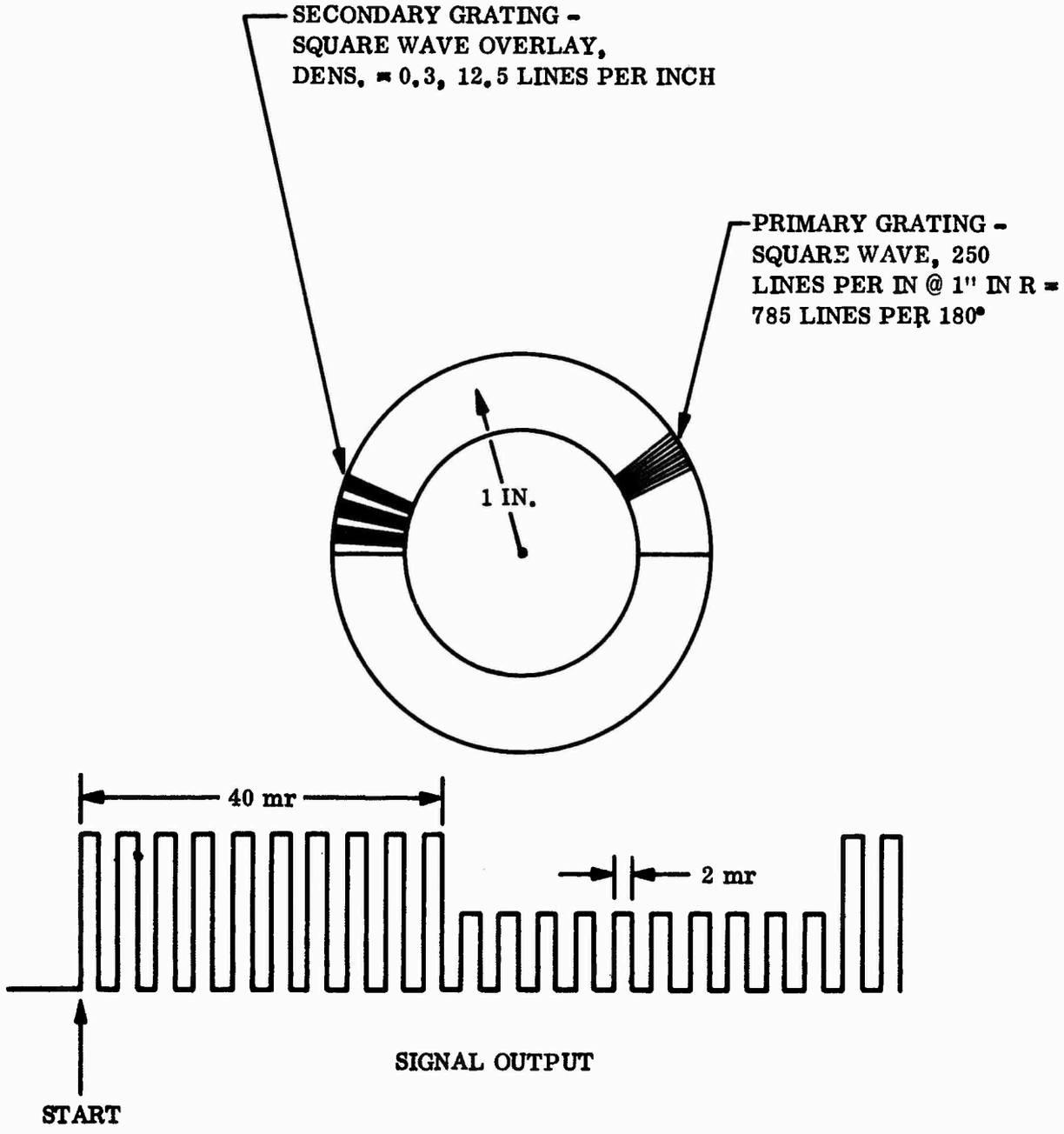

Figure 34. Shaft Position Encoder

6.3 Passive Target Projection Subsystem

In the passive optical intercept simulator, the target projection subsystem consists of the following components, which are taken up, in turn, below:

1. Target transparency
2. Target illuminator
3. Projection lens
4. Rotating diagonal mirror
5. Spherical zone mirror

6.3.1 Target Transparency. We have considered employing a target transparency with several degrees of freedom capable of realistically simulating much image detail. Although such realism is certainly feasible, we do not feel it is justified at present, considering the capability of present and immediately foreseeable scoring systems. Instead, we recommend a rather simple transparency with only one degree of freedom. Upgrading to more elaborate simulation can be done as the need arises.

In designing the transparency, we have considered two classes of intercepts:

1. Air-to-air intercepts involving small miss distances and targets subtending more than 20 degrees.
2. Other missions were targets subtend less than 20 degrees.

The 20-degree criterion enters primarily because of partial field obscuration by the project lens. The projection system allows a field of up to 90 degrees horizontally, but only 20 degrees vertically. This limitation is not serious because only air-to-air missiles approach closely enough to subtend more than 20 degrees, and then only in one dimension.

For the general case, we recommend the use of a simple iris whose diameter is electrically controllable. This would generate the image of a polyhedral target, which is close enough to many practical cases, especially satellites, to be quite useful. For the special case of an air-to-air missile with a rectangular profile, we recommend the superposition on the iris of a fixed rectangular slit. Of course, this also provides reasonable simulation of cylindrical satellite targets as well.

The two transparency designs are shown in Figure 35. A graphic illustration of how these appear to the scorer during an intercept cycle is shown in Figure 36.

Unfortunately, no electrically driven iris with the necessary frequency response is available on the market, so this component will involve an original design. The problem of frequency response can be overcome by sacrificing generality of function. The

1. SPACE MISSION

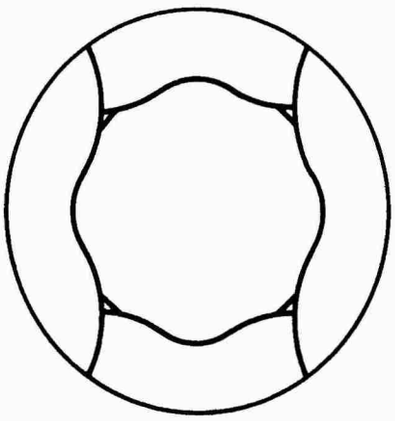

TIME-VARYING
APERTURE

2. AIR-TO-AIR

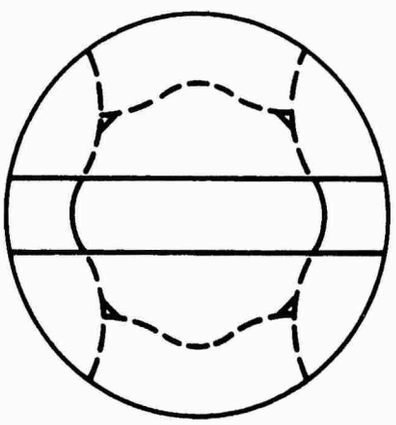

TIME-VARYING
APERTURE PLUS
FIXED RECTANGULAR
SLIT (REMOVABLE)

Figure 35. Target Transparency Design

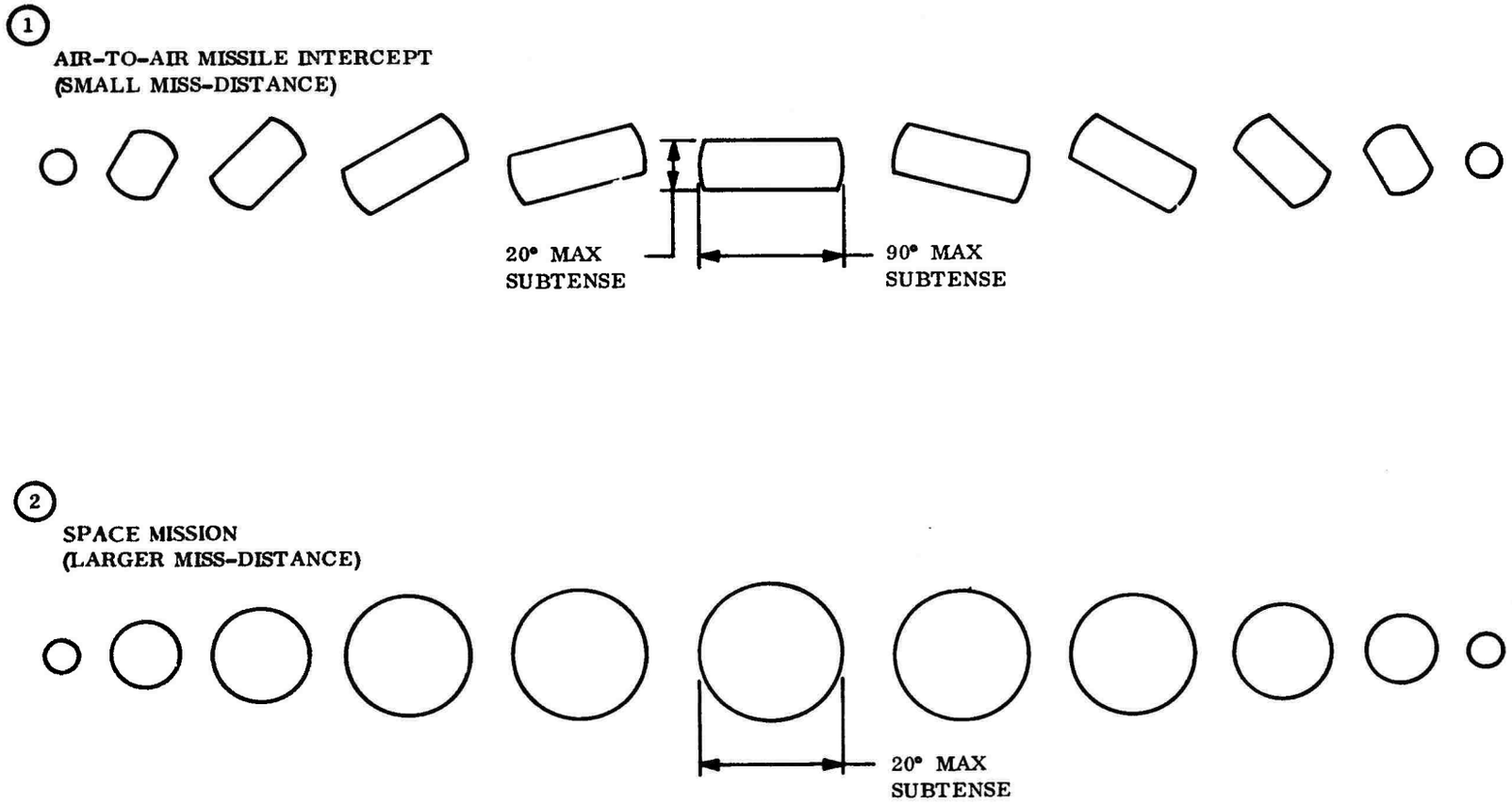

Figure 36. Projected Target Patterns

design recommended, which is illustrated in Figure 37, is an adaptation of a conventional shutter mechanism which requires only a constant speed drive. The design is simple in principle, and fabrication should be straightforward.

To simulate apparent size properly through the intercept, the size of the transparency opening must vary with time according to the law:

$$d = d_o \frac{1}{\sqrt{1 + \Omega^2 t^2}}$$

where $\Omega = \frac{V}{R_o}$ is the primary intercept parameter. If the shutter blades are given the shape, in polar coordinates:

$$r = r_o - 1/2 \frac{d_o}{\sqrt{1 + \Omega^2 t^2}}$$

where Ωt is allowed to vary over some appropriate range around the blade periphery, say from -10 to +10, and if the shutter blades are rotated at a constant speed, in this $\frac{\Omega}{20}$ rps, the size of the transparency opening will obey the required law. To accommodate various values of Ω, the speed must be variable. This is accomplished by using a DC servo motor and adjusting the voltage to produce the desired speed.

To simulate target vehicles of various sizes, the maximum iris opening should be variable. In the recommended design of Figure 35, this is not possible. Flexibility was sacrificed to avoid frequency response problems. Adding such a feature mechanically would introduce excessive complexity and cost or, as in the case of interchangeable shutter blades, undesirable opportunities for damage.

Two other ways to achieve the same effect are to use interchangeable iris modules, or to use interchangeable projection lenses. The use of interchangeable lenses is the cheapest way. Such lenses (including the condenser lenses, which should be changed at the same time) would cost about $200 per set.

Estimated materials and fabrication costs for the target transparency total $2000.

The controller need consist only of a suitably variable DC voltage supply, and a switch which can be activated by the Incredyne voltage. Estimated cost of the controller is $250.

6.3.2 Target Illuminator. The requirement of a 90-degree field has led to the choice of a projection lens with a 14.5 mm focal length. The target transparency must, therefore, measure 29 mm at its greatest enlargement, or slightly over an inch. The function of the illumination system is to provide reasonably uniform illumination over that 29-mm opening. The illumination must be sufficient to produce a final image

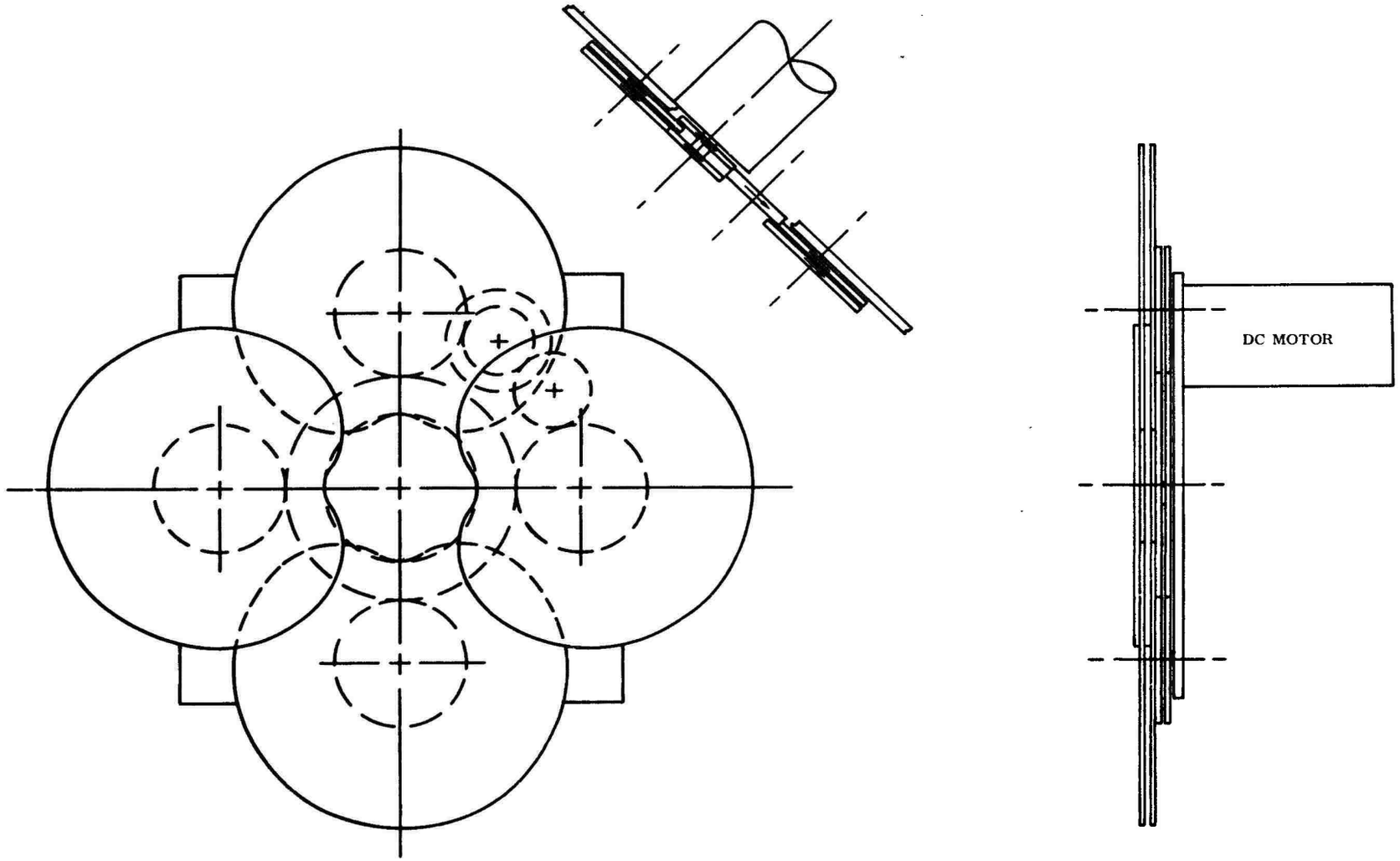

Figure 37. Time Variable Target Transparency

brightness, as seen by the scorer, of at least 4.5 stilb, which is equivalent to that of a perfect white diffusor in sunlight outside the atmosphere. This is a very easy requirement which can be met by a simple, conventional illumination system. A suitable design is sketched in Figure 38. Estimated materials cost is $250.

6.3.3 Projection Lens. The main requirement on the lens is field. Since the simulator must be able to handle air-to-air intercepts with miss distances as low as 5 feet, the field must be 90 degrees for a typical missile length of 10 feet. On the other hand, the lens must project through a diagonal mirror which, to keep inertia down, must be made as small as possible. These conflicting requirements make compromise necessary. All things considered, a suitable choice for the lens is the Angenieux R62, 14.5 mm F/3.5 with an advertised 90-degree field. Cost is $200. An outline drawing is shown in Figure 39.

6.3.4 Diagonal Mirror. A geometrical ray trace shows that projecting through a diagonal mirror results in an unavoidable obscuration in the vertical dimension which limits vertical field to 20 degrees. There is no limitation on horizontal field, however, which can go to the full 90 degrees provided by the lens. This is not a real disadvantage because the only targets which may subtend 90 degrees are air-to-air missiles, which conveniently have a rectangular cross section. A 90-degree x 20-degree field can perfectly well accommodate such targets. Since it is desirable to minimize the load on the motor, the mirror should be no larger than necessary to accommodate this 90-degree x 20-degree field and should have the lightest possible construction consistent with the stresses of rotation. Image quality does not have to be high. Limiting surface slope errors to one arc-minute is an easy specification to meet and will insure that the mirror cannot degrade the ultimate one milliradian angular resolution required of the system. A sketch of the recommended mirror design is shown in Figure 40. Estimated manufacturing costs are $250 each.

6.3.5 Spherical Field Mirror. The maximum vertical angular subtense allowed by the projection system is 20 degrees. Therefore, the spherical zone spherical field mirror need subtend no more than this. The need to accommodate apparatus of some physical size without operating too far off axis leads to a reasonable figure for mirror diameter of 10 feet. The mirror should then take the form of a 20-degree central zone of a 10-foot diameter sphere. A mirror of this type is most easily manufactured in sections. A total of nine 21-inch by 21-inch sections would be satisfactory. If was require the same 1 arc-minute accuracy as for the diagonal mirror, these sections can be readily fabricated either from machined and polished plexiglass or from sagged and polished glass. The price of either type would be about $400 per section, for a total cost of $3600. These nine mirror sections would need to be mounted in a jig allowing individual position adjustments. There is nothing unusual or complicated about such a structure, and satisfactory performance should be readily attained. A sketch of the mirror is shown in Figure 41. Estimated cost of the supporting structure is $2000.

6.3.6 Subsystem Costs. A summary of estimated costs, including the full cost of purchased components but only materials and fabrication costs on special items, is as follows:

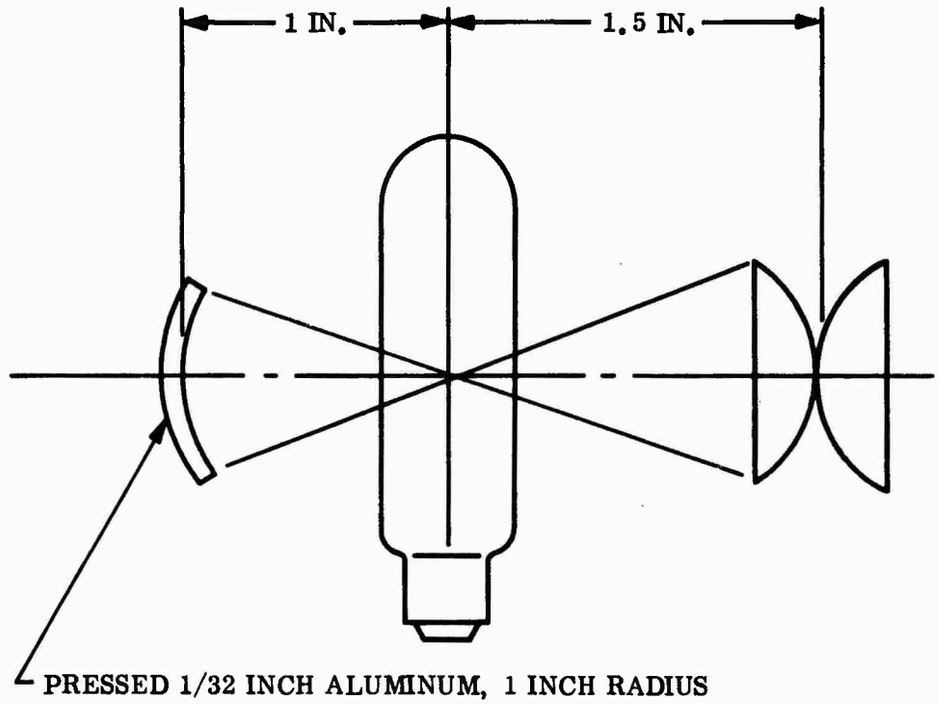

CONDENSER LENSES #1 & #2 ARE IDENTICAL AND MADE OF OHARA INFRA-RED ABSORBENT GLASS WITH $\eta_D = 1.512$, $v_{no} = 68.0$

LAMP, G.E., CDS, 100 WATT

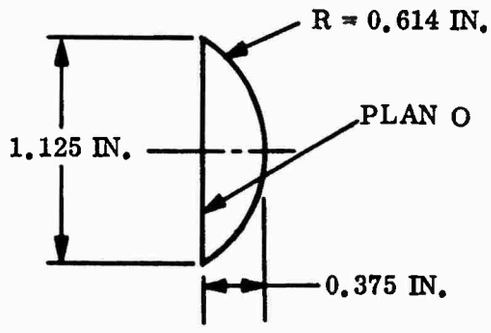

TOLERANCES:
±0.005 IN. ON
ALL DIMENSIONS

Figure 38. Transparency Illuminator

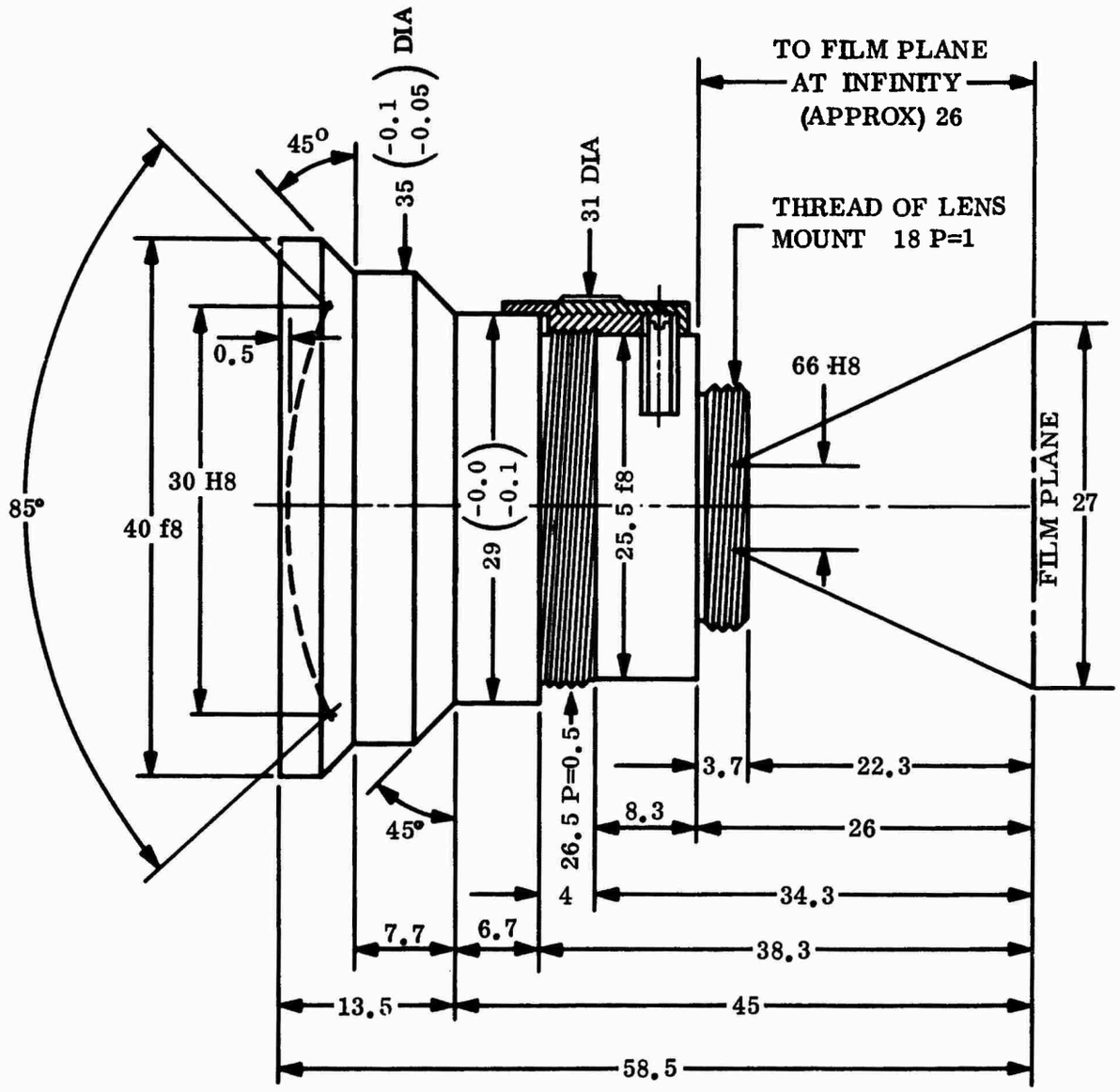

NOTE: ALL DIMENSIONS ARE IN MILLIMETERS.

Figure 39. Envelope Drawing

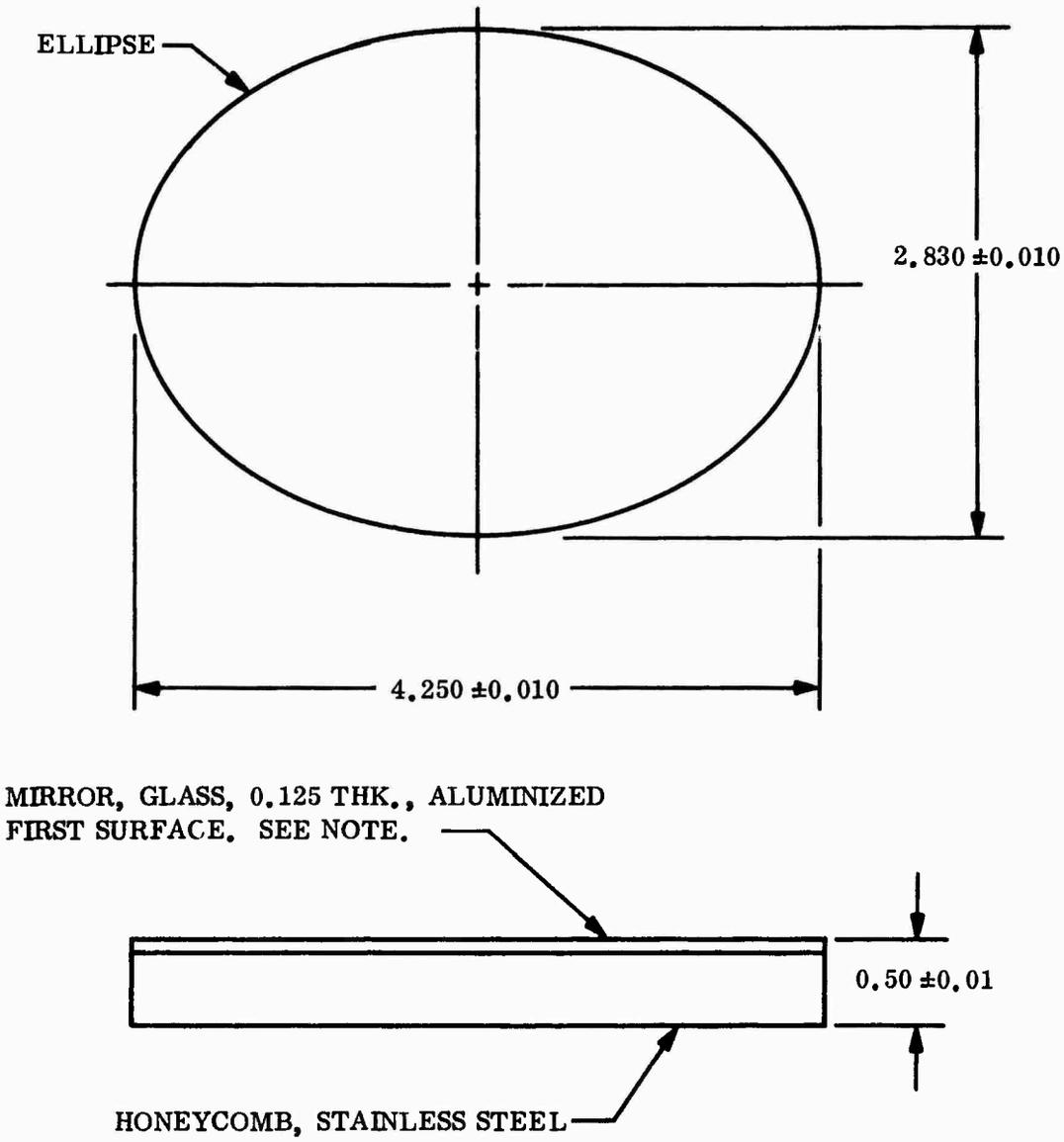

NOTE:

BOROSILICATE GLASS WITH HIGH REFLECTANCE ALUMINUM AND SiO OVERCOAT. SURFACE TO BE COMPLETELY POLISHED FLAT WITH NO SLOPE ERRORS GREATER THAN ONE MINUTE.

Figure 40. Rotating Diagonal Mirror

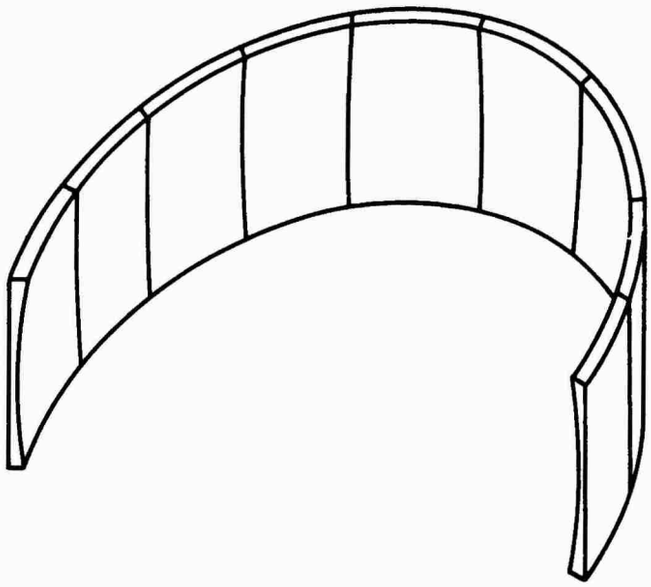

9 BLOCKS
21 IN. X 21 IN.
RADIUS OF CURVATURE
60 IN.
MAX SLOPE ERROR
1 ARC-MINUTE
MATERIAL
GLASS OR PLEXIGLASS
SURFACE
ALUMINIZED, S_iO OVERCOAT

Figure 41. Spherical Field Mirror

Target transparency	$2000
Controller	250
Target illuminator	250
Projection lens	250
Diagonal mirror	250
Spherical field mirror	3600
Supporting structure	2000
Total	$8570

6.4 Active Target Projection Subsystem

The target projection subsystem for the active optical intercept simulator consists of the following components:

1. Target transparency
2. Photosensor
3. Projection lens
4. Rotating diagonal mirror
5. Reflective fence

Components 1, 3, and 4 are identical with those previously described for the passive simulator. Where possible, component 2, the photosensor, is the scorer photoreceiver itself. Where the articulation of the scorer does not permit such use, the photosensor will consist of a target illuminator, as in the passive simulator, in which the lamp is replaced by a photocell and pre-amplifier. This package can be supplied for no more than $500 in materials and fabrication costs.

Except for size, the reflective fence, 5, will be similar to that recommended for use in the radar intercept simulator, and described in that section of this report. In the radar simulator, it is necessary only to accommodate a slightly diverging laser beam, and fence and folding mirrors need be only one-foot wide. In the active optical simulator it is necessary to accommodate the maximum vertical dimension of the target vehicle. If we assume a five-foot maximum vertical dimension, the extra cost of reflective sheeting, wall mirrors and supporting structure to allow one installation to serve both simulators is approximately as follows:

Scotchlite: 440 ft^2	$ 420
Mirrors: 240 ft^2	$3600
Alignment jig	$2000

6.4.1 Subsystem Costs. A summary of estimated costs, including the full cost of special items, is as follows:

Target transparency	$2000
Controller	250
Photosensor and preamplifier	500
Projection lens	220
Diagonal mirror	250
Reflective fence, additional costs over radar intercept simulator	6020
Total	$9240

6.5 Optical Intercept Simulator Costs

The cost of the optical simulator, excluding engineering costs, is found from the sum of the subsystem costs.

Mirror rotation subsystem	$22,575
Passive target projector	8,570
Active target projector (assumes construction of radar simulator)	9,240
Total	$40,385

7.0 DETAIL SUBSYSTEM DESIGN, RF SIMULATOR

7.1 Subsystem Definition

To implement the proposed design, three key subsystems must be assembled. These include:

1. The microwave processing subsystem, including the microwave receiving processor, the microwave transmitting processor, and the radar anechoic room.

2. The laser subsystem, including modulator, demodulator, reflective fence, and laser.

3. The mirror rotation subsystem.

The mirror rotation subsystem will be in all essentials similar to the one defined for the optical intercept simulator, and will require no further definition here. The remainder of this section will be devoted to a description of the microwave processing subsystem and the laser subsystem. Design is limited to L- and S-bands, extendable to higher frequencies by modular replacement.

7.1.1 Microwave Signal Processing Subsystem. The three areas of the Microwave Processing Subsystem are the Microwave Receiving Processor (MWRP), the Microwave Transmitting Processor (MWTP), and the Anechoic Chamber. The MWRP picks up the radar scorer signal, processes it at the incoming frequency and delivers it to the laser modulator. The MWTP obtains a demodulated signal from the travelling wave phototube (TWP) in the originating microwave frequency band, processes it, and transmits it back to the radar scorer. The Anechoic Chamber simulates an idealized space link.

The component configurations of the MWRP and MWTP, along with typical signal levels, are shown in Figures 42 and 43, respectively.

7.1.1.1 The MWRP. The signal levels for the MWRP are found as follows: A typical radar scorer, such as the BIDOPS system, has a transmitting power output of the order of 70 milliwatts, or about +18 dbm. The space loss for the antennae, spaced 4λ apart to simulate the far field is, from the one-way range equation:

$$\frac{P_t}{P_r} = \frac{(4\pi R)^2}{G_r G_t \lambda^2} = \frac{16\pi^2 (16\lambda^2)}{(1)(1)\lambda^2} = 2530 = 34 \text{ db}$$

The MWRP antenna has a mean gain of 10 db over an isotropic radiator and the insertion loss for the band pass filter is -1.5 db. For the variable attenuator when set at minimum, the loss is -5 db. Cascaded TWT amplifiers are used to provide an overall gain of 44 db, with the leading amplifier gain set at 20 db to give an output signal

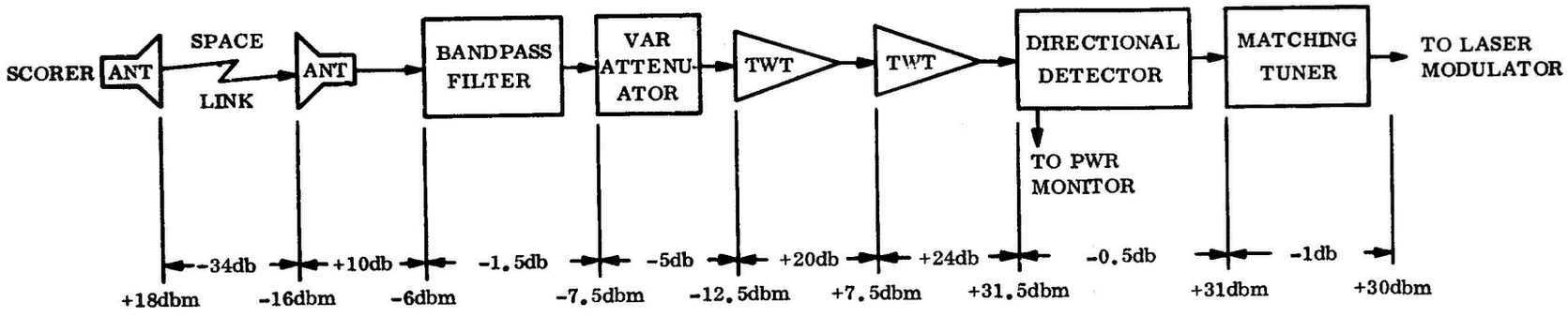

Figure 42. Microwave Receiving Processor

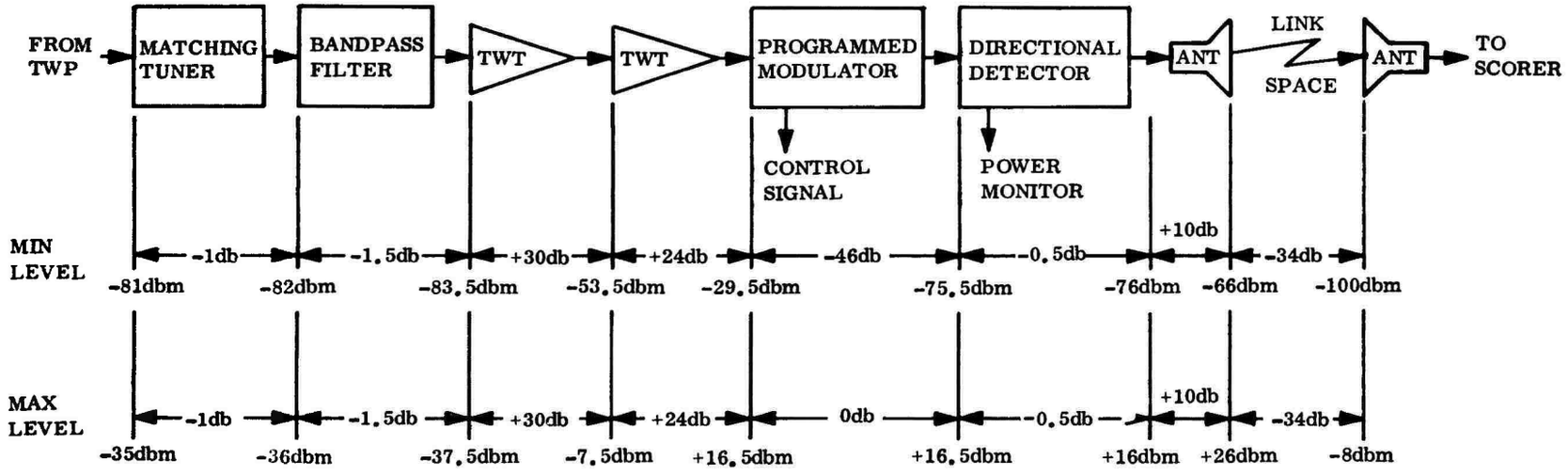

Figure 43. Microwave Transmitting Processor

level at this point of less than 10 dbm, which is within the linear signal range of the TWT. Following the amplifiers, a directional coupler with built-in crystal detector is used to isolate the MWRP from the laser modulator. The crystal detector is necessary to monitor the power level to the laser modulator. The variable attenuator takes care of higher power scorer signal levels and the TWT amplifiers have gain controls which can be readjusted to take care of lower power scorer signal levels. An anticipated range of control of power level is ± 10 db. A double stub matching tuner is used to reduce any VSWR reflection effects on the TWT amplifier to a tolerable magnitude. The microwave power level required at the laser modulator is 1 watt, or 30 dbm.

The question of signal to noise ratio was investigated to determine whether the TWT amplifiers were required to be of the low-noise variety. For a source impedance of R + j0 and a noise squared voltage of $E_n^2 = 4KTBR$, the available (matched power) noise input power is:

$$P_{na} = \frac{(1/2E_n)^2}{R} = \frac{E_n^2}{4R} = KTB$$

At a bandwidth of 1 Gc, the noise input power at 25°C is:

$$P_{na} = (1.38 \times 10^{-23})\ (298)\ (10^9) = 4.1 \times 10^{-12} w = -84 \text{ dbm}$$

At higher microwave frequencies and wider bandwidths, the noise input power will increase as shown below:

Band	Bandwidth	Noise Input Power
L	1 Gc	-84 dbm
S	2	-81
C	4	-78
X	4	-78
K	10	-74

Therefore, it is obvious that low noise TWT amplifiers are not necessary for the MWRP.

7.1.1.2 The MWTP. Referring to Figure 43, the laser subsystem will generate signals from a minimum power level of -81 dbm to a maximum power level of -35 dbm. This corresponds to a dynamic range of 46 db. The optical dynamic range has been restricted to 46 db because of the limited linear demodulation capability of the TWP. It is desired to have a 92-db dynamic range corresponding to a simulated target range from 5 to 1000 feet. Since only 46 db of power level variation can be accepted by the

TWP for reasonable signal-to-noise ratios, the remaining 46 db of variation will be simulated by the MWTP. The signal-to-noise ground rules are that, at the 1000-foot simulation range: (1) the signal-to-noise ratio is 20 db, and (2) the MWTP noise figure is 10 db maximum.

The noise figure F for a component is defined as $(SNR)_{in}/(SNR)_{out}$. However, if the component has more than one noise source, with gain interposed, then

$$F = F_1 + \frac{F_2 - 1}{G_1}$$

For the case at hand, the MWTP is to be designed for F = 10 db max, so that, by trading off low noise travelling wave amplifiers of a guaranteed noise figure value against power gain, an engineering analysis produces the optimum selection of components. With $F_1 = 8$ db, $F_2 = 30$ db, and $G_1 = 25$ db,

$$F = 6.31 + \frac{999}{316} = 9.47 \text{ or } 9.75 \text{ db}$$

To provide more safety margin, G_1 was increased to 30 db, making F = 8.65 db. If a lower noise figure TWT amplifier were used with, for instance, $F_1 = 5$ db, (the gain for this tube is 25 db maximum) the resulting component noise figure is

$$F = 3.16 + \frac{999}{316} = 7.32 = 8.65 \text{ db}$$

The cost factor being equal, the choice is in favor of the higher gain unit, since a still lower component noise figure could be obtained if G_1 were increased to the 35 db maximum value for this tube.

The required cascaded TWT amplifier power gain is 54 db. Simulation of the MWTP generated dynamic variation can be obtained by the recently announced Hewlett-Packard Microwave Modulator. A dynamic range of 80 db is possible with this equipment. The unit can be amplitude modulated externally at rates up to 10 mc by an electrical control signal. The sensitivity of control of modulation is 20 db per volt; therefore, for 46 db of modulation, 2.3 volts are required.

7.1.2 The Anechoic Chamber. The basic requirements on the anechoic chamber are that it be of sufficient size to provide far field communication with the outside at L- and S-bands and that there be sufficient isolation between transmitting and receiving links to prevent reflection ghosts and second-time-around returns.

A suitable chamber can be provided by Emerson and Cuming, Inc., to meet the following specifications:

1. Size: 14 ft cube

2. Absorber: Eccosorb HPY 18

3. Reflectivity: -40 db at 1 Gc, -50 db at 9 Gc and higher

4. Magnetic shielding: -60 db from 15 kc to 1 mc

5. Electric field shielding: -100 db from 15 kc to 100 mc

6. Leakage and spillover isolation: 60 db

The cost of this chamber is $17,500.

7.1.3 Component Selections and Subsystem Cost. The present effort is concerned with component implementation for L-band and S-band only. However, the choice of components has been made with due regard for implementation for the higher microwave frequency bands. Each of the components for L-band and for S-band is a readily available "off-the-shelf" item. Tables II through V give a compilation of the components required and include the costs.

TABLE II. MWRP COMPONENTS (L-BAND)

Quan.	Item	Mfg.	Part No.	Price
1	Antenna	AEL	H5001	$ 450
1	Band Pass Filter	H-P	8430A	210
1	Variable Attenuator	Alfred	E101	400
1	TWT Ampl.	Alfred	505	1950
1	TWT Ampl.	Alfred	560	2150
1	Directional Detector	H-P	786D	300
1	Matching Tuner	Omega	5568	120
			Total	$5580

TABLE III. MWTP COMPONENTS (L-BAND)

Quan.	Item	Mfg.	Part No.	Price
1	Matching Tuner	Omega	5568	$ 120
1	Band Pass Filter	H-P	8430A	210
1	TWT Ampl.	W-J	280	3500
1	TWT Ampl.	Alfred	560	2150

TABLE III. MWTP COMPONENTS (L-BAND) (Cont)

Quan.	Item	Mfg.	Part No.	Price
1	Modulator	H-P	8403A/ 8731B	$1200
1	Directional Detector	H-P	786D	300
1	Antenna	AEL	H5001	450
			Total	$7930

TABLE IV. MWRP COMPONENTS (S-BAND)

Quan.	Item	Mfg.	Part No.	Price
1	Antenna	AEL	H5101	$ 355
1	Band Pass Filter	H-P	8431A	210
1	Variable Attenuator	Alfred	E103	450
1	TWT Ampl.	Alfred	501	1650
1	TWT Ampl.	Alfred	561	2150
1	Directional Detector	H-P	787D	300
1	Matching Tuner	Omega	5572	90
			Total	$5205

TABLE V. MWTP COMPONENTS (S-BAND)

Quan.	Item	Mfg.	Part No.	Price
1	Matching Tuner	Omega	5572	$ 90
1	Band Pass Filter	H-P	8431A	210
1	TWT Ampl.	W-J	281	3500
1	TWT Ampl.	Alfred	561	2150
1	Modulator	H-P	8732B	500

TABLE V. MWTP COMPONENTS (S-BAND) (Cont)

Quan.	Item	Mfg.	Part No.	Price
1	Directional Detector	H-P	787D	$ 300
1	Antenna	AEL	H5101	355
				Total $7105

7.1.4 The Laser Subsystem. The design of the laser subsystem proceeds in the following order. We must first locate a suitable modulator and determine the modulation index possible with it. Next, we must locate a potential detector or demodulator. Knowing its properties and the signal modulation, we can calculate a minimum received optical power. Next, we must locate a suitable reflective material for the fence. With the reflectance of the fence and the minimum signal required by the demodulator, we can calculate, for the maximum operating range required, the necessary laser output power and select a laser.

7.1.4.1 Optical Modulator. What is desirable here is a single unit tunable over the whole L-band or S-band, requiring low power and delivering high modulation. Such devices do not seem to be available. It is possible, however, to obtain tuned-cavity modulators capable of high modulation at low input power, but they are very highly tuned indeed. The Sylvania SYD-4470 KDP modulator, for instance, will produce 25 percent modulation in the S-band for a 1-watt average input. The high-Q cavity has, however, a bandwidth of only 4 mc and cannot be tuned. Tunable modulators are available (Electro-Optical Systems, for instance), but their low-Q cavities typically deliver only 1 percent modulation or less. The percent modulation is very critical for the laser power requirement and it would be unwise to accept a lower figure than about 10 percent. Aside from undertaking development of a modulator with all the desirable characteristics, the most reasonable way around the problem is to buy a new modulator for each new scoring system to be tested (at $1500).

For the present system design we have assumed a modulation of 10 percent, which is reasonable and conservative.

7.1.4.2 Demodulator. The basic device for optical demodulation at microwave frequencies is the travelling wave phototube (TWP). Two kinds of TWP are available — those with a multiplier section, and those without. Without a multiplier section, the significant sources of noise are shot noise and thermal noise. The power signal-to-noise ratio (SNR) for this type of tube is given by:

$$SNR = \frac{1/2\,(mI_o)^2 R_{eq}}{kTB + 2eI_o BR_{eq}}$$

where:

m = modulation index

I_o = average beam current, amperes

R_{eq} = equivalent resistance of the TWP, ohms

k = Boltzmann's constant, 1.38×10^{-23} joules/degree

T = absolute temperature, ^oK

B = bandwidth, cps

e = electron charge, 1.60×10^{-19} coulomb

For a multiplier tube, the effect of thermal noise is removed, but the SNR due to shot noise only is degraded by the factor $\left(\frac{\sigma-1}{\sigma}\right)$, where σ is the gain per multiplier stage. A multiplier TWP thus has a higher SNR at low signal levels, and a lower SNR at high signal levels, than does the non-multiplier TWP. For the present application, SNR at the lowest levels is most important. Therefore, a multiplier tube is preferred.

The tube selected for application here is the RCA A1283M Multiplier Lasecon Microwave Phototube, with S-20 surface, available on 90-day delivery at the price of $8250. The SNR for this tube is given by:

$$SNR = \frac{m^2 q P_r}{Bh\nu} \left(\frac{\sigma-1}{\sigma}\right)$$

where, in addition to those constants already defined,

q = quantum efficiency of photocathode

P_r = received average optical power, watts

h = Planck's constant, 6.62×10^{-34} joule-sec

ν = optical frequency, cps

The numerical values of these parameters, assuming an argon laser ($\approx$5000 Å), include

$q = 0.12$

$h\nu = 4.0 \times 10^{-19}$ joule/quantum

$\sigma = 4.0$

The resulting expression for SNR is $SNR = 2.25 \times 10^9 P_r$.

This function has been plotted in Figure 44. For an assumed minimum SNR of 30 db, the optical requirement is $P_r = 4.5 \times 10^{-7}$ watt.

The A1283M TWP is supplied with a helix tuned to the 1-2 Gc band. Its use can be extended to the 2-4 Gc band by coupling in a 1-2 Gc signal from a low power, signal generator type local oscillator. A suitable equipment selection would be:

General Radio Model 1218-A Oscillator: $465

General Radio Model 1201-B Power Supply: $ 90

Alternatively, a second TWP can be purchased with a helix tuned to the 2-4 Gc band.

7.1.4.3 Reflective Fence. A survey of potential materials for this fence has led to the selection of Parkway Silver "Scotchlite" flat-top reflective sheeting, stock No. 3270, available with adhesive backing at $0.95 per square foot.

Scotchlite appears to have the best retroreflective properties of any commercially available material. Its gain characteristics are displayed graphically in Figure 45. Higher gains can be obtained with special fence structures, but the additional cost is not at present considered justified. The high optical gain of Scotchlite is most important at the extreme range of 1000 feet. To maintain the gain above 200 at this distance, it will be necessary to use the Scotchlite at or near normal incidence. This requires a periodic type of support structure. One simple arrangement which provides normal incidence at extreme ranges and reasonable accommodation to incidence angle at the shorter ranges is shown in Figure 46.

7.1.4.4 Laser. An argon laser has been selected because of the favorable combination of high laser power and high receiver sensitivity obtaining at argon wavelength (≈ 5000 Å). The power required of the laser is given by:

$$P_t = \left(\frac{\pi}{G}\right)\left(\frac{P_r}{\Gamma}\right)\left(\frac{R^2}{A_r}\right)$$

where:

Γ = overall optical transmission

P_r = minimum received optical power, watts

G = reflector gain

R = range, feet

A_r = receiver optics area, ft^2

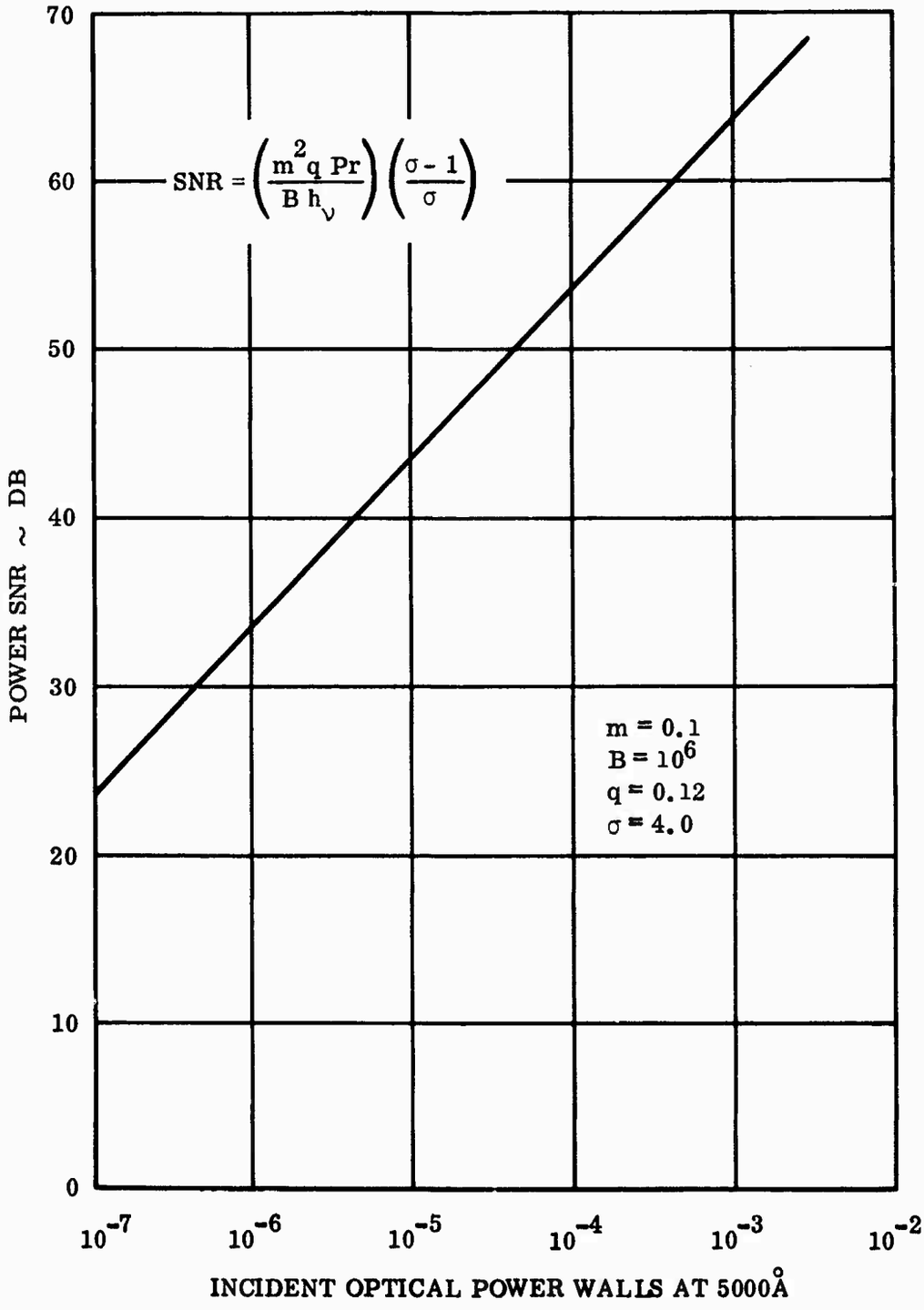

Figure 44. Power SNR for RCA A1283M Multiplier TWP

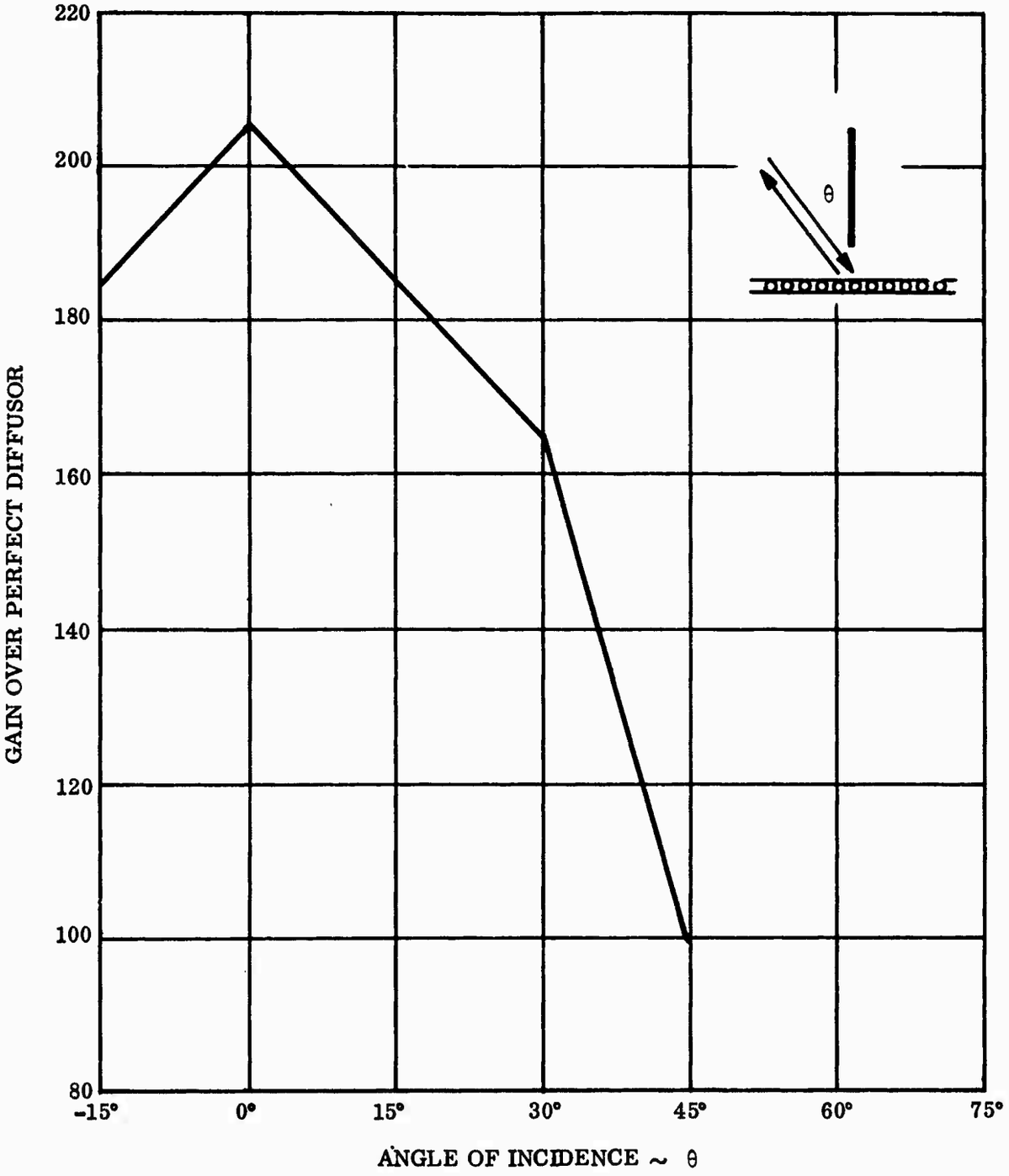

Figure 45. Retroflective Properties of Parkway Silver Scotchlite Flat Top Reflective Sheeting

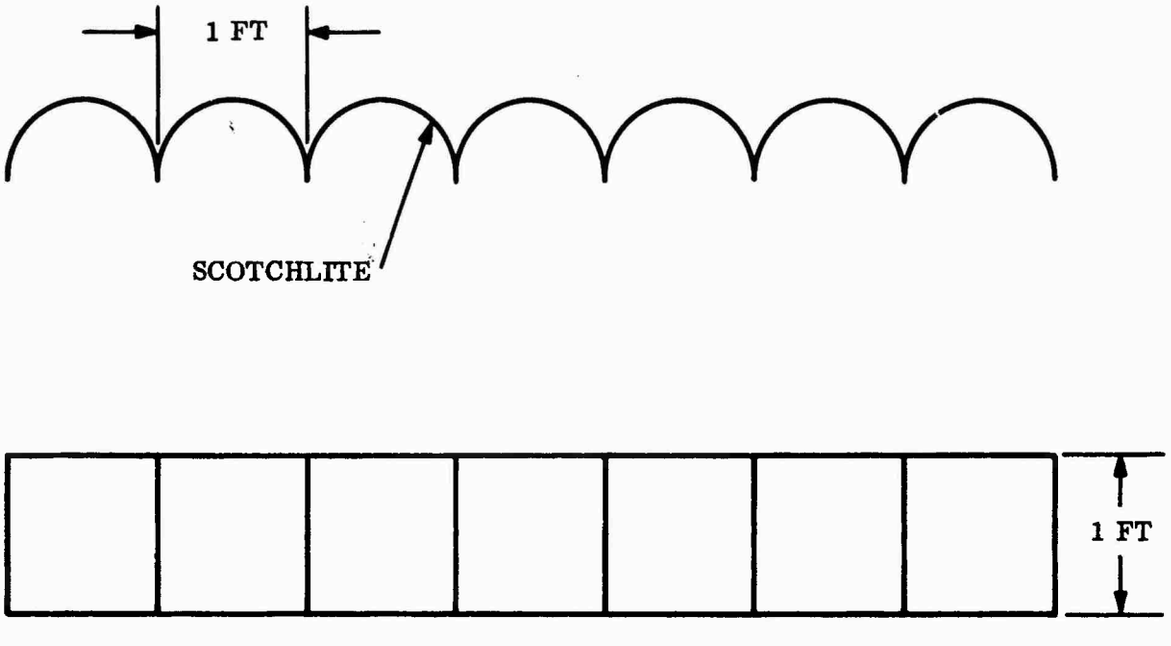

Figure 46. Reflective Fence Configuration

For the present case, the numerical values of these parameters are:

$P_r = 4.5 \times 10^{-7}$ watt

$G = 200$

$\Gamma = 0.5$

$R = 10^3$ ft

$A_r = 2.2 \times 10^{-2}$ ft^2

Substituting these numerical values yields:

$P_t = 0.64$ watt

This requirement can be met with power to spare by an off-the-shelf, one-watt, argon laser manufactured by Electro-Optical Systems. Its specifications are as follows.

Manufacturer and Model: Electro-Optical Systems Model 13 Argon laser

Power: 1 watt nominal at 4500 to 5000 Angstroms

Size: Head: 42 inches x 12 inches x 8 inches, weight 165 pounds
Power Supply: rack mounted, 6 feet x 21 inches x 24 inches, weight 1100 pounds

Power Requirement: 240 volts, 100 amps, single phase, 60 cps

Life: Tube guaranteed 300 hours (life experience exceeds 1000 hours)

Cost: $20,750 with power supply

Tube Replacement Cost: $2600 each

Ancillary Equipment Required: Heat Exchanger, liquid-liquid, $3500

7.1.4.4 Folded Reflective Fence. The reflective fence does not physically have to be 1000 feet in extent. Its effective length can easily be made infinite by using mirrors. The general scheme is illustrated in Figure 47. The penalty for this convenience is a loss at each reflection and a mirror accuracy requirement which grows more demanding with each reflection. The advantages include indoor installation with all weather capability and the removal of any background optical noise problem. If indoor installation is mandatory, the configuration of Figure 47 should give usable operation over most of the 180-degree relative trajectory.

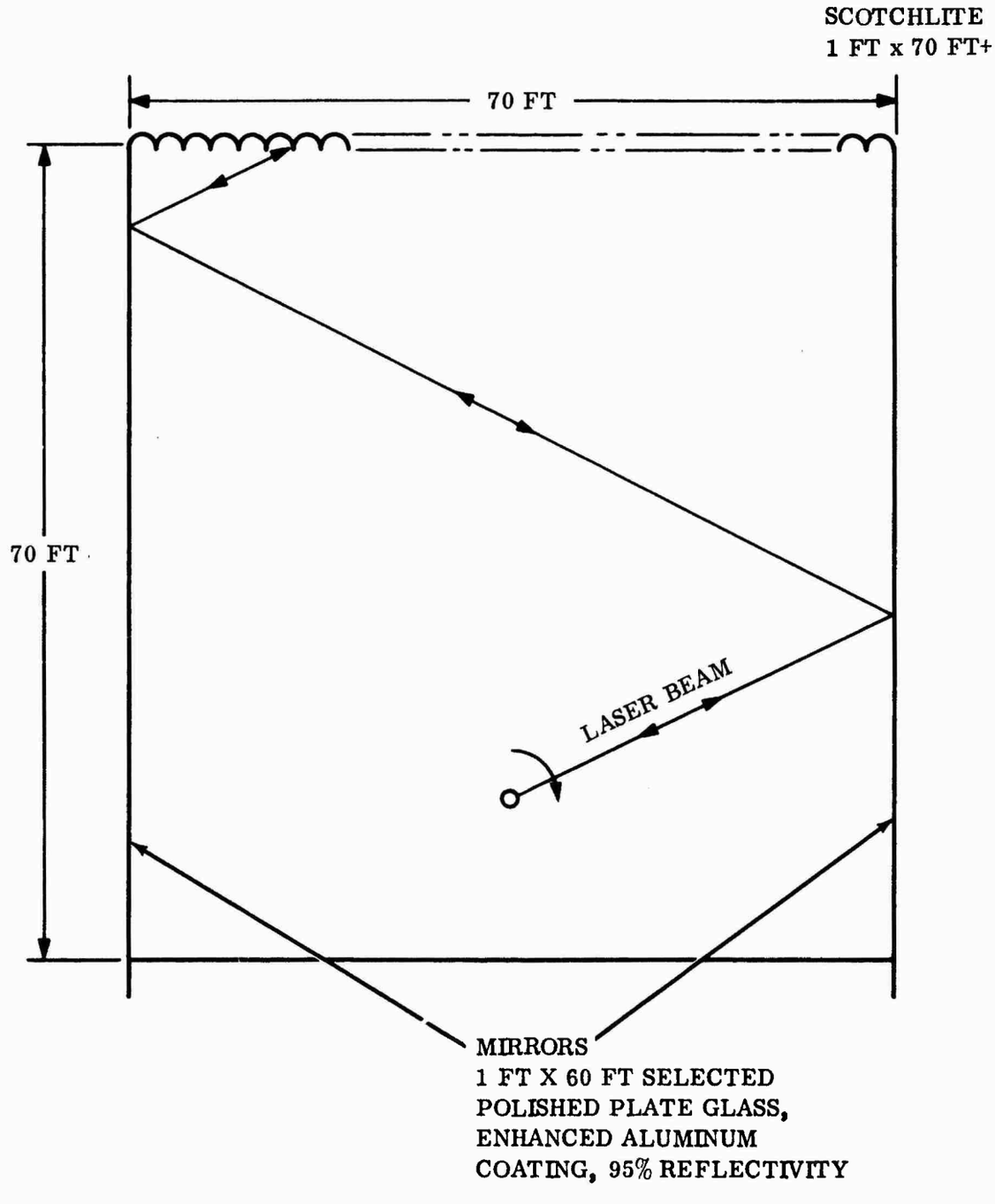

Figure 47. Folded Reflective Fence

Calculations (see below) support a prediction of useful performance in the open to 1000 feet. To calculate indoor range, the significant parameter is (Γ/R^2), where Γ is the overall system transmission and R is the range in feet. For the case of open air transmission, $(\Gamma/R^2) = 5 \times 10^{-7}$. Essentially equivalent performance may be expected for indoor operation as long as $(\Gamma/R^2) \geq 5 \times 10^{-7}$. If we assume operation inside a 70-foot wide room, we may write

$$\frac{\Gamma}{R^2} = \frac{0.5\,(0.95)^{2R/70}}{R^2} \geq 5 \times 10^{-7}$$

hence, we deduce that effective operation indoors is limited to about 600 feet, assuming a mirror reflectivity of 95 percent.

To achieve a reflectivity of 95 percent at 5000 Å, aluminum mirrors must be enhanced by a 2-layer dielectric coating. To limit angular position errors to 1 milliradian, the mirrors must exhibit a combined surface and position slope accuracy of not more than $10^{-3}/\sqrt{18}$ radians or 0.000235 radian. Hence, one-minute mirrors will suffice. One-minute mirrors of selected polished plate glass with enhanced aluminum surfaces can be supplied for about $15 per square foot. If the laser beam divergence is limited to 1 milliradian, the maximum mirror area required will be $2 \times 60 \times 1 = 120$ ft^2, assuming a room allowing a maximum miss distance of 60 feet. Mirror cost would be $1800. An alignment jig to hold the mirrors and allow for their adjustment would cost roughly an additional $2000. Total cost for folding the system would be $3800.

The indoor range calculation above assumed a beam modulation of 10 percent. This figure is conservative, because actually the modulator is rated at 25 percent. For 25 percent modulation, the received average power may be down by a factor of 6.25 and still yield the same SNR in the TWP. If we recalculate, taking this into account, we find

$$\frac{6.25\,(0.5)\,(0.95)^{2R/70}}{R^2} = 7.4 \times 10^{-7} \text{ for } R = 1000 \text{ ft}$$

Hence, it would appear possible to achieve a full 1000-foot range in an indoor installation, provided the modulator can be used at its full rated efficiency. Another factor working in the direction of increased range is that system calculations were based on a laser output power of 0.64 watt, whereas actually the laser is rated at one watt, and can be raised to two. It is good practice to base a design on conservative estimates of component performance, but we should recognize that the possibility of greater performance is still present.

7.1.5 Subsystem Costs. A summary of extimated costs, not including engineering costs, is as follows:

Modulator	$1500
Demodulator	8250
Oscillator	465
Power supply	90
Folded reflective fence	3800
Laser	20,750
Heat exchanger	3500
Total	$38,305

7.2 Radar Intercept Simulator Costs.

The materials costs for the radar simulator are found from the sum of the subsystem costs. No engineering costs are included.

Mirror rotation subsystem	$ 22,575
Microwave signal processors	25,820
Anechoic chamber	17,500
Laser subsystem	38,305
Total	$104,200

Unclassified
Security Classification

DOCUMENT CONTROL DATA - R&D

(Security classification of title, body of abstract and indexing annotation must be entered when the overall report is classified)

1. ORIGINATING ACTIVITY (Corporate author) General Electric Company Re-entry Systems Department Philadelphia, Pa.	2a. REPORT SECURITY CLASSIFICATION Unclassified 2b GROUP N/A

3. REPORT TITLE

Relative Motion Simulation Study

4. DESCRIPTIVE NOTES (Type of report and inclusive dates)

Final Technical Report, (February 1965 - December 1965)

5. AUTHOR(S) (Last name, first name, initial)

Ferrara, Peter J.

6. REPORT DATE	7a. TOTAL NO. OF PAGES	7b. NO. OF REFS
April 1966	121	None

8a. CONTRACT OR GRANT NO. AF08(635)-4911 b. PROJECT NO. 7848 c. d.	9a. ORIGINATOR'S REPORT NUMBER(S) ATL-TR-66-29 9b. OTHER REPORT NO(S) (Any other numbers that may be assigned this report)

10. AVAILABILITY/LIMITATION NOTICES This document is subject to special export controls and each transmittal to foreign governments or foreign nationals may be made only with prior approval of Air Force Armament Laboratory (ATWR), Eglin Air Force Base, Florida.

11. SUPPLEMENTARY NOTES	12. SPONSORING MILITARY ACTIVITY
	Air Force Armament Laboratory (ATWR) Eglin Air Force Base, Florida

13. ABSTRACT

The objectives of this study contract were to analyze the system requirements and establish design criteria for a relative motion simulation facility able to test and evaluate air-to-air or space mission scoring systems. In the pursuit of these objectives, numerous present and forseeable future scoring systems were studied and their essential features abstracted. The relative motion characteristic of the two classes of intercept was analyzed and the significance of maneuver capability evaluated. Those aspects of an intercept observable by scorers were summarized both quantitatively and qualitatively. With these general requirements in hand, various techniques for mechanizing the intercept simulation were considered. The technique finally selected as most practical employed a projection system whose line-of-sight was rotated by a high-performance, DC servo motor, driven open-loop in a manner duplicating the real-time sweep of the missile to target displacement vector. Relative velocity/miss distance ratios up to 500 can be simulated exactly, and ratios up to 1000 simulated acceptably, using this technique. Hardware implementation will be simple and straightforward, and all major components are obtainable off-the-shelf. A preliminary design was developed for a facility capable of accommodating L- and S-band radar scorers and both active and passive optical scorers. The design allows extension to higher radar frequencies or to infrared by modular replacement of components, without major redesign.

DD FORM 1 JAN 64 1473

Unclassified
Security Classification

14. KEY WORDS	LINK A		LINK B		LINK C	
	ROLE	WT	ROLE	WT	ROLE	WT
Relative Motion Simulation Scoring, Guidance, Homing Systems Infrared, Visible Optical, Radar						

INSTRUCTIONS

1. ORIGINATING ACTIVITY: Enter the name and address of the contractor, subcontractor, grantee, Department of Defense activity or other organization *(corporate author)* issuing the report.

2a. REPORT SECURITY CLASSIFICATION: Enter the overall security classification of the report. Indicate whether "Restricted Data" is included. Marking is to be in accordance with appropriate security regulations.

2b. GROUP: Automatic downgrading is specified in DoD Directive 5200.10 and Armed Forces Industrial Manual. Enter the group number. Also, when applicable, show that optional markings have been used for Group 3 and Group 4 as authorized.

3. REPORT TITLE: Enter the complete report title in all capital letters. Titles in all cases should be unclassified. If a meaningful title cannot be selected without classification, show title classification in all capitals in parenthesis immediately following the title.

4. DESCRIPTIVE NOTES: If appropriate, enter the type of report, e.g., interim, progress, summary, annual, or final. Give the inclusive dates when a specific reporting period is covered.

5. AUTHOR(S): Enter the name(s) of author(s) as shown on or in the report. Enter last name, first name, middle initial. If military, show rank and branch of service. The name of the principal author is an absolute minimum requirement.

6. REPORT DATE: Enter the date of the report as day, month, year; or month, year. If more than one date appears on the report, use date of publication.

7a. TOTAL NUMBER OF PAGES: The total page count should follow normal pagination procedures, i.e., enter the number of pages containing information.

7b. NUMBER OF REFERENCES: Enter the total number of references cited in the report.

8a. CONTRACT OR GRANT NUMBER: If appropriate, enter the applicable number of the contract or grant under which the report was written.

8b, 8c, & 8d. PROJECT NUMBER: Enter the appropriate military department identification, such as project number, subproject number, system numbers, task number, etc.

9a. ORIGINATOR'S REPORT NUMBER(S): Enter the official report number by which the document will be identified and controlled by the originating activity. This number must be unique to this report.

9b. OTHER REPORT NUMBER(S): If the report has been assigned any other report numbers *(either by the originator or by the sponsor)*, also enter this number(s).

10. AVAILABILITY/LIMITATION NOTICES: Enter any limitations on further dissemination of the report, other than those imposed by security classification, using standard statements such as:

(1) "Qualified requesters may obtain copies of this report from DDC."

(2) "Foreign announcement and dissemination of this report by DDC is not authorized."

(3) "U. S. Government agencies may obtain copies of this report directly from DDC. Other qualified DDC users shall request through

_____."

(4) "U. S. military agencies may obtain copies of this report directly from DDC. Other qualified users shall request through

_____."

(5) "All distribution of this report is controlled. Qualified DDC users shall request through

_____."

If the report has been furnished to the Office of Technical Services, Department of Commerce, for sale to the public, indicate this fact and enter the price, if known.

11. SUPPLEMENTARY NOTES: Use for additional explanatory notes.

12. SPONSORING MILITARY ACTIVITY: Enter the name of the departmental project office or laboratory sponsoring *(paying for)* the research and development. Include address.

13. ABSTRACT: Enter an abstract giving a brief and factual summary of the document indicative of the report, even though it may also appear elsewhere in the body of the technical report. If additional space is required, a continuation sheet shall be attached.

It is highly desirable that the abstract of classified reports be unclassified. Each paragraph of the abstract shall end with an indication of the military security classification of the information in the paragraph, represented as *(TS)*, *(S)*, *(C)*, or *(U)*.

There is no limitation on the length of the abstract. However, the suggested length is from 150 to 225 words.

14. KEY WORDS: Key words are technically meaningful terms or short phrases that characterize a report and may be used as index entries for cataloging the report. Key words must be selected so that no security classification is required. Identifiers, such as equipment model designation, trade name, military project code name, geographic location, may be used as key words but will be followed by an indication of technical context. The assignment of links, rules, and weights is optional.